NTNU
Norwegian University of
Science and Technology

Efficient heat recovery from industrial processes using heat pump

Pierfrancesco Fava

Mechanical Engineering
Submission date: January 2016
Supervisor: Trygve Magne Eikevik, EPT

Norwegian University of Science and Technology
Department of Energy and Process Engineering

NTNU

Norwegian University
of Science and Technology

Department of Energy
and Process Engineering

EPT-M-2015-xx

MASTER THESIS

for

Student Pierfrancesco Fava

Fall 2015

Efficient Heat Recovery from Industrial Processes through Heat Pumps

Effektiv varmegjenvinning fra industrielle prosesser ved hjelp av varmepumpe

Background and objective

The project objectives focus on development of industrial waste heat recovery solutions that aim at:
- recovering large quantities of waste heat, upgrading it to higher temperatures and reusing as thermal energy in internal industrial processes,
- high system durability expressed as at least 20 years life span
- reducing primary energy consumption,
- decarburization and resource efficiency of the energy supply

The first two statements define whether the proposed technological solutions and practices will be widely accepted by the end users or not, and are essential conditions, if we aim at their wide market penetration and large scale impact. The last two statements have a straightforward direct impact on optimum exploitation of the energy resources, as well as on environmental protection.

Recently, the heat pumps technology appears considerable application in household sector. Demonstrating the superior performance of the technology is essential in order to facilitate its large penetration in the industrial sector and demonstrate that can apply in pilot plants at industrial sites by improving this technology in terms of:
- heat supply at temperature range (+90 to +140°C or more)
- energy efficiency, e.g. heat recovery from 60°C waste heat (COP/SCOP 5.0 – 6.1)
- cost effectiveness

The following tasks are to be consider:
1. Literature review of heat pumps used in industrial applications
2. Determine suitable working fluids for high temperature heat pump
3. Developing a simulation model using EES for a given case
4. Evaluate the different working fluids in different cases
5. Implementing an economical model taking into account the size of the components
6. Make a draft scientific paper of the results from the project

7. Make suggestion for further work

-- " --

Within 14 days of receiving the written text on the master thesis, the candidate shall submit a research plan for his project to the department.

When the thesis is evaluated, emphasis is put on processing of the results, and that they are presented in tabular and/or graphic form in a clear manner, and that they are analyzed carefully.

The thesis should be formulated as a research report with summary both in English and Norwegian, conclusion, literature references, table of contents etc. During the preparation of the text, the candidate should make an effort to produce a well-structured and easily readable report. In order to ease the evaluation of the thesis, it is important that the cross-references are correct. In the making of the report, strong emphasis should be placed on both a thorough discussion of the results and an orderly presentation.

The candidate is requested to initiate and keep close contact with his/her academic supervisor(s) throughout the working period. The candidate must follow the rules and regulations of NTNU as well as passive directions given by the Department of Energy and Process Engineering.

Risk assessment of the candidate's work shall be carried out according to the department's procedures. The risk assessment must be documented and included as part of the final report. Events related to the candidate's work adversely affecting the health, safety or security, must be documented and included as part of the final report. If the documentation on risk assessment represents a large number of pages, the full version is to be submitted electronically to the supervisor and an excerpt is included in the report.

Pursuant to "Regulations concerning the supplementary provisions to the technology study program/Master of Science" at NTNU §20, the Department reserves the permission to utilize all the results and data for teaching and research purposes as well as in future publications.
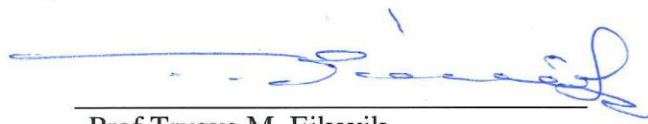
The final report is to be submitted digitally in DAIM. An executive summary of the thesis including title, student's name, supervisor's name, year, department name, and NTNU's logo and name, shall be submitted to the department as a separate pdf file. Based on an agreement with the supervisor, the final report and other material and documents may be given to the supervisor in digital format.

☐ Work to be done in lab (Water power lab, Fluids engineering lab, Thermal engineering lab)
☐ Field work

Department of Energy and Process Engineering, August 28th 2015

Prof. Olav Bolland	Prof Trygve M. Eikevik
Department Head	Academic Supervisor
	e-mail: Trygve.m.eikevik@ntnu.no
Research Advisor:	e-mails
PhD Ignat Tolstorebrov	Ignat.tolstorebrov@ntnu.no

Preface

This dissertation thesis, which is the conclusion to my Master's Degree in Mechanical Engineering, has been carried out at the Energy and Process Engineering department of the NTNU University during the fall semester of 2015.

I would like to thank my supervisor, Professor Trygve Magne Eikevik. for the enormous opportunity I have been offered, for his helpfulness and for his support during the writing of the thesis. During this experience, I have been faced with the resolution of both theoretical and practical problems that undoubtedly improved how I manage critical issues.

Special acknowledgments go out to Professor Coriolano Salvini who gave me his support for this challenge.

Pierfrancesco Fava

Efficient heat recovery from industrial processes using heat pump

Summary

List of figure

List of table

Introduction

Ever since the Kyoto Protocol came into being, the acceding States have pledged to conclude agreements in order to reduce greenhouse gas emissions and limit the damages caused by the release of pollutants into the atmosphere.

According to the International Energy Agency, the industrial sector absorbs 31% of the primary energy generated globally, only a little less than the transportation sector. It is clear that these systems need improvement, if we wish to strongly reduce polluting emissions.

In order to do so, there is a tendency to reduce the consumption of primary energy by recovering heat and materials that would otherwise become waste.

Heat pumps technology is making its way in this trend: it has already been used for some time in space heating and, more recently, in the industrial sector.

This system allows heat recovery from a low temperature source to a source with a higher energetic level by introducing work in the system. The result of this technology, therefore, is the reduction of primary energy within a process, but not its complete substitution.

This technology is mainly applied to low temperatures, with a few cases of temperature raising above 80 °C, even though it is already well-established for a number of industrial processes, such as wood drying, and in the food and chemical industry.

For this reason, studies on pilot plants are carried out in order to establish this technology fit also for these uses, which will surely give high benefits as a result.

The main aim of this thesis is to show the possibilities that heat pumps hold within the industrial sectors in high-temperature applications, easing their inclusion within this field.

The thesis will focus on a heat pump system used in a tomatoes-working facility in Kyknos, Greece to recover heat. It will estimate its performances, especially the reduction of primary energy consumption, within a broader analysis of the pollutants

released and of its economic efficiency, by drawing a comparison with the same situation if the recovery system had not been used.

This writing is an analysis of the state of the art of heat pumps, and it follows the development of a highly efficient recovery system through the software EES.

I will begin by describing the working principles of these machines and their performances, followed by a brief description of the types of machines available on the market.

Subsequently, the circulation of these systems within the industrial sector is analysed, along with the fluids used by these machines.

Following that, a model for such heat pump is presented according to the characteristics of the given case. First, the ideal case is considered, through which the characteristics of the machines used within the system can be determined; later on, I analyze more accurately the real case, since it allows to determine the actual performances of the system.

An economic analysis of the system was carried out, which resulted in the definition of an optimized cycle according to its costs.

I gave a great deal of importance to the choice of the refrigerant fluid, which has been chosen among a range of natural fluids. To make this choice, simulations for each refrigerant fluid selected for the study have been carried out using the aforementioned software, which helped in determining the most performant fluid for the specific given case.

1. Working principles

It is called heat pump (HP) a machine that continuously transfers heat from a low temperature source to a higher temperature one by introducing work in the system. [1]
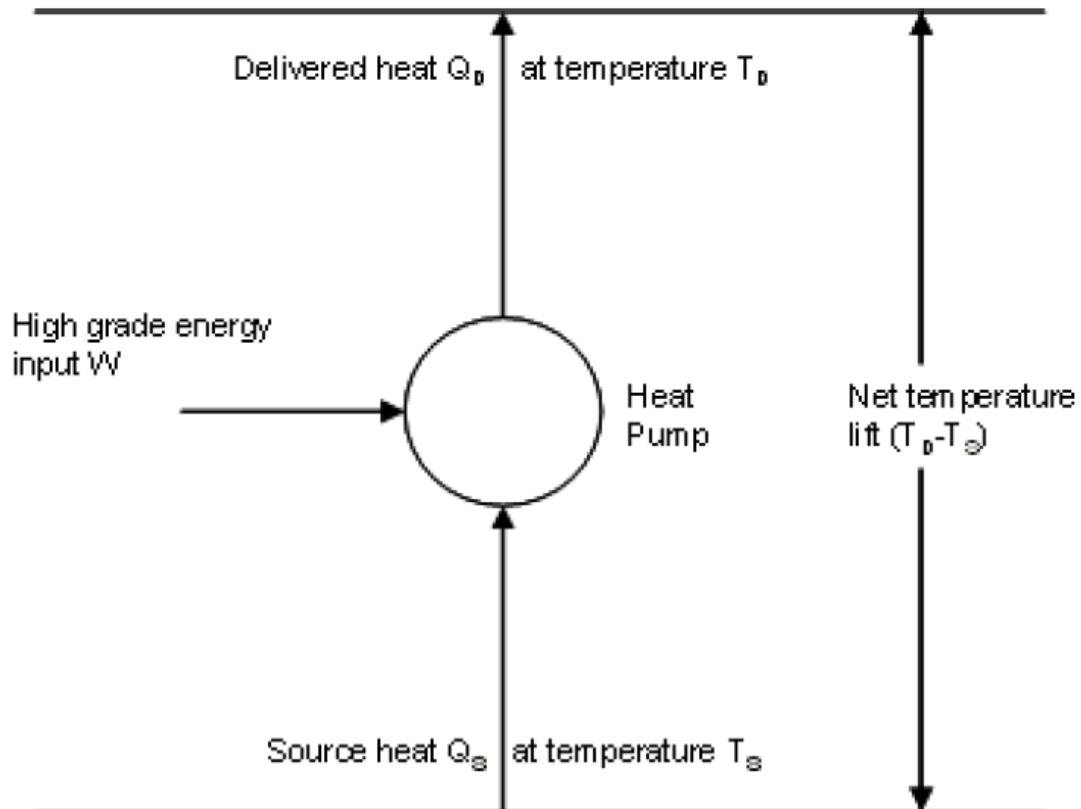
Figure 1: Heat Pump principle (Bohdan Soroka, 2015)

Thermic sources can have natural origins, such as ambient air and water, or artificial origins: that is the case of waste heat flows derived from any process inside a factory.

This technology can increase the efficiency of industrial processes through the recovery of waste heat flows. They will be requalified and made available at higher temperatures, reducing the primary energy consumption of the entire process

2. HP Performances

An analysis of the relevant parameters and performances of HPs follows.

The heat transfer at high temperature Q_d, is equal to the heat transfer from the source at low temperature Q_s plus the amount of high energy input W.

$$Q_d = Q_s + W$$

Therefore, it is possible to define the coefficient of performance for heat pumps COP, which is represented by the ratio between the purposed effect and the energy required to obtain it.

$$COP = Q_d/W$$

In addition, we can also define a COP_c involving a Carnot cycle which represents the maximum value that the COP can reach between temperatures T_s e T_q, and which is defined as follows:

$$COP_c = T_d/(T_d - T_s)$$

However, many types of HP that can be driven by mechanical or thermal energy exist. It is therefore useful to introduce another parameter to compare the different HP technologies. This parameter is the primary energy ratio PER, defined as:

$$PER = \frac{useful\ heat\ deliverd}{primary\ energy\ input}$$

This can be related to the COP with the following equation:

$$PER = COP * \eta$$

In the equation, the parameter η indicates the transformation efficiency of the primary energy used within the HP.

3. HP Classification

This paper will now draw up a first possible classification of HPs, followed by a more accurate description of how they work, their implant schemes and their applications in the industrial sector. [2]

A first possible classification divides HPs in Open-Cycle (OC) and Closed-Cycle (CC) systems. The work fluid of OC pumps can be either water in its different aggregation states (liquid and gaseous); on the other hand, CC systems use other fluids, called refrigerant fluids: they can have natural origins, synthetic origins, or they can be a mixture of more than one component. This is a necessary distinction, since they can have different effects on the environment and human beings.

HPs can also be divided according to the type of energy supplied to the system to make it work. Heat pumps can be mechanical-driven, using an electric or a diesel motor to move the compressor, or they can be thermal-driven. This classification refers respectively to mechanical compression cycles and to absorption or thermal vapour compression cycles.

The following list comprises of the major Industrial Heat Pumps (IHPs) that will be analyzed in this paper:
- Closed Compression Cycle – CCC;
- Mechanical Vapor Recompression – MVR;
- Thermal Vapor Recompression – TVR;
- Absorption Heat Pump – AHP.

3.1 Closed Compression Cycle – CCC

Below is the implant plan of the Closed Compression Cycle Heat Pump, one of the systems most used worldwide for industrial applications in different production environments:
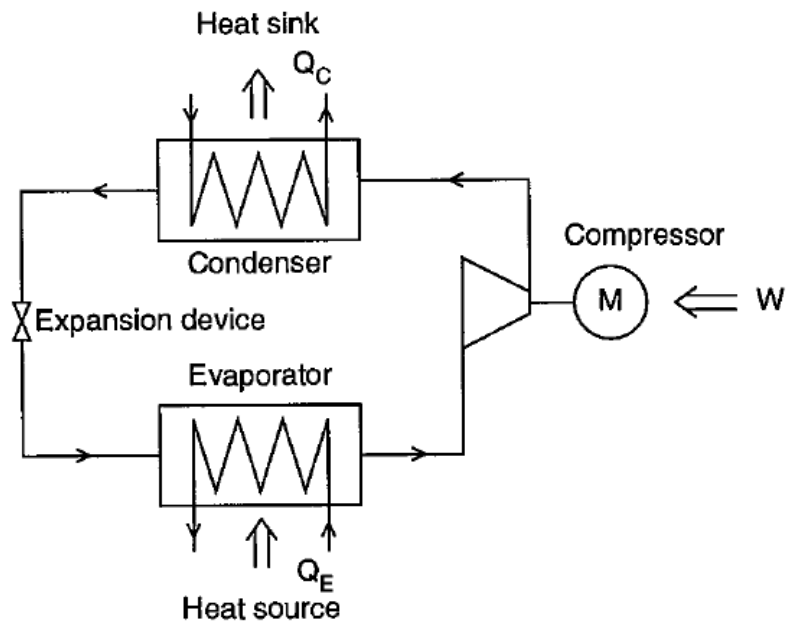
Figure 2: Simple Closed Compression Cycle (CCC)

This machine is composed of: [1]

- Evaporator – recovers the waste heat supplied by the heat source:
- Condenser – supplied the recover heat;
- Expansion valve – decreases the pressure of the condenser;
- Compressor – an engine that can be electric or a diesel driven.

Taking into account an electric-driven compressor, it is possible to represent the performances of this system: in the diagram below, the COP of the machine according to the evapouration temperature of the work fluid is parameterized for the type of compressor and for the sink temperature, the highest temperature in which heat can be released.

Figure 3: Closed Compression Cycle COP vs Temperature (Bohdan Soroka, 2015)

The diagram previously shown refers to the basic configuration of the HP, but performances can be increased with the appropriate modifications. [1]

The most effective modification possible would be to use multistage cycles. In this case, the compression would be split into more than one stage, in order to decrease the pressure ratio and increase the efficiency of each stage w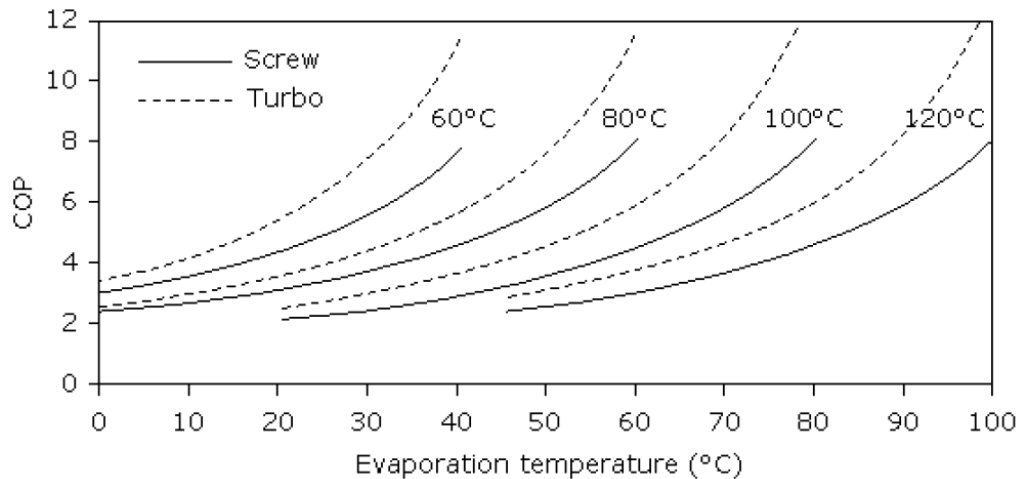hen compared to a single stage system. Usually, an intercooler is placed between the stages to further reduce the work of the downstream compressor.

Another modification that could improve the performances of this HPs would be sub-cooling the condensate to increase the purposed effect, and therefore the COP, without increasing the work needed to power the compressor. This can be achieved by introducing a heat exchanger downstream of the condenser.

Further improvements can be obtained with the insertion of an economizer or a flash sub-cooler: they both reduce the temperature change that the fluid needs, and so reduce the work needed for the compression.

3.2 Mechanical Vapor Recompression – MVR

This technology is used to increase pressure and temperature of a waste flow in order to reuse it. Two different layouts can apply to this machine. [2]
In the MVR type I the steam is compressed directly, and it later goes inside of a condenser.
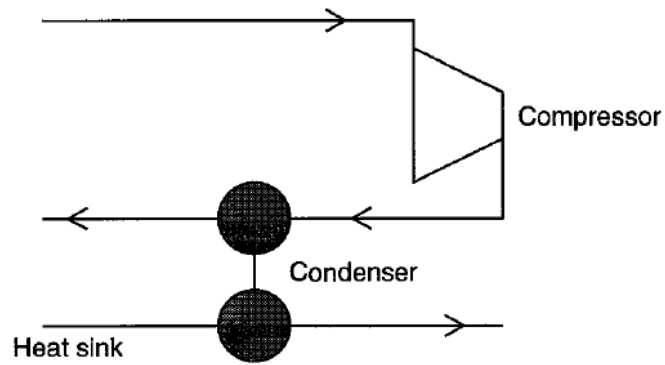
Figure 4: MVR Type I (International Energy Association, 1995)

In the MVR type II, the heat source goes through an evaporator instead of a condenser, as seen in all the previous HPs. This solution is adopted when the heat flow which is to be recovered might present a contaminant which needs to stay isolated. The flow first goes through an evaporator; only after this can the steam produced go inside the compressor and achieve the required pressure and temperature characteristics.
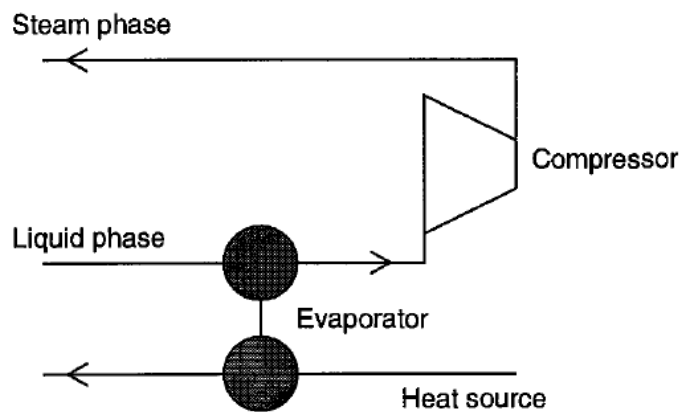
Figure 5: MVR Type II (International Energy Association, 1995)

These HPs have an especially high COP value, even though it depends on difference of temperature between the heat source and the temperature at which heat is released, as shown in the diagram below.
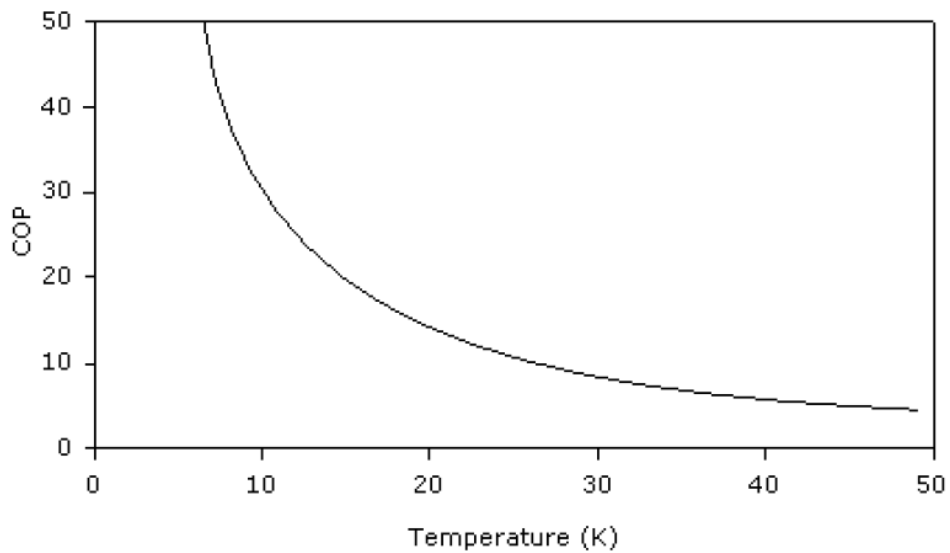
Figure 6: MVR COP vs Temperature Lift (Bohdan Soroka, 2015)

This means that, to achieve high values of COP, it is necessary to have heat exchangers with a large exchange surface, which are more expensive.

3.3 Thermal Vapor Recompression – TVR

IHPs can be made using an ejector and high pressure and temperature steam. Contrary to MVR, which are driven by an electrical or Diesel motor, IHPs work thanks to the heat of the jet of high temperature and pressure steam introduced in the system by the ejectors.

The layout is shown below. [2]
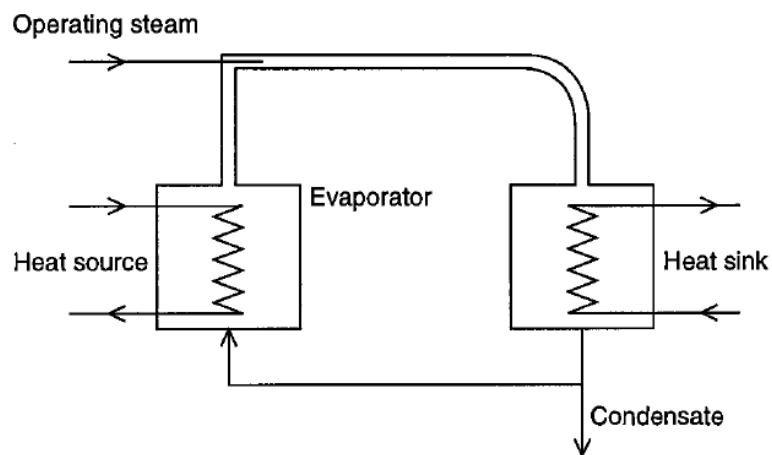
Figure 7: TVR (International Energy Association, 1995)

9

The heat source goes through an evaporator. The steam produced will be blended with the high pressure one and with temperature introduced by the ejector. The resulting steam with an higher energetic level reaches the condenser. Part of the condensation goes back to the evaporator, and part of it comes out of the system to keep the flow to the heat exchangers, and thus the heat exchanged, stable.

This type of TVR system is simple to design, and has the benefit of not containing any moving part. It requires however a constant stream of high pressure and temperature vapour, usually between 7 and 15 bar of pressure. [1]

In this case, the COP is defined as the ratio between the latent heat of the condensation of the vapour coming out of the TVR, and the sum of the inlet heat and the heat provided by the vapour jet.

The following figure shows the trend of the COP depending on the temperature difference between the heat source to recover, and the temperature at which the heat is exchanged.

Figure 8: TVR COP vs Temperature Lift (Bohdan Soroka, 2015)

3.4 Absorption Heat Pump – AHP

Also this kind of HPs are thermal-driven. The heat absorbed from the outside is used to generate as purposed effect a heat carrier with a higher energetic level than that of

the source. The heat is the result of an isothermal chemical reaction which happens inside the absorber.
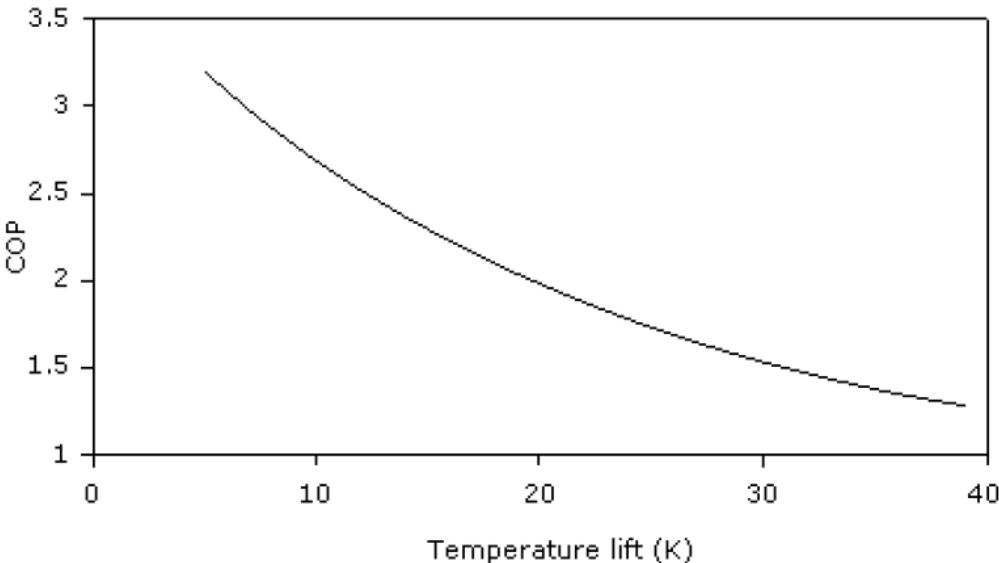
These systems take advantage of how fluids or salts absorb a certain quantity of the working fluid. [2]

In industrial applications the working fluid is a lithium bromide solution in water $LiBr/H_2O$. This system can produce heat at a maximum temperature of 100 $°C$.

In industrial applications, water is used as a working fluid, and $LiBr$ (lithium bromide) as an absorbent. These systems can produce heat at a maximum temperature of 100 $°C$. However, a new mixture specifically designed for high temperature applications, called Alkitrate™, is being developed with the collaboration of the U.S. Department of Energy, and it can reach a condensation temperature of 200 $°C$. [1]

In the next diagram, the working principles of the absorbing and generating system are shown in detail.
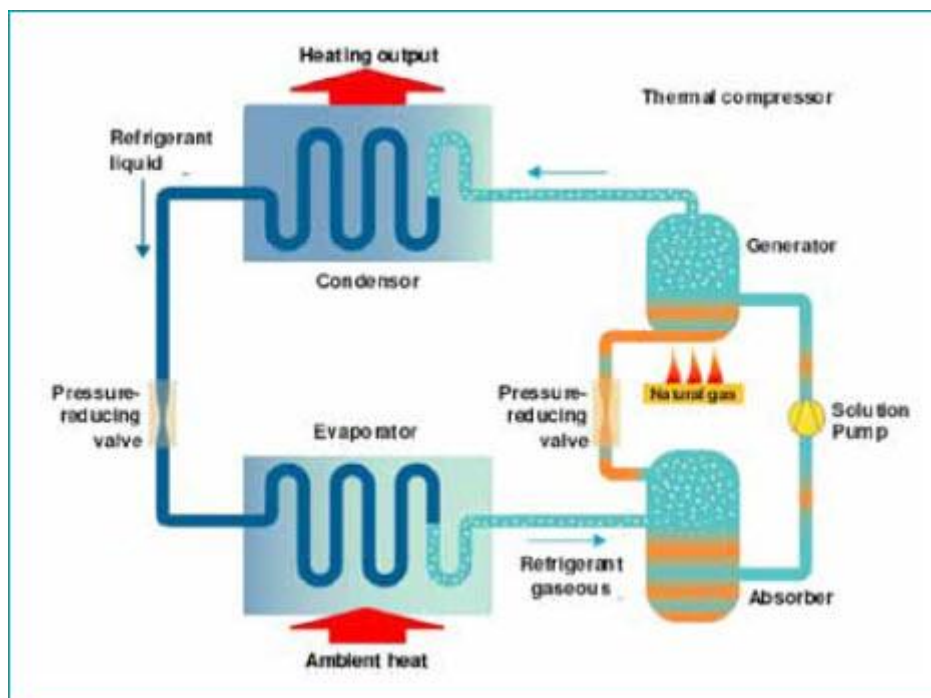

Figure 9: Absorption Heat Pump principles

As shown in the image, the vapour of the working fluid goes through the absorber and it is absorbed by salts; this is a strong exothermic reaction that increases the temperature of the mixture. Nevertheless, the absorber loses its capacity to absorb the working fluid vapour, therefore in order to return to its initial conditions, the

11

mixture is forced into the generator. Once it has reached the generator through the insertion of further heat, the two mixtures separate, and the steam with a higher energetic level than that of the outcoming one, is sent to the condenser where it will release its latent heat.

AHPs can be divided in two types:

- AHP type I;
- AHP type II or heat generator.

The following figure shows the layout of a AHP type I.
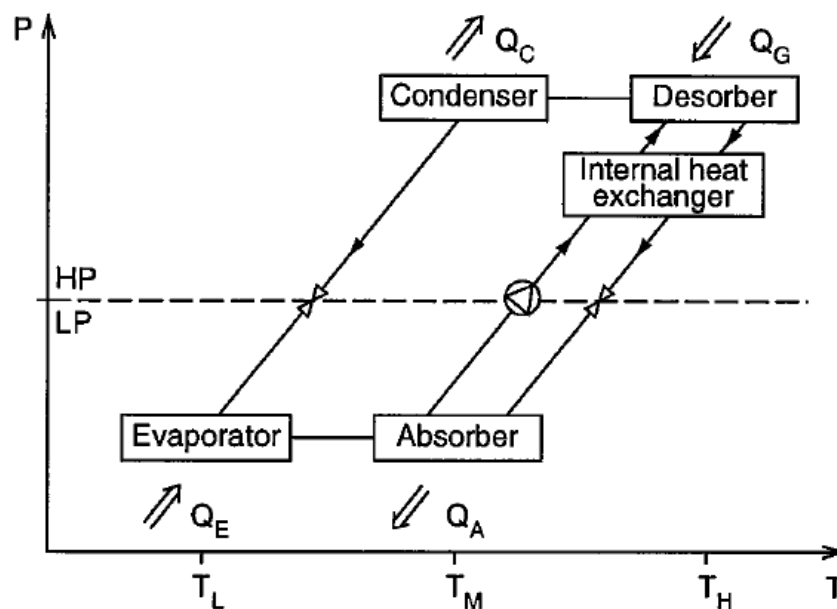
Figure 10: AHP Type I (International Energy Association, 1995)

In this case, the source from which the heat will be recovered is at a low temperature level T_L: thanks to the supply of heat, a heat carrier at medium temperature level T_M. The steam goes from the evaporator to the absorber, which increases its energetic level. The mixture is then pumped into the generator where, with the supply of high temperature heat T_H, the steam is extracted and then sent to the condenser.

AHPs type II, on the other hand, have a medium temperature level T_M source, and thanks to the cycle shown in the figure below they can supply high and low temperature heat at the same time.
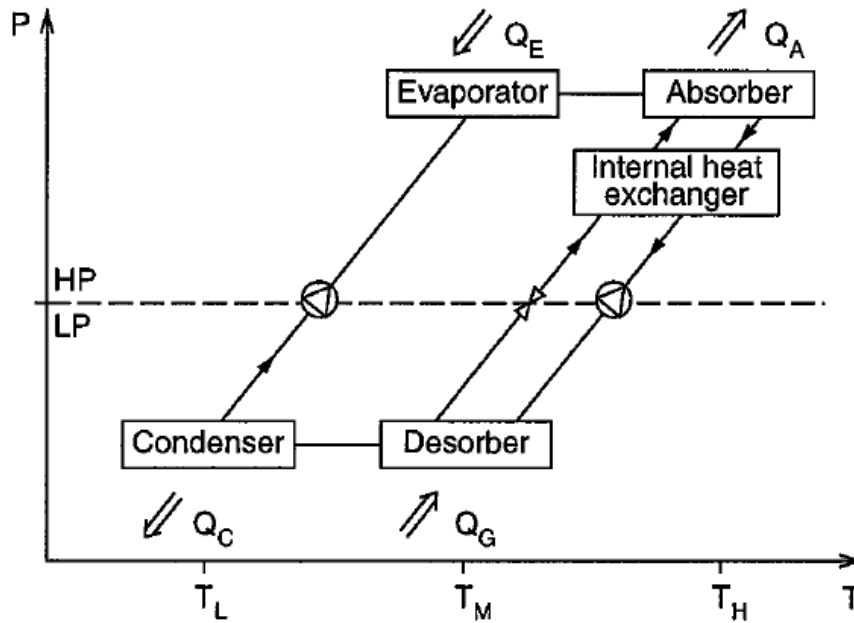
Figure 11: Heat Generator (International Energy Association, 1995)

This system is used for heat recovery in industrial processes where there is an excess of waste heat at a medium level.

The table below shows brief and immediate data on the performances and the operating ranges for each of the IHPs analysed above.

		COP	Max Sink Temperature [°C]	Max Temperature lift [°C]
CCC		3 ÷ 8	120	80
MVR		10 ÷ 30	190	90
TVR		1.2 ÷ 3	150	40
Absorption Type I	LiBr/H$_2$O	1.6 ÷ 1.7	100	50
	Alkitrate		200	
Absorption Type II		1.6 ÷ 1.7	150	60

Table 1: Perfromances Abstract

4. Applications of IHPs

In this section, we will analyze closely the market for IHPs and the applications in which they are well integrated and their potentiality will be listed.

According to current data published by the International Energy Association (IEA, 2015), the industrial sector consumes about 31% of the total primary energy in the OECD countries; the only industry consuming more is the transportation one. [4] This situation is shown in the diagram below.
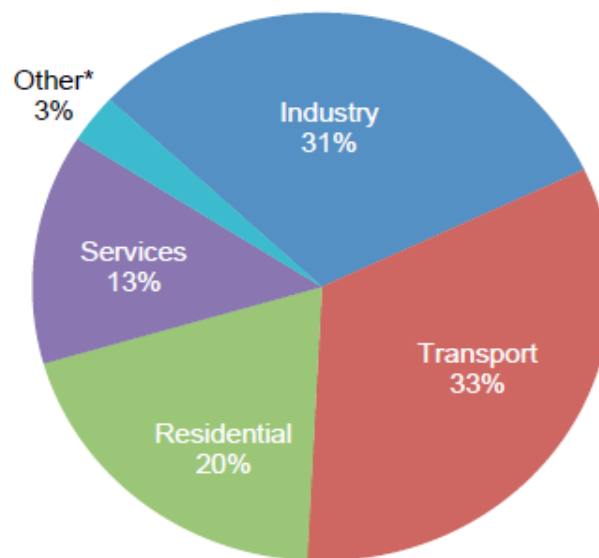
Figure 12: OECD Total Final Energy consumption by sector 2013 (IEA, 2015, p. vii)

Using a benchmarking analysis of the industrial sector, it was possible to evaluate the improvement potential for each sector with the best technology available for that sector.

The results of this analysis reveal that is possible to achieve considerable savings on primary energy consumption and thus on CO_2 production. These savings – according to 2008 data - are synthetically estimated between 18% and 26%. [5]

Below is a complete table of the most important applications of industrial heat pumps. [6]

	Improvement potential (%)		Total Savings Potential (EJ/yr)		Global Subtotal (EJ/yr)
	Industrialized countries	Developing countries	Industrialized countries	Developing countries	
Chemical and petrochemical					
High value chemicals	15–25	25–30	0.4	0.3	2.3
Ammonia, methanol	10–15	15–30	0.1	1.4	
Non-ferrous metals					
Alumina production	30–40	40–55	0.1	0.5	1
Aluminium smelters	5–10	5	0.2	0.2	
Cast non-ferrous and other non-ferrous	35–60				
Ferrous metals					
Iron and steel	10–15	25–35	0.7	5.4	6.1
Cast ferrous	25–40				
Non-metallic minerals					
Cement	20–25	20–30	0.4	1.8	2.8
Lime					
Glass	10–40	20–50	0.4	0.2	
Ceramics					
Pulp and paper	20–30	15–30	1.3	0.3	1.6
Textile					
Food, beverages and tobacco	25–40		0.9	1	1.9
Other sectors	10–15	25–30	2.5	8.7	11.2
Total	10–20	30–35	7.2	20.1	27.3
Total (excl. feedstock)	15–20	30–35			

Source: Saygin et al., 2010.

Figure 13: Enery Efficiency Improvement Potenial in the Manufacturing Industry based on Benchmarking and Indicator Data, 2007 (Rangan Banerjee, 2012)

Industry	Manufacturing activity	Process	Heat pump type
Petroleum refining and petrochemicals	Distillation of petroleum and petrochemical products	Separation of propane/propylene, butane/butylene and ethane/ethylene	Mechanical vapour compression, open cycle
Chemicals	Inorganic salt manufacture including salt, sodium sulphate, sodium carbonate, boric acid	Concentration of waste streams to reduce hydraulic load on waste treatment facilities	Mechanical vapour compression, open cycle
	Treatment of process effluent	Concentration of waste streams to reduce hydraulic load on waste treatment facilities	Mechanical vapour compression, open cycle
	Heat recovery	Compression of low-pressure steam or vapour for use as a heating medium	Mechanical vapour compression, open cycle
	Pharmaceuticals	Process water heating	Mechanical vapour compression, closed cycle
Wood products	Pulp manufacturing	Concentration of black liquor	Mechanical vapour compression, open cycle
	Paper manufacturing	Process water heating	Mechanical compression
	Paper manufacturing	Flash-steam recovery	Thermocompression, open cycle
	Lumber manufacturing	Product drying	
Food and beverage	Manufacturing of alcohol	Concentration of waste liquids	Mechanical vapour compression, open cycle
	Beer brewing	Concentration of waste beer	Mechanical vapour compression, open cycle
	Wet corn milling/corn syrup manufacturing	Concentration of deep water and syrup	Mechanical vapour compression, open cycle, thermocompression, open cycle
	Sugar refining	Concentration of sugar solution	Mechanical vapour compression, open cycle, thermocompression, open cycle
	Dairy products	Concentration of milk and whey	Mechanical vapour compression, open cycle
	Juice manufacturing	Juice concentration	Mechanical vapour compression, open cycle
	General food-product manufacturing	Heating of process and cleaning water	Mechanical vapour compression, closed cycle
	Soft drink manufacturing	Concentration of effluent	Mechanical vapour compression, closed cycle
Utilities	Nuclear power	Concentration of radioactive waste	Mechanical vapour compression, open cycle
		Concentration of cooling tower blowdown	Mechanical vapour compression, open cycle
Miscellaneous	Manufacturing of drinking water	Desalination of sea water	Mechanical vapour compression, open cycle
	Steam-stripping of waste water or process streams	Flash steam recovery	Thermocompression, open cycle
	Electroplating industries	Heating of process solutions	Mechanical vapour compression, closed cycle
		Concentration of effluent	Mechanical vapour compression, open cycle
	Textiles	Process and wash-water heating	Mechanical vapour compression
		Space heating	Mechanical vapour compression
		Concentration of dilute dope stream	Mechanical vapour compression
	General manufacturing	Process and wash-water heating	Mechanical vapour compression
		Space heating	Mechanical vapour compression
	District heating	Large-scale space heating	Mechanical vapour compression
	Solvent recovery	Removal of solvent from air streams	Mechanical vapour compression, open cycle

Figure 14: Overview of HPs applications in manufacturing activities (K.J. Chua, 2010)

The main application of IHPs is in the food industry. In this field, they are usually exploited for the distillation process in the production of alcohol.

However, there are many other applications that apply to different industrial environments. For example, IHPs are used to recover heat that would otherwise be lost, as an evaporator and in drying processes. [3]

5. Refrigerants

This part shows a classification of the working fluids used in IHPs.

Along with thermo-dynamical aspects, which are essential when choosing the right working fluid, another very important characteristic is the evaluation of their impact on the environment.

The following is a list of the major parameters used to evaluate environmental impact caused by refrigerants. [7] The parameters are:

- ODP (Ozone Depletion Potential) – The quantity of layer ozone depletion caused by the refrigerant, compared with the depletion caused by R-11 refrigerant;
- GWP (Global Warming Potential) – The quantity of heat trapped by greenhouse gases, compared to the one trapped from the same quantity of CO_2, which represents the greenhouse gas of reference, due to its GWP of 1. This parameter is evaluated in a period of fifty years; another parameter, called IIR, represents the same effect but over a period of 10 years;
- TEWI (Total Equivalent Warming Impact) – The total amount of greenhouse gases produced by direct and indirect sources with this technology.

Some of the refrigerants used by HPs are going to be presented.

5.1 Synthetic refrigerants

CFC, HCFC and HFC are synthetic refrigerants. [8]

CFCs, or Halocarbons, arise from the substitution of an atom of hydrogen contained in a chain of hydrocarbon, like butane or isobutane, with one of chlorine. They have a high chemical stability, but due to their harmful effects on the environmental, that both causes layer ozone depletion and contributes to the greenhouse effect, their production first, and later their sale and use has been banned.
This category contains the following refrigerants: R-11, R-12, R-13, R-113, R-114, R-115, R-500, R-502, R-13B.

HCFCs, Hydrochlorofluorocarbons, arise from the partial replacement of hydrogen with chlorine and fluorine. Even though they are less dangerous compared to CFCs, the use of these refrigerant fluids has been progressively limited over time until their use in all UE countries was definitely banned in January 2015. This category contains the following refrigerants: R-22, R-401, R-402, R-403, R-408 e R-409.

References on the timing and methods of the reduction of the use of refrigerants previously mentioned were taken from the following EU regulations: EC no. 2037/2000 and EC No. 842/2006.

HFCs, Hydrofluorocarbons, are used as short and long term replacements for HCFCs because they don't contain chlorine, which is dangerous for the ozone, even though they contribute to the greenhouse effect. Nevertheless, it is necessary to pay attention to the use of lubricants, because mineral oils are non-miscible with these refrigerants. It is therefore necessary to polyester oils when re-adapting systems. The refrigerants mostly used to substitute CFCs and HCFCs are R-134a, R-152a, R-32, R-125e R-507.

5.2 Natural refrigerants

A description of natural refrigerants, which have a ODP and GPW value of zero or approximately zero, follows. The most important are: water, air, CO2, ammonia and hydrocarbons. [9]

Water H_2O $(R-718)$

H_2O is neither inflammable nor toxic; this condition, with its thermodynamic properties – such as high critic temperature and high heat capacity – makes it suitable for industrial applications. However, the low volumetric mass of the steam makes the compression at downstream of the evaporator difficult. High compression ratios are needed, which making the compressor more hulking and expensive.

Air $(R-729)$

It is not used in typical thermodynamic cycles, where, the refrigerant evaporates and condenses to achieve the heat transfer. Therefore this fluid is used only for specific applications. Beside it has a low heat transfer ability due to its low latent energy.

Hydrocarbon HC

These working fluids constituted on Hydrocarbon are based on short-chained molecules as butane $(R-600)$ and isobutane $(R-600a)$. They have relevant thermodynamic properties, such as a high critical temperature of $136°C$ and $151°C$ respectlively, that allows to reach high temperatures when releasing heat. Their use is restricted to 150g if installed in a location accessible to the general public because of its flammability. For industrial environments, no quantity restriction is set but severe security measures are needed. For example, the HP needs to be confined inside a machinery room or external building, and the lights used must be suitable for inflammable atmospheres. [10]

Ammonia NH_3 (R-717)

Ammonia is both toxic and flammable. Nevertheless, its thermodynamic characteristics are quite interesting. It has a critical temperature of 132,4°C, allowing to increase the temperature of the heat supplied. Indeed, it is possible to rise the temperature of water from 8°C up to 90°C.

Usually, ammonia is used in mechanical compression systems but applications with thermal-driven systems, particularly in absorption cycles, are being studied. It can be used as the volatile element in liquid form, as a mixture blended with water, or even in the form of salts.

However, it is an aggressive fluid towards lots of materials, so attention must be paid to the seals, and the entire system must be made of steel.

Carbon dioxide CO_2 (R-744)

Carbon dioxide is neither inflammable nor toxic, moreover it does not present any incompatibility with common lubricants and with usually utilised construction materials.

Its use is rapidly increasing, especially with small and medium sized HPs. This is due to the excessive working pressure, exceeding 100 bar, which occurs in large facilities.

5.3 Blends

Blends need to be discussed separately. They are composed by two or more pure fluids, and they are often created for specific processes.

They can be divided into:

Azeotropic – the phase change occurs with stable temperature;

Near-Azeotropic – the phase change is less marked than the zeotropic one;

Zeotropic – evaporation/condensation occurs at more than one temperature value, the difference in temperature is called *glide temperature*.

They are widely used as replacements for HCFC and are made by a mixture of HFC and short-chain hydrocarbon.

The most used ones are: R-407, in system which previously used R-22; R-402 for creating new implants. They have large application in air conditioning systems.

6. Case of study

The developed case of study is a highly efficient heat recovery system for industrial applications using HP technology. This system is to be inserted into the Kyknos transformation implant, located in Savalia, Greece, a factory that uses fresh vegetables to produce all kinds of canned tomato products. This project is part of a broader European project to reduce emissions.

The main energy consuming process of the implant is the generation of steam at 180° C of temperature and 10 bar of pressure, which is used for treating vegetables, peeling and cooking tomatoes, thermic treatments on vegetables, cooking and sterilization of the cookers. Four oil powered boilers currently produce the steam flow.

Another important stream within the implant is the waste water flow, containing tomato particles that shall later be filtrated.

Finally there is the high temperature condense and pressure which are sent to the boilers, which will then produce the steam used by the implant internally.

The table below shows the characteristics of the stream analyzed above.

Stream	Temperature [°C]	Pressure [bar]
Steam	180	10
Waste water	50	1
Condensate	95	10

Table 2: Stream summary

The purpose of this heat recovery system is to absorb heat from the waste water flow, downstream of the filtering, raise its temperature level and release it to the stream of condense going towards the boilers in order to pre-heat it and thus reduce the fuel consumption of the boilers.

To obtain this result, a Mechanical Vapour Compression heat pump (MVC) is used: it will work between the temperatures supplied by the manager of the factory, as shown below.

Stream	Mass flow [ton/h]	Inflow Temperature [°C]	Outflow Temperature [°C]
Waste water	20	50	47
Condensate	16	95	100

Table 3: HP stream characteristic

The study has been conducted taking into account the limits of the temperatures of the thermic sources mentioned above.

The following figure shows the layout of the implant, with all the equipment necessary for its working.
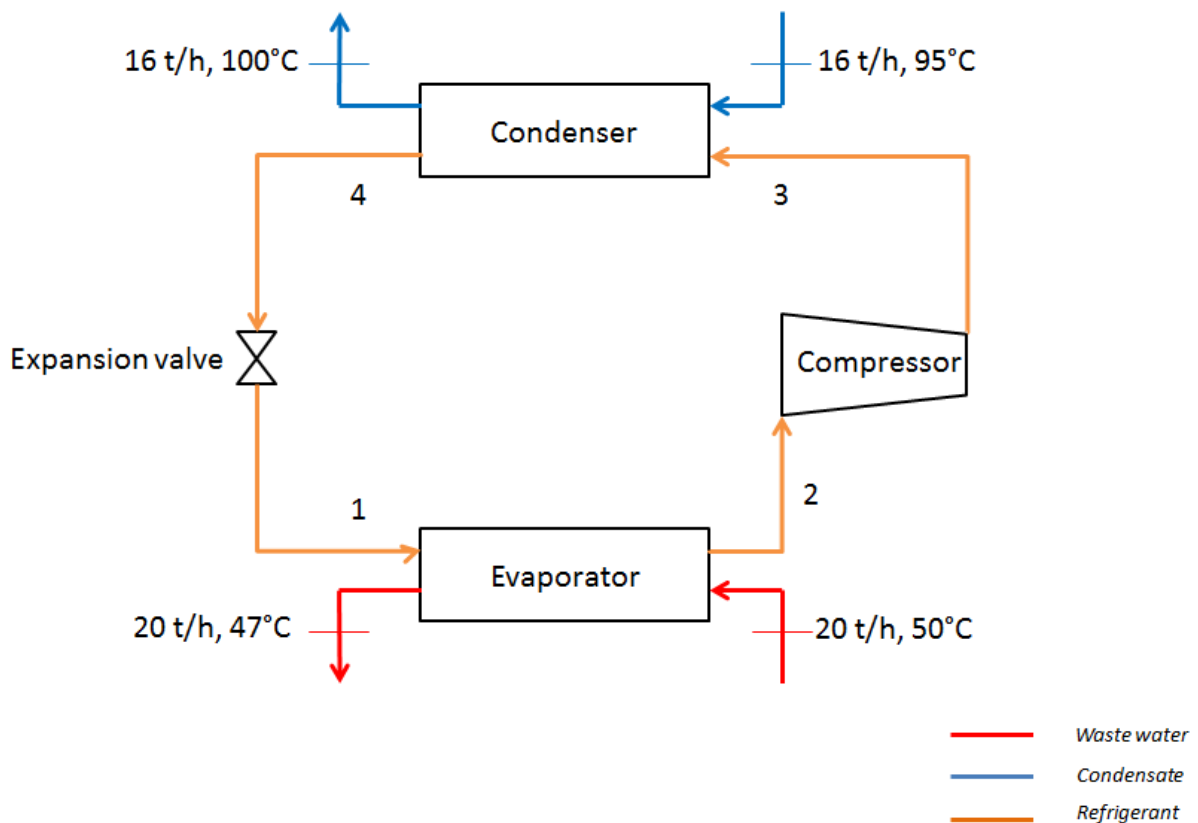

Figure 15: HP layout

As the diagram above shows, there are an evaporator, a compressor, a condenser and an expansion valve. Considering the refrigerant's cycle within the implant, the following conditions will take place in quick succession:

1. low-temperature heat, necessary for the refrigerant evaporation, is exchanged within the evaporator;

2. the steam is sent to the compressor where its energetic level is increased;
3. the steam is sent to the condenser, where it will release heat at high temperature;
4. the condense is dispatched to the expansion valve that brings the fluid back to its initial conditions.

Further considerations can be made about the refrigerant. Because of the nature of this project, only natural fluids were used, since they present a limited danger for the environment. A list of refrigerants particularly appropriate for this process was drawn up from academic literature, with special regards to the constraints on the maximum permissible operating temperatures and their critical pressure.

Below is the list of the refrigerants which will be used in the study reported here:

Ammonia (R-717)

Butane (R-600)

Isobutane (R-600a)

R-245fa

Even though the latter is not a natural refrigerant, it was used in the study to make a comparison with the traditional refrigerants (HFC).

7. Model, ideal case

For the definition of the system and the evaluation of its performances, a simulation model was created with the aid of the Engineering Equation Solver (EES) software.

The main function of the EES is solving of a set of algebraic equations. EES can also solve differential equations, equations with complex variables, and do multi-dimensional optimizations.

The software uses specific libraries that make the performance of mathematical operations easier; lots of thermodynamic properties of many fluids, including the most used refrigerants, are also implemented in the software.

7.1 Hypothesis and boundary conditions

It is to be noted that the almost static case will be considered, thus without analyzing how the system works during its startup and switch off , and generally during transients.

When considering the heat exchange, the supposition was that no heat losses towards the exterior would occur, considering the heat exchangers as adiabatic. The heat exchange along the longitudinal wall was neglected and the phase changings were considered happening at stable pressure and temperature. [11]

First of all, the ideal study of the system was considered, adding further hypothesis later on, which would then be removed during the analysis of the real case.

The losses within the heat exchangers, the isentropic compression, the expansion inside the valve, isenthalpic, were ignored.

After defining the ideal cycle of the heat pump, it was possible to determine the necessary characteristics for the dimensioning and, to choose from a catalogue, the machines needed to build the system.

To generate the model, and thus to determine the cycle of the heat pump, the use of degrees of freedom was needed in order to determine operating temperatures.

The minimum temperature at which the hot fluid and the cold fluid can be near inside an exchanger was defined as the pinch point temperature difference (ΔT_{pp}). This parameter is essential to determine the exchange surface and consequently the cost of the heat exchangers. The difference was set to be ten degrees, for both the evaporator and the condenser.

Two more values were drawn from academic literature: the values of the difference of the superheating temperature of steam (ΔT_{sh}) and the difference of the sub-cooling temperature (ΔT_{sc}). The first one is the temperature difference between the conditions of saturated dry vapour and the conditions when entering the compressor; the second one is the temperature difference between the saturated liquid conditions and the conditions when entering the expansion valve.

The following table lists these values applied to the refrigerants used during this study.

Refrigerant	ΔT_{ppe}	ΔT_{she}	ΔT_{ppc}	ΔT_{scc}
R717	10	5		
R600a	10	15		
R600	10	15	10	3
R245fa	10	15		

Table 4: Temperature restrictions

As the table shows, the difference of the superheating temperature of the evaporator, with the exception of ammonia, is higher than the values reported in the academic literature. This phenomenon is caused by the peculiar shape of the state diagram, which will be shown later in the $p - h$ plane: it needs a high superheating value in order to avoid falling into the upper limiting curve during the final stage of the compression.

In the following parts, hypothesises will be removed, and the losses inside the machines used will be determined.

7.2 Ideal model

In order to determine the cycle of the heat pump, the starting point was the evaporator outlet section. Considering the superheating temperature difference in this point, the minimum temperature at which two fluids inside the first exchanger can be close is recorded. The temperature of the fluid entering the compressor was thus determined.

Since the inlet temperature is known, by removing the difference of superheating temperature the result will be the temperature of the working fluid at the end of the evaporation stage. This point can be determined since the temperature of the fluid and its strength are both known. Using specific functions implemented in the software, it was possible to determine all of the thermo-dynamical properties of the fluid in this state.

Using these functions, if two thermo-dynamical properties of a fluid in the same state are known, it is possible to determine any other of its proprieties, given that the fluid is listed in the database. The following function was used in this particular case. Similar functions were used in other sections of the heat exchanger.

$$P_i = pressure(T = T_i; x = x_i)$$

The pressure when exiting the evaporator is then determined; the pressure drops within the heat exchangers will be ignored, since we are analyzing the ideal case. It is clear that the pressure and temperature when entering the exchanger are known. This is a bivariate area, so the enthalpy of the entering section of the evaporator is not known, but it will be determined later with the analysis of the condenser.

The following chart shows the typical trend of a heat exchange inside the evaporator.

Figure 16: Heat transfer of the evaporator R-717

The following step is the analysis of the second heat exchanger. There is an area where the vapour exiting from the compressor is de-superheated, and another where the condensation of the refrigerant occurs, followed by a sub-cooling process until the desired temperature is reached. Therefore, it is more complicated to identify the section where the minimal temperature approach occurs. To do so, another temperature difference - called approach temperature difference ($\Delta T_{approch}$) – is defined: it represents the difference between the considerable temperature of the inlet fluid and that of the fluid flowing out of one of the ends of the exchangers. In this case, the ingoing fluid will be the condense that will be heated, and the outflowing fluid will be the refrigerant. This means that, if we change this parameter, we can change the extent of the minimum temperature approach between the fluids.

This parameter is set to 10°C.

By doing so, the thermodynamic characteristics of the end of the condensation are defined univocally. The temperature of the fluid to which heat is going to be released is added to the sub-cooling temperature difference and the approach temperature difference. The function is as follows:

$$T_{F_6} = T_{condensate_6} + \Delta T_{sc} + \Delta T_{approch}$$

After determining this temperature value, since it has to be on the lower limiting curve, we can find pressure, enthalpy and entropy using the aforementioned functions.

Consequently, the characteristic of the beginning of condensation can be determined, since temperature and strength are known and that section needs to be on the upper limiting curve.

The point of compression end can be determined, ignoring also the pressure drops this time, for the same reasons explained before. Knowing the pressure inside the condenser, and since the compression is isentropic, the characteristics of the end of the compression are determined univocally.

In the same way, the characteristics of the refrigerant coming out of the heat exchanger are determined.

Once the enthalpy of the refrigerant fluid coming out of the condenser is determined, it is possible to define the starting point of the vapourization inside the first heat exchanger thanks to an isenthalpic expansion inside a valve.

The following is the typical trend of the process inside a condenser.
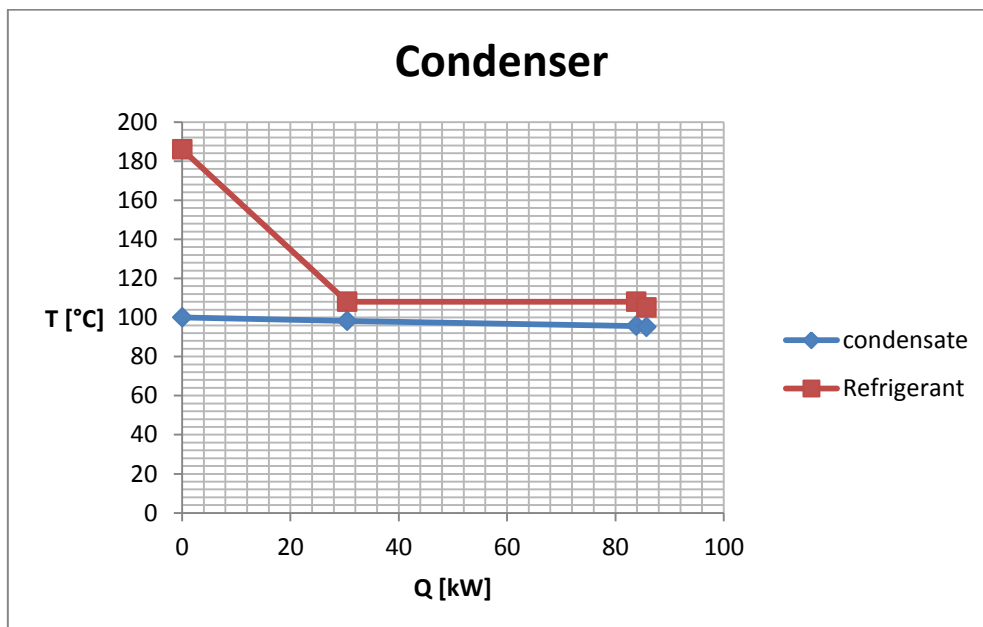
Figure 17: Heat transfer of the condenser R-717

In order to determine ΔT_{pp} inside the condenser and identify the section in which it will be positioned, it is necessary to apply the energy conservation equation to the different sections of the second exchanger, and to verify where the minimum temperature difference between the two fluids occurs.

By fixing the temperatures of the sources, it is possible to determine the ideal cycle of the heat pump.

The following image is the ideal cycle of an HP which uses R – 717 as a refrigerant in the p – h planes. When the same considerations are applied to the other refrigerant fluids, the results are similar graphics that can be found in the appendixes of this writing.
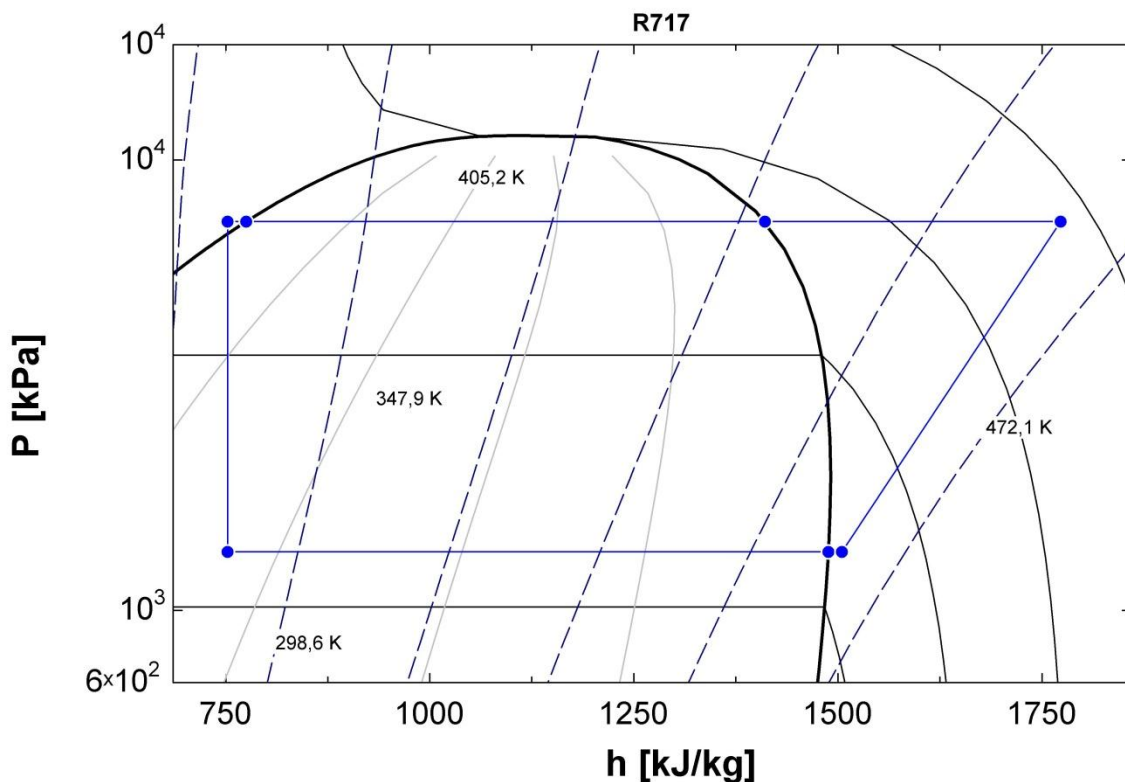
Figure 18:Ideal Cycle for R-717

7.3 Preliminary dimensioning of the machines

Once the cycle of the HP is determined, it is necessary to dimension the other machines. The process focused more on the heat exchangers, while the compressor was chosen from a catalogue.

Naturally, the choice of the refrigerant fluid will have consequences on both the choice of the materials and the frequency of the maintenance.

The following part explains the procedure to determine the necessary parameters to decide or dimension these machines; a set of boundary conditions specific for each machine is taken into account.

7.3.1 Compressor

The information needed for choosing the compressor is: the volumetric flow rate of the fluid transitioning, the maximum exhaust temperature, the pressure reached by the system, and the pressure ratio that the compressor needs.

In order to determine this information, the following equation of energy conservation needs to be applied. The function is applied to the first heat exchanger in the case of the stream from which heat needs to be recovered – which is the stream of waste water.

$$Q_{he_1} = \dot{m}_{waste\ water}(h_{waste\ water_3} - h_{waste\ water_1})$$

Where:

- Q_{he_1} represents the heat released from the low temperature source, which needs to be the same absorbed by the refrigerant;
- $\dot{m}_{waste\ water}$ represents the mass flow of the low temperature source;
- $h_{waste\ water_3}$ is the enthalpy of the fluid when entering the heat exchanger;
- $h_{waste\ water_1}$ is the enthalpy of the fluid when exiting the heat exchanger.

Through this process, we could determine the heat exchanged by the first heat exchanger. Applying the same equation to the refrigerant fluid, while knowing the enthalpies when entering and exiting the machine, the refrigerant mass flow can be determined.

To choose the compressor from a catalogue, we will need to determine the volumetric flow rate.

The last value necessary is the compression pressure ratio, that is defined as the ratio between the maximum and minimum pressure of the cycle.

$$\beta = \frac{P_{max}}{P_{min}}$$

7.3.2 Heat exchangers

First of all, in order to design the heat exchanger, it is necessary to choose the refrigerant fluid that will be used, and the operating pressures and temperature.

Later, we will need to choose the kind of heat exchanger to be used. In this case study, there are two possible scenarios: the first one employs a shell and tube heat exchanger, while the second one uses compact plate-fin exchangers.

In the following part, I will explain how to dimension the heat exchangers. Only the evaporator case will be analyzed, for the sake of simplicity, but the exact same procedure will be used for the condenser too.

7.3.2.1 Shell & Tube heat exchangers

The first step is the thermic sizing of the heat exchanger using the $\varepsilon - NTU$ method, that I will briefly describe.

This method expresses the exchanged heat using the following equation:

$$Q = \varepsilon C_{min}(T_{hi} - T_{Ci})$$

ε is the efficiency of the heat exchanger, which is defined as the ration between the thermic power exchanged in the analyzed conditions, and the maximum thermic power that could be exchanged – such as in the case of infinite exchange surfaces.

$$\varepsilon = \frac{Q}{Q_\infty}$$

Within the ratio, the minimum per hour thermic capacity of the fluids employed in the thermic exchange C_{min} is taken into consideration; it is the result of the mass flow for the specific heat at constant pressure.

For this method to be applicable, the value needs to be constant. For this exact reason, we will perform a separate analysis for each portion of the exchanger where a significant change of the per hour thermic capacity occurs, as in the case of the

31

phase change of the refrigerant. Each portion of the exchanger thus identified will be consequently considered as a separate machine.

Because of this, the analysis of the exchangers inside the model has been split in different parts. For the first exchanger, two areas were identified: the evaporator and the superheater. The second exchanger, on the other hand, has an area where the vapour is de-superheated, an area where the condensation occurs, and another area where the steam is subcooled.

The number of transfert unit NTU is defined as:

$$NTU = \frac{uA}{C_{min}}$$

Where A is the surface through which the heat exchange happens, and u is the global heat exchange coefficient.

Using the considerations drawn from the energy conservation equation, the exchanged thermic power was determined; moreover, since the cycle was defined, the temperatures are known. Therefore, it is possible to calculate the heat exchanger efficiency. [12]

After calculating its efficiency, the following ratio can be used to determine the value of NTU:

$$NTU = \frac{\ln(\frac{1 - \varepsilon C_R}{1 - \varepsilon})}{(1 - C_R)}$$

This equation can be applied only to counterflow shell and tube exchangers with only one tubepass -side, with no phase change occurring. The term C_R represents the ratio between the maximum and minimum thermic capacity of the fluids involved in the heat exchange.

$$C_R = \frac{C_{max}}{C_{min}}$$

The equation is not valid, however, when a phase change occurs, since the fluid affected by this phenomenon will have a per hour thermic capacity that will tend towards infinity, therefore the parameter will have that same value.

In this case, the equation that needs to be used is the following:

$$NTU = -\ln(1 - \varepsilon)$$

The next value to be determined is the exchange surface of the evaporator. To do so, we first need to find the global heat exchange coefficient of this scenario, which is not known to us beforehand.

The following equation designs a method used to determine the global heat exchange coefficient:

$$U = \left(\left(\frac{1}{\alpha_{shell}}\right) + R_{shell} + \left(\frac{d_{internal}}{d_{external}}\right)\left(R_{tube} + \left(\frac{1}{\alpha_{tube}}\right)\right)\right)^{-1}$$

The values R_{tube} and R_{shell} respectively represent the coefficients of tube side and shell side fouling. These status parameters can reduce the global heat exchange coefficient, so as to oversize the exchange surfaces to take into account the fouling of the surfaces, a consequence of the regular use of the machine.

The values used during the simulations with the refrigerant fluids employed for this study have been reported in the following chart.

Fouling factors	
Fluid	Factor * 10^{-4}
R717	1,75
R717 vapour	1,75
R600	1,75 - 3,5
R600 vapour	1,75 - 3,5
R600a	1,75 - 3,5
R600a vapour	1,75 - 3,5
R245fa	3,5
R245fa vapour	3,5
Waste water	1,75
Condensate	0,9 - 1,75

Table 5: Fouling factors (W. M. Rosenhow 1998)

The other two parameters α_{tube} and cα_{shell} are the coefficient of local exchange, respectively for the tube side and shell side. The latter coefficient has been determined for both the exchangers using appropriate values drawn from the

literature. [13] In order to determine the tube side coefficient, the following formulation by Dittus-Boelter [14] was employed:

$$\alpha_{tube} = 0{,}023 \left(\frac{\lambda_{tube}}{d_{internal}}\right) Re_{tube}^{0,8} Pr_{tube}^{(1/3)}$$

The formulation includes the Reynolds number and the Prandlt number of the tube side fluid, raised to the proper coefficients. Moreover, there is the ratio between the conductivity of the tube side fluid and the internal diameter of the tubes used inside the machine.

The formulation can only be applied to the liquid phase; determining the coefficient during the phase change appears to be more complex.

Nevertheless, a specific database inside the software can be used to calculate the average exchange coefficient inside the tubes if phase change should occur.

This function takes into account convective and nucleation-evaporation, according to Saha's reports (1982) [15]. Some information needed to use in this function include: first of all the type of refrigerant fluid used; the quantity of fluid entering and exiting; its saturation temperature. Another important quantity is the mass velocity G, which represents the mass flow for surface unit represented by the passage surface.

$$G = \dot{m}/S_{ortogonal}$$

Another parameter needed to use this function is the thermic power for surface unit, given by the following ratio:

$$q'' = \frac{Q_{he_1}}{\pi d_{internal} L}$$

The L value is the length of the tube sections.

The last information we will use to determine the average tube side exchange coefficient is whether the exchanger is horizontal or vertical, which will modify the constants used by the software to perform the calculations.

Here is how the function was developed in the model.

$$\alpha_{tube} = Flow_{Boiling,\text{avg}}(\text{Fluid}; \text{T}_{\text{sat}}; \text{G}_{\text{tube}}; \text{d}_{\text{internal}}; \text{x}_{\text{in}}; \text{x}_{\text{out}}; q''; Horizontal)$$

A similar function was used when considering condensation. The only further parameter needed was the wall temperature of the tubes during condensation. The following formulation is how the function was reported inside the code.

$$\alpha_{tube} = Cond_{horizontiube,\text{avg}}(\text{Fluid}; \text{T}_{\text{sat}}; \text{T}_{\text{wall}}; \dot{m}; \text{d}_{\text{internal}}; \text{x}_{\text{in}}; \text{x}_{\text{out}})$$

It is now possible to calculate the global heat exchange coefficient for the exchanger or a section of it. The last value we need to determine is the surface needed in order for the heat exchange to occur with the temperatures identified using the equation for the number of transfer unit NTU.

Once the exchange surface is found, all of the heat exchanger geometrical parameters can be defined.

$$A = \pi d_{internal} L n_{tube}$$

The number of tube sections needed to achieve the desired exchange surface is thus determined.

The previous process works inside the evaporation area. In order to determine the exchange surface where the superheating will occur, once the number of tube sections is calculated thanks to the analysis of the evaporation section, the unknown factor will be the length of the tube that will need to be added to the previous value.

Nevertheless, the equation system elaborated cannot be directly solved, since there is the need to insert some freedom degrees, especially geometrical-related, that will allow to determine the exchange surface of the exchanger, which is a key information when calculating its cost.

The following chart shows the values of the quantities used. Some of these values have not been mentioned during the dimensioning process, but they will be later used to determine the pressure drops inside the heat exchanger and thus will be analyzed more in detail in the chapter determining the real model.

Shell & Tube Heat exchanger	
R717	
d_e [m]	0,01905
d_i [m]	0,01483
pass [m]	0,0238
$n_{pass\ tube}$	1
$n_{pass\ shell}$	1
Lenght [m]	4,515
$\alpha_{wastewater}$ [W/m^{2}K]	5678
$\alpha_{condensate}$ [W/m^{2}K]	8517

Table 6:Shell & Tube characteristics

7.3.2.2 Plate & Fin heat exchangers

This type of exchangers has similar relations with regards to its thermal dimensioning.

On the other hand, the process to calculate the heat exchange coefficient is different. In this case, given how difficult it is to determine the exchange coefficient if a phase change is occurring, the choice has been to increase by 30% the exchange coefficient identified for the shell and tube exchanger. The experience has later validated this choice.

Different formulations were necessary to determine the exchange surfaces which are defined in a completely different way for this type of machinery, given the diverse conformation of the exchanger.

The EES software includes a wide database to calculate this kind of heat exchanger; for the purpose of this study, a plate-fin exchanger was chosen. The diagram below shows its characteristics.
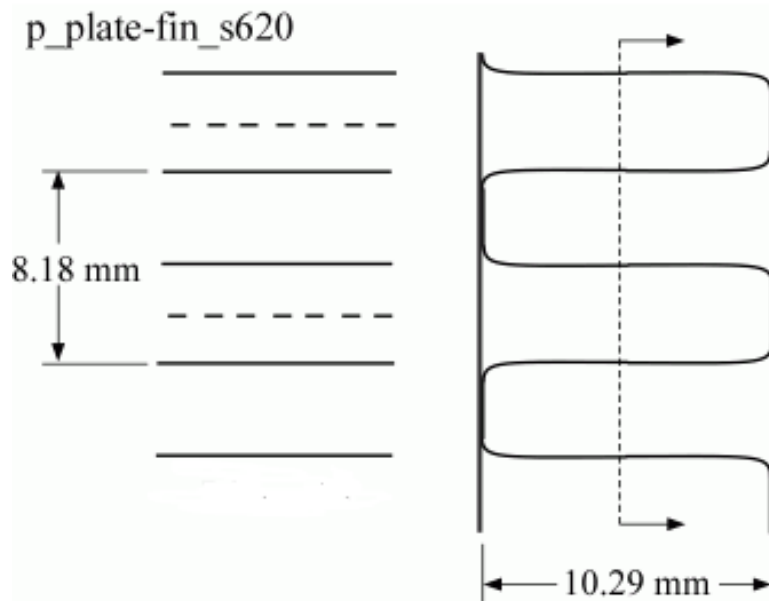
Figure 19: Plate & Fin geometrical characteristics (A. Klein, 2013)

These dimensions apply to both the internal layer where the hot fluid flows, and to the layer where the cold fluid passes.

Naturally, the hot fluid inside the evaporator is the flow of water waste, while the refrigerant represents the cold fluid; inside the condenser, on the other hand, the refrigerant is the hot fluid and the condense is the cold one.

Below is an outline of how this type of heat exchangers is composed; reported are also the reference magnitudes that will be used to determine the exchange surfaces.
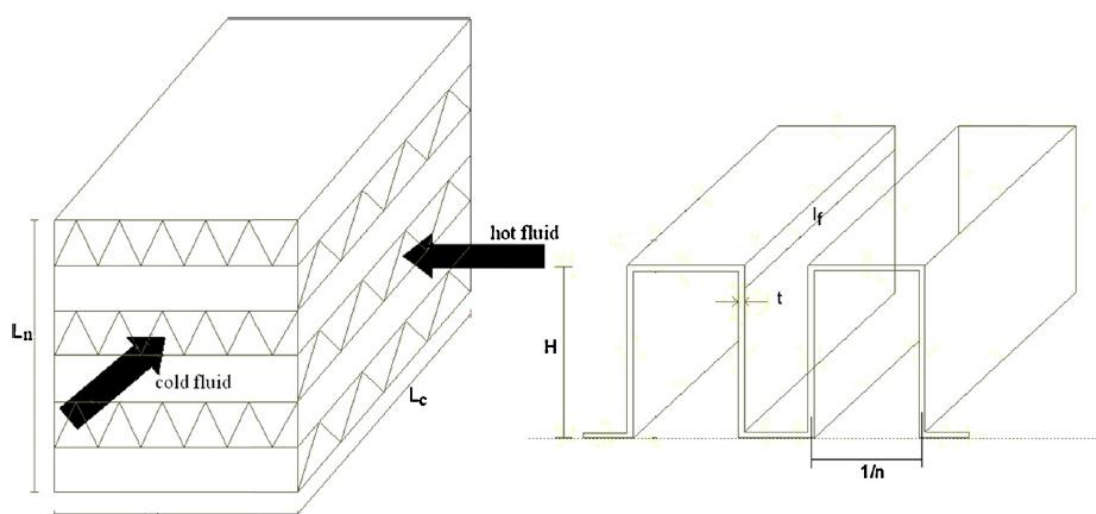
Figure 20: Plate & Fin heat exchanger layout (V. Patel 2014)

At this point, it is necessary to define two surfaces, one touched by the hot fluid and the other one touched by the cold fluid; their sum will determine the total heat exchange surface, on which the cost of the machine will depend, among other factors.

Following are the relations used to determine such surfaces. [16]

$$A_h = L_h L_c N_h [1 + 2n_h(H_h - t_h)]$$

$$A_c = L_c L_h N_c [1 + 2n_c(H_c - t_c)]$$

$$A = A_h + A_c$$

The relations include the number of layers N_h e N_c , the density of the fins n_h e n_c, the thickness of the fins t_h e t_c, and the length of the layer L_h e L_c, respectively for the hot side and the cold side.

For this type of machinery, it is also necessary to determine the passage surface, which does not appear to be immediate, due to the particular arrangement of the corrugated sheets. The following formulations relate to this issue.

$$A_{ff\,h} = (H_h - t_h)(1 - n_h t_h)L_c N_h$$

$$A_{ff\,c} = (H_c - t_c)(1 - n_c t_c)L_h N_c$$

Below is the illustration of a section of the machine, to show the arrangement of the corrugated sheets, so as to understand how complex it is to determine the passage section.
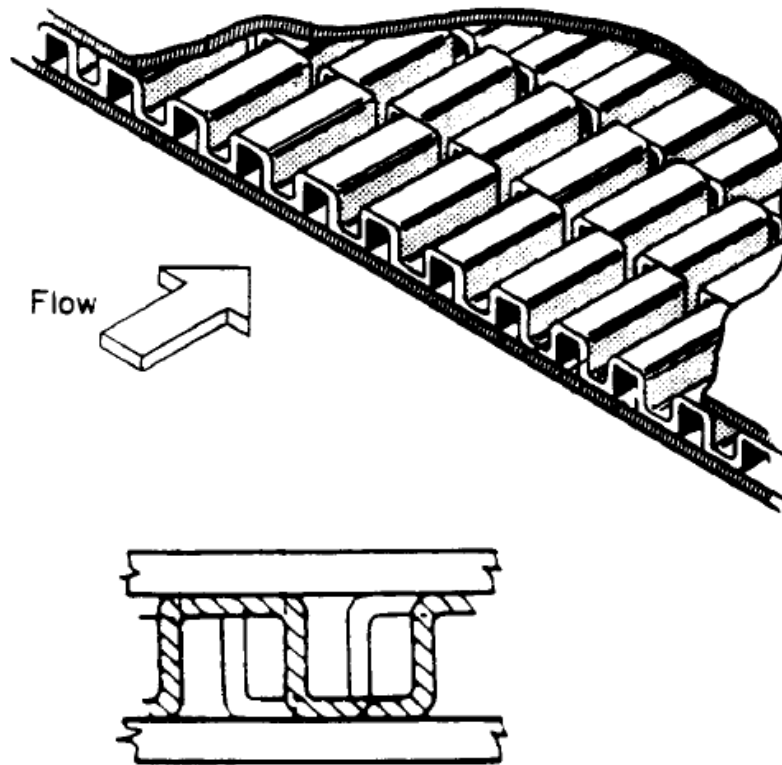
Figure 21: Plate & Fin Heat Exchanger Flow Area (R. M. Manglik, 1994)

7.4 Results of the ideal case and choice of the refrigerant

The previous chapters have shown how to define the ideal cycle while considering the constraints of the study, and the choosing and dimensioning process for the equipment needed to operate the plant.

It is already possible to make some considerations on the performances of the system, even though they come from the ideal conditions. This allows to determine the most performant fluid for the application considered. By doing so, we can reduce the time needed to create the model, and largely reduce the number of simulations.

Presented below are the results from the simulations using the refrigerants mentioned above.

It should be reminded that these results were achieved with the same pinch point temperature difference (10 ° C) inside the evaporator and the condenser, in order to make this comparison.

Refrigerant	ΔT_{ppe}	ΔT_{she}	ΔT_{ppc}	ΔT_{scc}	$\dot{m}$ [kg/s]	p_4 [kPa]	β	T_4 [K]	COP
R717	10	5			0,084	7302	5,405	459	2,807
R600a	10	15			0,4835	2381	5,415	383,4	1,998
R600	10	15	10	3	0,387	1845	7,571	383,3	1,941
R245fa	10	15			0,734	1574	10,65	384	1,967

Table 7: Ideal Cycle Simulation Result

As the chart shows, the highest coefficient of performance appears when the refrigerant *R-717* is used. The cause is the superheating value of the steam before entering the compressor, which turns out to be considerably greater for the other refrigerants because of the peculiar shape of the state diagram.

As a matter of fact, if such value were not imposed, the last stage of the compression would have happened inside the upper limiting curve.

Despite this necessity, a simulation was carried out imposing the same ΔT_sh found in the literature like in the case of R-717. Despite the whole coefficient of performance arose up to the value of 2.2, it appears to be rather lower than the value obtained in the case of ammonia nevertheless.

This situation is shown in the following state diagram for the refrigerant *R-600a* on the *p-h* plane.
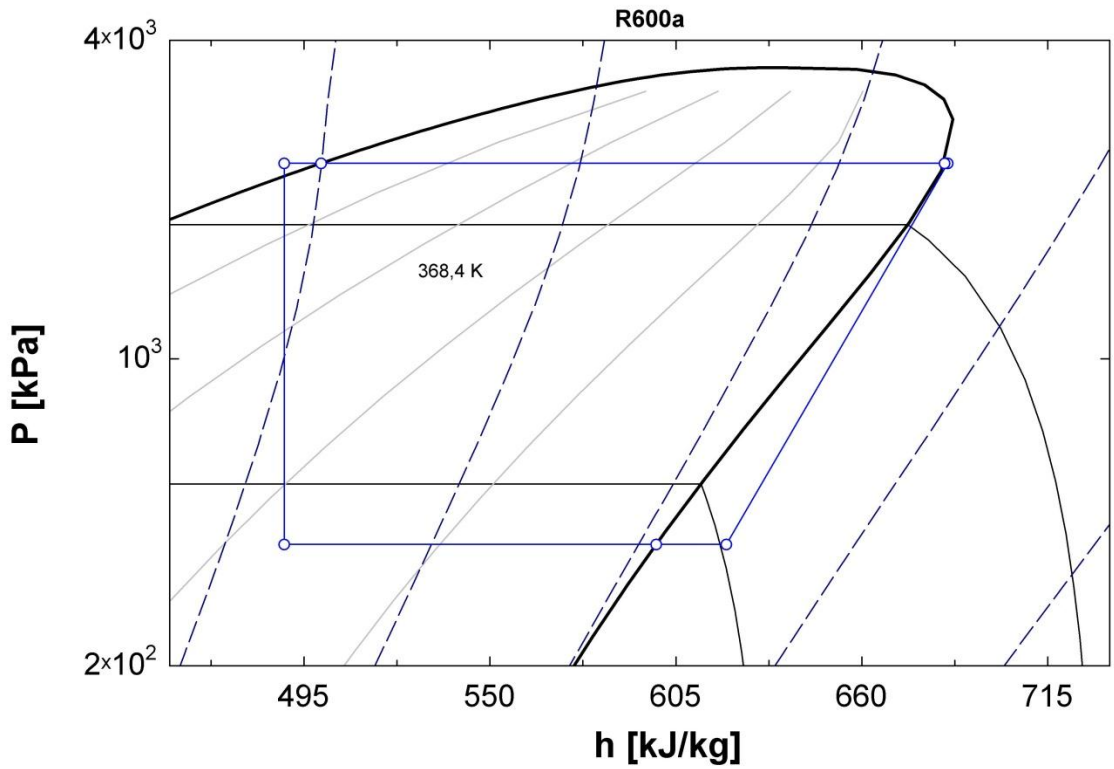
Figure 22: Ideal Cycle R-600a

The diagram shows that the end point of compression has been brought as close as possible to the limiting curve, in order to reduce as much as possible the superheating temperature difference of the evaporator, with the same difference of ΔT_{pp}.

This link between the coefficient of performance and the temperature difference of superheating appear more clearly in the following graph.
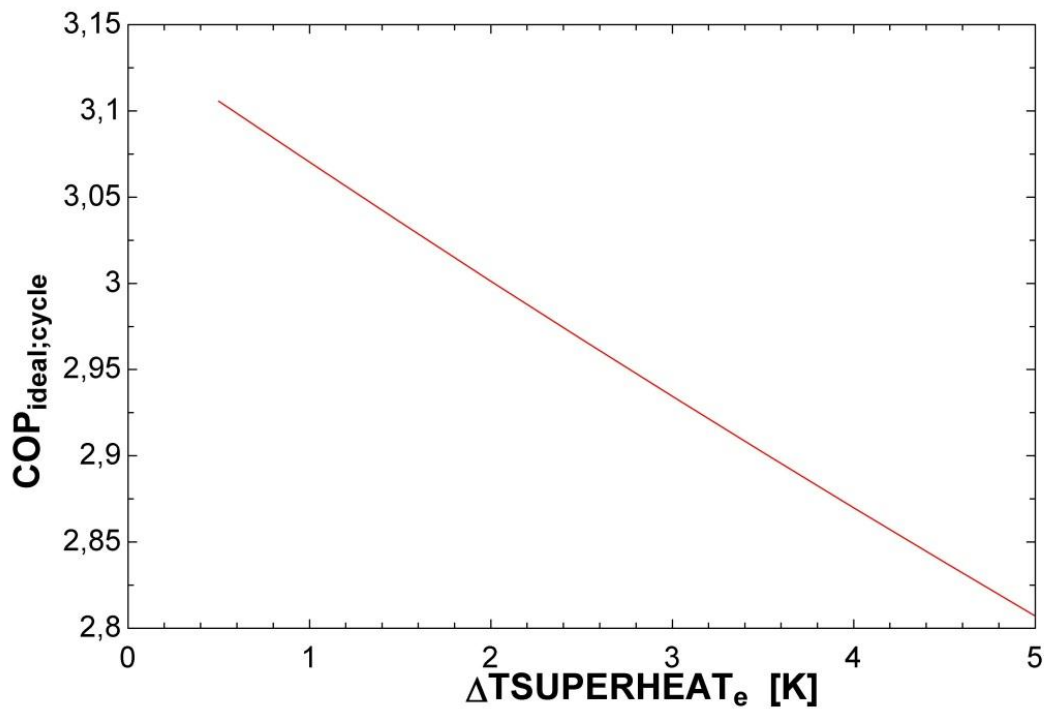
Figure 23: COP Ideal Cycle vs ΔT_{sh_e} for R-717

This graph is the result of a cycle where ammonia was used as a refrigerant, but the trend in the case of other refrigerants used is clearly identical.

A decisive factor on which the value of the coefficient of performance depends, is the minimum temperature value at which the two flows in the evaporator can be combined. This value establishes the temperature of the refrigerant fluid downstream of the heat resulting from the recovery of heat, which would have otherwise been thrown outside. Since the temperature that needs to be reached inside the condenser is already fixed, the higher is the temperature reached by the coolant by refrigerant during the heat recovery, the less work will need to be supplied by the compressor in order to achieve the desired characteristics in the condenser.
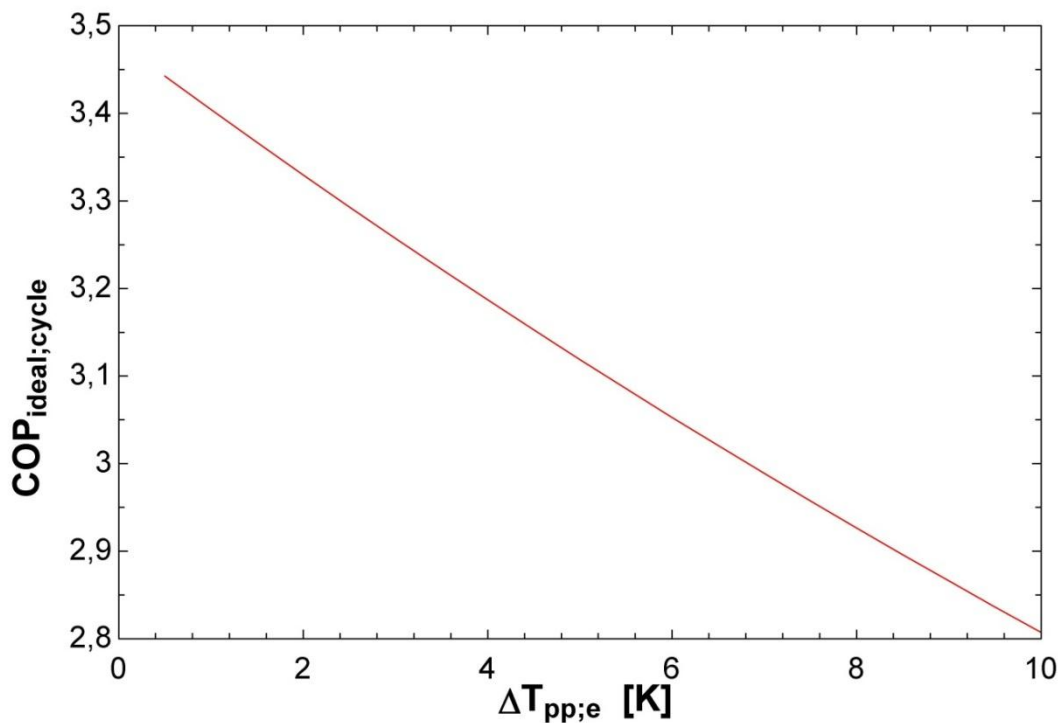
Figure 24: COP Ideal Cycle vs ΔT_{pp_e} for R-717

The previous graph shows exactly the trend described above. The coefficient of performance decreases with the increasing of the ΔT_{pp}.

The operating conditions of the system require other consideration. The operating temperatures, in the case of butane, isobutane and *R-245fa*, are all very similar, with an average of 110 ° C; on the other hand, when using ammonia, the temperature reached at the compressor outlet is significantly higher, around 185 ° C . One must of course take into consideration that, in the real case, the temperature of the end compression will be greater, because of its pressure drops.

The same thing happens when looking at the operating pressures. In the case of isobutane the compressor output pressure will be of about 23 bar, while in the case of ammonia, it will be three times higher, amounting to 73 bar.

Indeed, these heavy operating conditions, difficult to overcome, limit the use of the R-717 refrigerant in the case of similar temperatures.

Despite these difficulties, the coefficient of performance cannot be compared to the other fluids; for this reason, the R-717 was the refrigerant of choice in the following study.

8 Real case – methodology

In order to determine the characteristics of the equipment, the ideal cycle needed to be defined; the definition of the real cycle, on the other hand, needed the determination of the actual characteristics of the implant components.

8.1 Compressor

Once the temperature of the refrigerant entering the compressor is known, it is necessary to determine the temperature at the end of the compression. Knowing the compression end pressure, a result drawn from the analysis of the ideal cycle, will allow to univocally define such point on the plane *p-h*. This is because, despite the ideal case conditions, the compression is not isentropic anymore, consequently pressure drops will occur, which will generate entropy and thus result in a further increase of the temperature of the cooling fluid after going through the compression.

The pressure at the beginning of the compression is already known in the light of the considerations that will be made further on in the study; thus, the next step is to calculate the actual pressure ratio of compression, using the same formulation shown in the previous chapters.

Once this is done and the compressor is chosen from catalog as shown above, the determination of the isentropic efficiency of the compressor is carried out: this can be easily achieved from the nameplate information of the component.

We then proceed to calculate the enthalpy of the end compression using the following formulation.

$$h_{F_{real4}} = h_{F_{real3}} + \frac{(h_{F_4} - h_{F_{real3}})}{\eta_{compressor}}$$

After calculating this value and knowing the pressure of the compression end, the point is determined univocally; the appropriate functions within the software mentioned previously can now determine the remaining thermodynamic properties of the refrigerant. Below is how the function used for the determination of the temperature was reported within the code; it represents the maximum temperature reached inside the cycle.

$$T_{f_{real4}} = Temperature(h = h_{f_{real4}}; P = P_{F_{real4}})$$

8.2 Heat exchangers

In this paragraph, the correlations used for the determination of pressure drops inside the heat exchangers will be presented, along with the procedure for the determination of the operating real cycle of the heat pump.

For the calculation of the real cycle, the starting point was the input section of the first heat exchanger.

Firstly, the pressure and temperature of the entering point to the evaporator were fixed. The methodology here described determined the conditions occurring when leaving the exchanger.

The correlations reported in the following paragraphs were used to calculate the pressure drops within the tubes, with the average thermodynamic properties of the fluid in the evaporator inlet sections and in the section at the end of the evaporation process referring to the ideal case. After determining the pressure drops of the given section, the new pressure at the end of the evaporation process in the heat exchanger was determined; knowing its title allows to determine, using the functions implemented within the software, the new outlet temperature of that section of the tube bundle.

At this point, pressure drops were calculated again using the average properties and updating them with the new pressures and temperatures found. A new value for the pressure drops is thus determined; lastly, the new pressure and temperature of the end of evaporation section are calculated.

This process is iterative; it repeats itself until the conditions previously chosen occur.

An error δ is defined: it identifies the difference between the pressure found in the previous case, and the pressure found in the following case. If the value is less than $10^{-3}\ Pa$, the process stops, because the real pressure at the end of the analyzed portion of the exchanger has been found.

A clearer definition of the error is shown below.

$$\delta_i = P_{i-1} - P_i$$

The procedure must be repeated for each portion taken into consideration during the dimensioning of the heat exchanger.

The process for the second heat exchanger is similar; the only difference is that the thermodynamic characteristics at the end of the compression are known.

The same procedure was used to determine the real cycle with the aid of the compact plate-fin heat exchangers.

The formulas below were used for the calculation of the pressure drops inside the exchangers; the analysis of shell and tube exchangers will come first, followed by that of plate-fin exchangers.

8.2.1 Shell and tube exchangers

When talking about shell and tube exchangers, it is important to separate what happens on the tube side and what happens on the shell side. [18]

The formulation used in this case is the following:

$$\Delta P_{shell} = \frac{\rho_{shell} v_{shell}^2}{2} f_{shell} n_{pass_{shell}} \left(\frac{L}{b}\right) \left(\frac{D_{internal_{shell}}}{D_{eq}}\right)$$

This equation appears to be valid if the Reynolds number values on the shell side are less than 40000.

There are various geometric factors inside the formulation: the diameter of the shell enclosing the equipment, the equivalent diameter - defined as the ratio between the pass surface of the tube and the perimeter of the same -, the distance between the baffles, the number of shell side passes, the friction factor - representative coefficient of the frictional losses caused by the passage of the fluid inside the shell - which depends on the conditions of the flow.

With the exception of the number of passes on the shell side, which is a distinct constructive parameter and was set to one in this case, the other parameters have very precise formulations.

Below are the formulas that determine the geometric parameters described above.

$$b = 0{,}3 D_{internal_{shell}}$$

$$D_{internal_{shell}} = \sqrt{\left(\tfrac{4}{\pi}\right) n_{tube} p^2 \Big/ CPT}$$

Where *p* is the tube pass and *CPT* is the space between the tube bundle and the exterior shell. These values too were previously set: they were reported inside a table where all the other constructive parameters of the equipment were united; the table in question can be found in the previous chapters.

$$D_{eq} = \frac{4\left(p^2 - \left(\tfrac{\pi}{4}\right) d_{external}^2\right)}{\pi d_{external}}$$

This geometric factor will have a different formulation according to the kind of mesh chosen for the tubes. The formulation above applies to a squared mesh.

The following part will analyze the parameters that depend on the thermodynamic state of the fluid.

The shell-side velocity of the fluid is defined as follows.

$$v_{shell} = \frac{\dot{m}_{shell}}{\rho_{shell} S_{f_{shell}}}$$

$$S_{f_{shell}} = \frac{\pi (D_{internal_{shell}}^2 - d_{external}^2)}{4}$$

The latter is the formulation for the fictitious passage surface of the fluid through the shell.

The last parameter is the friction factor, defined as follows.

$$f_{shell} = 2 \times 0{,}72 Re_{shell}^{-0{,}15}$$

The formulation above is to be considered valid in the case of a fully developed turbulent flow; in case of laminar flow, the coefficient would depend linearly on the Reynolds number.

Naturally, within the shell-side Reynolds number, the reference characteristic length appears to be the equivalent diameter, of which the formulation was previously shown.

The flow inside the tubes will now be defined using relations similar to the previous case. The formulation below determines the pressure drops.

$$\Delta P_{tube} = \frac{\rho_{tube} v_{tube}^2}{2} (f_{tube} + 4) n_{pass_{tube}} \left(\frac{L}{d_{internal}}\right)$$

The formulations presents a constant, which is summed to the tube side friction factor, since it also takes into account the tube bundles inlet and outlet losses.

Other geometric quantities are included, such as the number of tube side passes, which in this case has a value equal to one, the inner diameter of these passes, and the length of the tubes.

In this case too, it is necessary to make explicit the terms that depend on the thermodynamics conditions of the fluid.

Here below are the relations which allow to determine the friction factor and the flow velocity.

$$f_{tube} = \sqrt{(1{,}82 \times \log_{10} Re_{tube}) - 1{,}64}$$

$$v_{tube} = \frac{\dot{m}_{tube}}{\rho_{tube} \left(\frac{\pi}{4}\right) d_{internal}^2 \left(\frac{n_{pass_{tube}}}{n_{pass_{shell}}}\right)}$$

The tube side velocity is correlated to the ratio between the number of tube side passes and shell side passes. This aspect was given particular importance since it shows how, for an equal mass flow rate, the constructive peculiarities of the equipment can have an enormous influence on the characteristics of the fluid.

When considering shell and tube exchangers, these relations can determine the pressure drops within the machines.

It should be noted that losses greater than 0.5 bar pressure are avoided as much as possible in practice; this is because this pressure drop is related to a variation of the saturation temperature of the fluid that is used in the exchanger. Exactly because of

the ultimate purpose of this equipment, a reduction in saturation temperature greater than 2 °C is to be avoided. Naturally, this good design rule was respected.

8.2.2 Plate and fin heat exchangers

The following relations are used to calculate the pressure drops of this kind of exchangers. [16]

$$\Delta P_h = \frac{2 f_h L_h G_h^2}{\rho_h D_{h_h}}$$

$$\Delta P_c = \frac{2 f_c L_c G_c^2}{\rho_c D_{h_c}}$$

The subscript h refers to the hot fluid, and the subscript c refers to the cold fluid.

These formulas include some geometric parameters previously introduced: the friction factor, the mass velocity and the hydraulic diameter.

These parameters will now be defined starting from the mass velocity: the following formulation is to be considered valid for both the hot fluid and the cold fluid, with the only condition of making the appropriate substitutions.

$$G = \frac{\dot{m}}{A_{ff}}$$

The other parameters need the introduction of geometric coefficients.

$$\alpha = \frac{f_s}{H - t}$$

$$\delta = \frac{t}{l_f}$$

$$\gamma = \frac{t}{f_s}$$

$$f_s = \left(\frac{1}{n} - t\right)$$

In this case too, the definition of the coefficients resorts to the same formulation for both the fluids. It is now possible to determine the hydraulic diameter for the exchanger used.

$$D_h = \frac{4 f_s l_f (H - t)}{2\big(f_s l_f + (H - t)l_f + (H - t)t\big) + t f_s}$$

The friction factor is the last parameter to be evaluated. For this type of heat exchangers a correlation, validated by experimental data, was discovered: it allows to evaluate f regardless of the flow regime; this is extremely important in case of off-design, although this specific treatment was not analyzed in this study. [17]

$$f = 9{,}6243 Re^{-0{,}7422} \alpha^{-0{,}1856} \delta^{0{,}3053} \gamma^{-0{,}2659} (1 + 7{,}669 \times 10^{-8} Re^{4{,}429} \alpha^{0{,}920} \delta^{3{,}767} \gamma^{0{,}236})^{0{,}1}$$

8.3 Real case result

The trends described in the ideal case do not need further consideration, since they remain unaltered.

Nevertheless a variation of the coefficient of performance will occur, caused by a combination of effects.

The first one is related to difference between the outlet pressure from the heat exchanger and its input pressure; the latter will be lower, thus varying the enthalpy exiting from the machine. This means that the value of the numerator in the formula of the COP will change; the modification is not very relevant if the standard rules on pressure drops are applied.

The second effect is caused by the pressure drops within the compressor, which will further rise its outlet temperature. This means that the enthalpy of the fluid entering the capacitor will be greater than the one calculated in the ideal case. This will determine the increase of the denominator in the formulation of the COP.

The coefficient of performance in the real case will therefore be smaller, with respect to the one of the ideal case.

The graphic below shows the ideal cycle and the real one at the same time, in case of the pinch point temperature difference of the evaporator being equal to 10 ° C. They are nearly completely superimposed inside the heat exchangers; their differences will be more marked when the compressor analysis will be carried out.

Naturally, within the computing environment, where it is possible to shift with high precision inside the refrigerant state diagrams, the pressure drop of the heat exchangers can be appreciated more easily; as mentioned earlier, this drop appears to be limited.
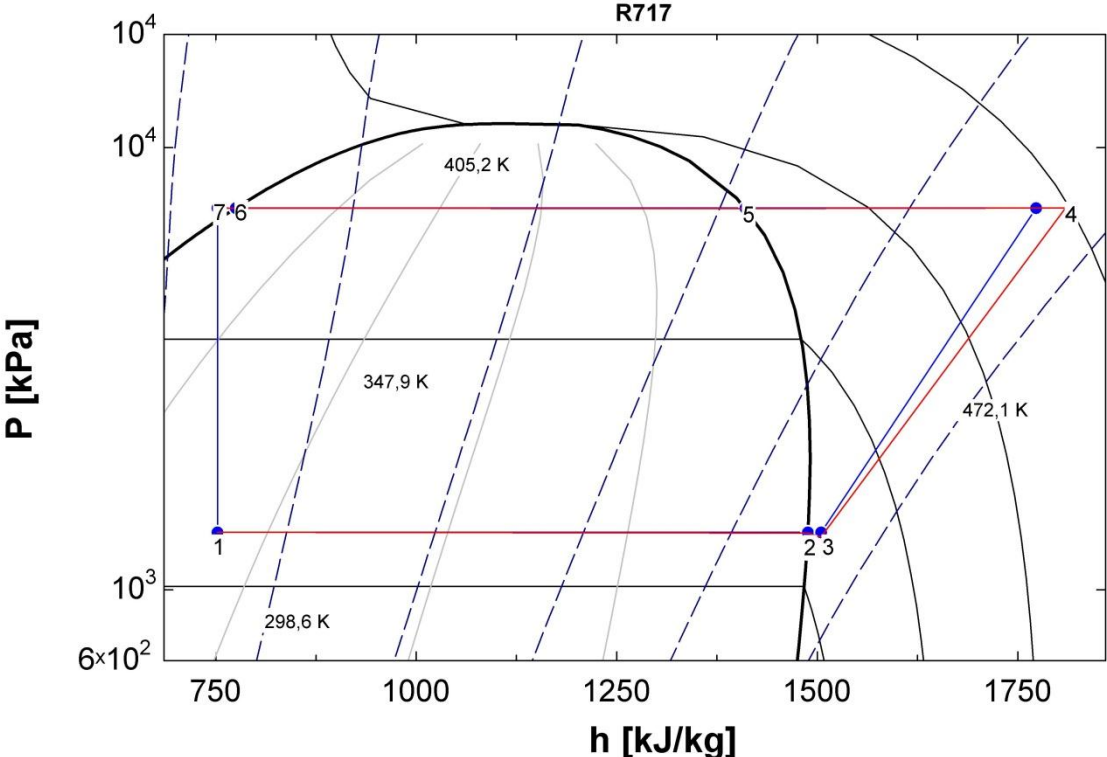
Figure 25: Real Cycle R-717

The following summary tables include the geometric quantities of the two different types of heat exchangers, and the cycle performances with these configurations.

It should be noted that the difference of the coefficient of performance with an equal ΔT_{pp} among the presented solutions does not appear to be significant. For this reason, only one value for the COP_{real} is shown.

Refrigerant	ΔT_{ppe}	ΔT_{she}	ΔT_{ppc}	ΔT_{scc}	$\dot{m}$ [kg/s]	β	p_4 [kPa]	T_4 [K]	T4 real [K]	COP ideal	COP real
R717	10	5	10	3	0,084	5,405	7302	459	470	2,807	2,469

Table 8: Real Cycle Simulation Result

	R717	n_{tube}	d_e [mm]	d_i [mm]	pass [mm]	$n_{pass\ tube}$	$n_{pass\ shell}$	$D_{i\ shell}$ [mm]	Pitch	CPT	Total lenght [m]	Total surface [m²]
S&T	Heat exchanger 1	10	19,05	14,83	23,8	1	1	91,57	square	0,85	4,515	2,67
	Heat exchanger 2	10	19,05	14,83	23,8	1	1	92,85	square	0,85	4,968	3,02
												5,69

Table 9: Real Cycle S&T heat exchangers characteristics $\Delta T_{pp_e} = 10°\ C$

		H [mm]	t [mm]	L_{hot} [mm]	L_{cold} [mm]	l_f [mm]	n [mm⁻¹]	S_{layer} surface [m²]	Total surface [m²]
PFHE	Heat exchanger 1	10,3	0,1	200	1000	10	0,2041	1,033	2,065
	Heat exchanger 2			1100	200			1,136	2,272
									4,337

Table 10: Real Cycle Plate&Fin heat exchangers characteristics $\Delta T_{pp_e} = 10°\ C$

9 Economic analysis

The previous chapters addressed all the aspects relevant to the design of the system. In particular, the ideal cycle of the heat pump was determined, the machinery was preliminarily dimensioned, and an assessment determined the most performant fluid for this specific application. Pressure drops were introduced, and the real cycle and is performances for the refrigerant identified with the ideal cycle analysis were determined.

The entire modeling was carried out with a well determined value of the ΔT_{pp} of the evaporator which was assumed as given. It is now necessary to determine the structural setting of the system with the best performance. For this purpose the following economic analysis was conducted; its function is the minimization of the costs that need to be met to change as suggested the existing plant.

The results of the analysis will make a comparison possible, in order to see whether this change is economically viable. The costs for the construction of this implant modification and other operating costs will then be compared with the estimated expenses needed to achieve the same purposed effect using fuel oil in an evaporator.

In order to do so, the parameter ΔT_{pp_e} was changed; the exchange surface of the evaporator, and the amount of heat recovered on which the coefficient of performance depends, are governed by this parameter. This will also determine a variation of the operating costs of the compressor: as the COP increases, the purchase cost of the electrical work required to drive the compressor is reduced.

The estimate cost of the plant has an error margin of ± 25%.

Assuming that the system would work 8,000 hours a year for 20 years, the cost of the electrical work supplied by the network was considered to be 0.12 € / kWh.[19]

The cost items that need to be taken into account when determining the cost of the economic enterprise will be now listed.

Firstly, there are the costs of the system:

• Cost of purchase of the compressor;

• Cost of purchase of the two heat exchangers.

The following are the operating costs:

• Purchase of electrical work to power the compressor;

• Special and ordinary maintenance of the compressor.

The manufacturing firm of the compressor, Mykom, provided the purchase price for its alternative volumetric compress HS series.

The determination of the cost of the heat exchangers in the case of shell and tube exchangers exploited a series of cost correlations whose validity scope was extended in order to determine the cost of these machines also in the case of limited exchange surfaces.

The correlation used is the Hall correlation; nevertheless, this formulation has a validity range function of the diameter of the shell which cannot be smaller than 60 $inch^2$. [20]

The correlation is the following:

$$C_{heat\ exchanger\$} = 8500 + 409A^{0,85}$$

This value represents the cost of the machine installed during the year referenced in the correlation whose result was the cost of the equipment, 2003.

To determine the current cost of the equipment, it will be necessary to multiply this cost for the ratio between the cost indexes of the reference year and the indexes of the current one, as shown in the following formulation. [21]

$$C_{real,heat\ exchanger\$} = C_{heat\ exchanger\$}\left(\frac{I_{equipment\ cost\ index\ 2003}}{I_{equipment\ cost\ index\ 2015}}\right)$$

The cost is expressed in dollars: it will have to be converted in euros. To change the currency, the amount has to be multiplied by the following factor $0,81553\frac{€}{USD}$. [19]

A similar situation arises in the case of compact plate-fin heat exchangers, where the cost of the heat exchanger needs to be determined, then referred to the current cost index and later converted from USD to €.

The relation used to calculate the cost of the compact heat exchangers is the following.

$$C_{heat\ exchanger\$} = 231A^{0,639}$$

The following formula too has its separate range of validity; as a matter of fact, the exchange surface must be between the following values: $4,65\ m^2 < A < 836\ m^2$.

Now, the calculation of the operating costs is analyzed. The costs for the handling of the compressor are defined by the following relation.

$$C_{operating\ compressor\$} = \left(\frac{h_{F\,4real} - h_{F\,3real}}{\eta_{compressor}}\right) \dot{m}_F N_{working\ hours} C_{electricity}$$

This relation represents the yearly cost of the purchase of electric work expressed in dollars; to have the price in euros, it is necessary to multiply the entire factor above by the conversion factor mentioned above.

What must be determined is the discounted cost of the total expenditure due to the purchase of electrical work to power the compressor during the entire lifetime of the system. This was the formula used to determine the compound actualised rate, with an interest rate of $i = 0.1$.

$$C_{operating\ compressor,ctualyzed} = \sum_{k}^{N_{year}} \frac{C_{operating\ compressor€}}{(1+i)^k}$$

Other operating costs are represented by the maintenance costs of the compressor.

They were calculated as a percentage of the purchase cost of the component, ranging from 2 to 10%. [22] In the specific case, given the size of the component, the maintenance cost was set to 10% of the basic cost of the compressor.

This cost too will apply to the whole period of life of the plant; it must therefore be actualised with the formulation previously reported.

It is now possible to calculate the total cost of the project.

$$C_{tot} = C_{he1_{\euro}} + C_{he2_{\euro}} + C_{operating\ compressor,actualyzed} + C_{mantenience\ compressor,actualyzed}$$

Once the overall costs are determined, the next stage is the minimization of these costs using the ΔT_{pp_e} . This factor is changed from the value taken as a reference when choosing the refrigerant, until it reaches values lower than the Celsius degree. As a result, since the exchange surfaces are not extremely sizeable, the heat exchanger will also turn out to be not very expensive; it will thus affect less the total cost, compared to the benefits obtained from the reduction of the operating costs of the heat exchanger. Naturally, if the cancellation of the ΔT_{pp_e} is imminent, the cost of the exchange surfaces will diverge.

For this reason, the ΔT_{pp_e} value was set at 3 ° C for technological reasons.

The last calculation is to determine the cost that should have been borne in order to buy fuel oil, had this recovery system had not been introduced.

This cost equals the thermal power that is exchanged, multiplied by the number of operating hours per year and the cost per heating kWh produced by the fuel oil. This value comes to € 0.0834 / kWh.

$$C_{oil} = Q_{he_2} N_{working\ hours} C_{kWh\ from\ oil}$$

It will then have to be actualised, like in the previous cases.

The following tables show the costs of the chosen solution.

		H [mm]	t [mm]	L_{hot} [mm]	L_{cold} [mm]	l_f [mm]	n [mm^{-1}]	S_{layer} surface [m^2]	Total surfice [m^2]	Cost [€]
PF HE	Heat exchanger 1	10,3	0,1	200	1000	10	0,2041	1,033	6,169	1644
	Heat exchanger 2			1100	200			1,136	6,816	1783
									12,985	3427

Table 11:Plate and Fin heat exchangers costs $\Delta T_{pp_e} = 3° C$

It is clear that, with the same coefficient of performance and a fixed ΔT_{pp_e} in both the case of shell and tube heat exchangers and that of plate-fin exchangers, the compact heat exchangers solution results in greater savings and less space occupied.

About € 200,000 were saved during the total lifespan of the system. Therefore, the economic benefits produced by the introduction of this recovery system within the plant are very clear.

10 Environmental impact assessment

Naturally, the economic aspect is not the only parameter to analyze when verifying if a technological solution is appropriate. The environmental impact is as much important, especially during these hard times in which all countries are facing the needs of planet Earth: reducing emissions is necessary to stop global warming.

The solution analyzed, by employing heat recovery, can reduce carbon dioxide atmospheric emissions.

Moreover, this work analyzed the use of natural refrigerants fluids for high temperature applications, demonstrating how these fluids, and particularly the refrigerant fluid $R-717$, appear to be not only more efficient, but also less hazardous to the environment.

In order to highlight the positive contributions of the system, the process followed is here described.

In this case too, two different scenarios were analyzed: a first case where fuel oil resulting from natural gas was used, and a second case using residual oil from other combustibles. Using the standards SEF emission factor and knowing the combustible used, it will be possible to determine the quantity of carbon dioxide that would have been introduced into the atmosphere due to the combustion of fuel oil, had the heat recovery system designed not been used.

The next step is to determine the emissions coming from the purchase of electrical work from the national network needed to operate the compressor. Two different emission factors were once again considered: the first factor is the average emission of European Union countries; the other one is the average emission of Scandinavian countries only. In the latter case, given the large presence of renewable energy sources on the Scandinavian territory, the SEF appears to be considerably lower, compared to the European one.

The table below shows the standard emission coefficients mentioned above: they represent the carbon dioxide emissions resulting from a set amount of work produced. [23]

	[tonCO$_2$/MWh]
SEF$_{Europe}$	0,46
SEF$_{Scandinavian countries}$	0,222
SEF$_{gas oil}$	0,267
SEF$_{residual oil}$	0,279

Table 12: Standard Emission Factor (Convenant of Mayors, 2006)

The emissions will now be determined. The formulation used is the same for both the emissions caused by oil combustion, and those deriving from the purchase of electrical work from the network.

$$CO_{2\,emission} = \left(\frac{h_{F\,4real} - h_{F\,3real}}{\eta_{compressor}} \right) \dot{m}_F N_{working\,hours} SEF$$

To determine all of the emissions previously mentioned, it is sufficient to change the value of the standard emission factor.

The results can be seen in the table below, which reports all the combinations analyzed. It is apparent that, using fuel oil derived from natural gas and considering the European SEF, the atmospheric emission avoided would amount to $1900\ [tonCO_2]$; in the case of residual oil from other fossil combustibles and with a SEF value such as that of Scandinavian countries, the emission savings would increase up to $2900\ [tonCO_2]$.

		CO$_2$ emission no HP per year [tonCO$_2$/year]	CO$_2$ emission no HP life [tonCO$_2$]	CO$_2$ emission HP per year [tonCO$_2$/year]	CO$_2$ emission HP life [tonCO$_2$]	CO$_2$ saving per year [tonCO$_2$/year]	CO$_2$ saving life [tonCO$_2$]
R717	Gas oil - Europe	176,5	3530	81,18	1624	95,32	1906
	Gas oil - Scandinavia			39,18	783,5	137,32	2746,5
	Residual oil - Europe	184,4	3689	81,18	1624	103,22	2065
	Residual oil - Scandinavia			39,18	783,5	145,22	2905,5

Table 13: CO_2 Emission Reduction

11 Conclusions

The present experiment shows the potentiality of heat pumps, a technology that has widespread application in the space conditioning field.

They are already used in the industrial sector too, for instance within a number of drying systems in the food, wood and paper industry and in the chemical industry; nevertheless, their use was limited to temperatures lower than 90 °C, with very few exceptions. Therefore, this technology has not yet fully expressed its potentialities in the production industry at higher temperatures.

Therefore, this project is an example of innovative experimentation aimed at proving the aptitude of this technology to possible applications in contexts of production characterized by higher temperatures. As a matter of fact, in the case studied, the condense, whose energetic level is increased, reaches a temperature of 100 ° C.

This temperature is reached by raising the refrigerant temperature up to 185° C, providing heat with a temperature of about 110° C through the condenser.

The refrigerant fluids used for these high-temperature applications were also analyzed, and the refrigerant fluid *R-717* turned out to be the most performing.

This result has even greater relevance when considering the environmental impact: natural refrigerants are proven to be superior to synthetic ones (an example is the *R-245fa* fluid, analyzed during the study).

This solution has a double advantage. Firstly, it is economically convenient, since the introduction of the heat recovery system produces savings. However, the most important effect is the reduction of carbon dioxide emissions; as a matter of fact, in the best case, the emission reduction amounts to almost 80%, compared to a case where fuel oil exclusively provides the thermal power needed by the fluid to raise its temperature.

In the current socio-economic context, great importance is given to environmental issues and to the impact that emissions can have on the planet; these results can represent the essential success factor that would help to spread the use of heat

pumps in high-temperature applications, with a consequent decrease of industrial emissions.

Another important result is the mathematical model that was developed to guide the designing process and maximizing the results. The model can be applied to any industrial context, with only some simple modifications that need to be carried out based on the constraints of the heat recovery and on the dimensions of the equipment; it will thus allow to easily determine the ideal cycle, the preliminary sizing of the machines and finally the real cycle.

This model, which was designed in specialized development environments, can be largely adjusted to specific parameters; it takes into account the constraints of each solution, and it adapts its development to such constraints, highlighting the most interesting results.

12 Future projects

This work is only an example, though significant, of the potential that heat pumps have in the industrial sector: they would improve the primary energy consumption, and reduce atmospheric carbon dioxide emissions.

In the future, other studies that could be carried out, could include heat recoveries of larger entity: they would probably give even greater results in terms of cost and emission reduction.

The present case used a mechanical vapour-compression closed-cycle heat pump (CCC); a valid alternative is represented by absorption heat pumps, which have already been used in high-temperature applications.

These heat pumps can reach even higher temperatures, but they tend to have a superior complexity level.

The aim of this study is to further develop similar projects that can stimulate the spreading of this heat recovery system in high-temperature industrial fields; as a result, the sector technological level would increase, leading to better performances of the implants and, in conclusion, more economical and environmental-conscious productions.

References

[1] Bohdan Soroka, 2015. *Application Note - Industrial Heat Pumps.* [pdf] European Copper Institute. Available at: http://www.leonardo-energy.org/sites/leonardo-energy/files/Cu0118%20-%20Industrial%20Heat%20Pumps%20-%20v2.pdf [Accessed August 2015];

[2] International Energy Association, 1995. *Industrial Heat Pumps – Experiences, Potential and Global Environmental Benefits.* [pdf] Sittard: International Energy Association Heat Pump Centre;

[3] K.J. Chua *, S.K. Chou, W.M. Yang, 2010, Advances in heat pump systems: A review. Applied Energy [e-journal] 87, pp. 3611-3624;

[4] International Energy Association, 2015. Recent Energy Trends in OECD, excerpt from: Energy Balance of OECD Countries. [pdf] Paris, International Energy Association. Available at: http://www.iea.org/publications/freepublications/publication/EnergyBalancesofOECDcountries2015editionexcerpt.pdf [Accessed August 2015];

[5] International Energy Association, 2008. Worldwide Trends in Energy Use and Efficiency. [pdf] Paris, International Energy Association – Key Insights from IEA Indicator Analysis. Available at: https://www.iea.org/publications/freepublications/publication/Indicators_2008.pdf [Accessed August 2015];

[6] Banerjee, R., Y. Cong, D. Gielen, G. Jannuzzi, F. Maréchal, A. T. McKane, M. A. Rosen, D. van Es and E. Worrell, 2012: Chapter 8 - Energy End Use: Industry. In *Global Energy Assessment - Toward a Sustainable Future*, Cambridge University Press, Cambridge, UK and New York, NY, USA and the International Institute for Applied Systems Analysis, Laxenburg, Austria, pp. 513-574;

[7] International Energy Association Heat Pump Center. Heat Pump Working Fluids. [online] Available at:
http://www.heatpumpcentre.org/en/aboutheatpumps/refrigerants/Sidor/default.aspx [Accessed September 2015];

[8] Bricic, M., 2014. *High temperature heat pumps applying natural fluids.* Master thesis. Norwegian University of Science and Technology. Available at:
http://brage.bibsys.no/xmlui/bitstream/handle/11250/235504/726775_FULLTEXT01.pdf?sequence=2&isAllowed=y [Accessed September 2015];

[9] Gaute, G., 2013. *High temperature heat pumps for industrial applications.* Master thesis. Norwegian University of Science and Technology. Available at:
http://brage.bibsys.no/xmlui/bitstream/handle/11250/235192/649637_FULLTEXT01.pdf?sequence=2&isAllowed=y [Accessed September 2015];

[10] Pearson, A., 2012. High temperature heat pumps with natural refrigerants. *IEA Heat Pumps Center Newsletter.* (1/2012), pp. 33-35;

[11] Warren M. Rohsenow and James P. Hartnett, Young I. Cho, 1998. Handbook of heat transfer. 3rd ed. New York: McGrow-Hill;

[12] Gregory Nellis, Sanford Klein, 2012. Heat transfer. Cambridge University Press;

[13] http://www.hcheattransfer.com;

[14] Marwan Chamoun, Romual Rulliere, Philippe Haberschill, Jean Francois Berail, 2012. Dynamic model of an industrial heat pump using water as refrigerant. *International Journal of Refrigeration,* [online] Available at:
http://www.sciencedirect.com/science/article/pii/S0140700711003082 [Accessed November 2015];

[15] S. A. Klein, 2013. Engineering Eqation Solver. Available at:
http://www.fchart.com;

[16] Vivek Patel, Vimal Savsani, 2014. Optimization of a plate-fin heat exchanger design through an improved multi-objective teaching-learning based optimization (MO-ITLBO) algorithm. *Chemical Engineering Research and Design*, [online] Available at: http://www.sciencedirect.com/science/article/pii/S0263876214000732 [Accessed November 2015];

[17] Raj M. Manglik, Arthur E. Bergles 1994. Heat transfer and pressure drop correlations for the rectangular offset strip and fin compact heat exchanger. *Experimental thermal and fluid science* [online] Available at: http://www.sciencedirect.com/science/article/pii/089417779400096Q [Accessed November 2015];

[18] M.S. Peters, K.D. Timmerhaus, 1991. Plant Design and Economics for Chemical Engineers. New York: McGraw-Hill

[19] Antonio C. Caputo, Pacifico M. Pelagagge, Paolo Salini 2008. Heat exchanger design based on economica optimization. *Applied Thermal Engineering* [online] Available at: http://www.sciencedirect.com/science/article/pii/S1359431107002839 [Accessed December 2015];

[20] Marcel Taal, Igor Bulatov, Jiri Klemeš, Petr Stehlìk 2003. Cost estimation and energy price forecast for economic evaluation of retrofit project. *Applied Thermal Engineering* [online] Available at: http://www.sciencedirect.com/science/article/pii/S1359431103001364 [Accessed December 2015];

[21] M&S equipment economical index;

[22] Turton, Bailie, Whiting,Shaeiwitz, Bhattacharyya, 2012. Analysis, Synthesis and Design of Chemical Processes, 4rd ed. Prentice Hall;

[23] Convenant of Mayors, 2006. Technical annex to the SEAP template instructions document: the emission factors. [pdf] Convenant of Mayors.

Appendix A

Below is shown the model developed with the aid of the software Engineering which analyzed the case of using plate and fin heat exchangers with a ΔP_{pp_e} of $3°\,C$.

{known informations}

F$ = 'R717'

{heat source}

T_waste_water[3] = 323,15 [K]
T_waste_water[1] = 320,15 [K]
m_dot_waste_water = 5,04 [kg/s]
P_waste_water = 100 [kPa]

{heat recovered characteristics}

T_condensate[4] = 373,15 [K]
T_condensate[7] = 368,15 [K]
m_dot_condensate = 4,032 [kg/s]
P_condensate = 1000 [kPa]

DELTAT_pp_e = 3 [K]
T_F[3] = T_waste_water[3] - DELTAT_pp_e

DELTAAPPROCH_c = 8 [K]

DELTATSUPERHEAT_e = 5

DELTAT_sc = 3 [K]

DELTAT_pp_c = min(T_F[5]-T_condensate[5];T_F[4]-T_condensate[4])

{Ideal cycle of the HP}

T_F[1] = T_F[2]
P_F[1] = P_F[2]   {pressure losses have been neglected in the heat exchanger}
h_F[1] = h_F[7]   {isoentalpic valve}
s_F[1]=Entropy(F$;h=h_F[1];P=P_F[1])
x_F[1] = Quality(F$;P=P_F[1];h=h_F[1])

T_F[2] = T_F[3] - DELTATSUPERHEAT_e
x_F[2] = 1
P_F[2]=Pressure(F$;T=T_F[2];x=x_F[2])

h_F[2]=Enthalpy(F$;T=T_F[2];x=x_F[2])
s_F[2]=Entropy(F$;T=T_F[2];x=x_F[2])

P_F[3] = P_F[2]   {pressure losses have been
neglected in the heat exchanger}
h_F[3]=Enthalpy(F$;T=T_F[3];P=P_F[3])
s_F[3]=Entropy(F$;T=T_F[3];P=P_F[3])

T_F[4]=Temperature(F$;P=P_F[4];h=h_F[4])
P_F[4] = P_F[6]   {pressure losses have been
neglected in the heat exchanger}
h_F[4]=Enthalpy(F$;s=s_F[4];P=P_F[4])
s_F[4] = s_F[3]

T_F[5] = T_F[6]
x_F[5] = 1
h_F[5]=Enthalpy(F$;T=T_F[5];x=x_F[5])
P_F[5] = P_F[6]
s_F[5]=Entropy(F$;T=T_F[5];x=x_F[5])

T_F[6] = T_condensate[7] + DELTAAPPROCH_c
x_F[6] = 0
P_F[6]=Pressure(F$;T=T_F[6];x=x_F[6])
h_F[6]=Enthalpy(F$;T=T_F[6];x=x_F[6])
s_F[6]=Entropy(F$;T=T_F[6];x=x_F[6])

T_F[7] = T_F[6] - DELTAT_sc
P_F[7] = P_F[6]
h_F[7]=Enthalpy(F$;T=T_F[7];P=P_F[7])
s_F[7]=Entropy(F$;T=T_F[7];P=P_F[7])

beta = P_F[4] / P_F[3]

{Determination of mass flow of the refrigerant & heat transfer }

Q_he_1 = m_dot_waste_water * (h_waste_water[3] - h_waste_water[1])
Q_he_1 = m_dot_F *(h_F[3] - h_F[1])

h_waste_water[3]=Enthalpy(Water;T=T_waste_water[3];P=P_waste_water)
h_waste_water[1]=Enthalpy(Water;T=T_waste_water[1];P=P_waste_water)

Q_he_2 = Q_sh_c + Q_c + Q_sc_c

COP_ideal_cycle = (h_F[3] - h_F[1]) / (h_F[4] - h_F[3])

{Heat exchanger 1}

H_waste_water_e = H_F_e
H_waste_water_e = 10,3 [mm]

t_waste_water_e = t_F_e
t_waste_water_e = 0,1 [mm]

L_waste_water_e = 200 [mm]
L_F_e = 1000 [mm]

n_waste_water_e = n_F_e
n_waste_water_e = (1 / 4,9) [(mm)^(-1)]

N_layer_waste_water_e = N_layer_F_e
N_layer_waste_water_sh_e = N_layer_F_sh_e

l_f_hot_e = l_f_cold_e
l_f_hot_e = 10 [mm]

{Evaporator}

Q_e = m_dot_waste_water * (h_waste_water[2] - h_waste_water[1])
Q_e = m_dot_F *(h_F[2] - h_F[1])

T_waste_water[2]=Temperature(Water;h=h_waste_water[2];P=P_waste_water)

{Hot fluid}
mu_waste_water_2_e=Viscosity(Water;T=T_waste_water[2];P=P_waste_water)
mu_waste_water_1_e=Viscosity(Water;T=T_waste_water[1];P=P_waste_water)
mu_waste_water_e = (mu_waste_water_2_e + mu_waste_water_1_e) / 2

rho_waste_water_2_e=Density(Water;T=T_waste_water[2];P=P_waste_water)
rho_waste_water_1_e=Density(Water;T=T_waste_water[1];P=P_waste_water)
rho_waste_water_e = (rho_waste_water_2_e + rho_waste_water_1_e) / 2

k_waste_water_2_e=Conductivity(Water;T=T_waste_water[2];P=P_waste_water)
k_waste_water_1_e=Conductivity(Water;T=T_waste_water[1];P=P_waste_water)
k_waste_water_e = (k_waste_water_2_e + k_waste_water_1_e) / 2

cp_waste_water_2_e=Cp(Water;T=T_waste_water[2];P=P_waste_water)
cp_waste_water_1_e=Cp(Water;T=T_waste_water[1];P=P_waste_water)
cp_waste_water_e = (cp_waste_water_2_e + cp_waste_water_1_e) / 2

C_waste_water_e = cp_waste_water_e * m_dot_waste_water

{Cold fluid}
mu_F_2_e=Viscosity(F$;T=T_F[2];x=x_F[2])

3

mu_F_1_e=Viscosity(F$;T=T_F[1];x=0)
mu_F_e = (mu_F_2_e + mu_F_1_e)/2

rho_F_2_e=Density(F$;T=T_F[2];x=x_F[2])
rho_F_1_e=Density(F$;T=T_F[1];x=0)
rho_F_e = (rho_F_2_e + rho_F_1_e) / 2

Q_e = epsilon_e * C_waste_water_e * (T_waste_water[2] - T_F[1])

NTU_e = -ln(1 - epsilon_e)

NTU_e = (U_e * A_e) / (C_waste_water_e * convert(kJ/K*s;W/K))

A_waste_water_sl_e = L_waste_water_e * L_F_e * (1 + 2 * n_waste_water_e *
(H_waste_water_e - t_waste_water_e))

A_F_sl_e = L_waste_water_e * L_F_e * (1 + 2 * n_F_e * (H_F_e - t_F_e))

A_waste_water_e = A_waste_water_sl_e * N_layer_waste_water_e
A_F_e = A_F_sl_e * N_layer_F_e

A_e = A_F_e*convert(mm^2;m^2) + A_waste_water_e*convert(mm^2;m^2)

U_e_s&t = 1949
U_e = U_e_s&t + ((U_e_s&t *30) / 100)

A_ff_waste_water_e = (H_waste_water_e - t_waste_water_e) * (1 -
(n_waste_water_e * t_waste_water_e)) * L_F_e * N_layer_waste_water_e
A_ff_F_e = (H_F_e - t_F_e) * (1 - (n_F_e * t_F_e)) * L_waste_water_e *
N_layer_F_e

{Super heater of the evaporator}

Q_sh_e = m_dot_F *(h_F[3] - h_F[2])

{Hot fluid}
mu_waste_water_2_sh_e = mu_waste_water_2_e
mu_waste_water_3_sh_e=Viscosity(Water;T=T_waste_water[3];P=P_waste_water)
mu_waste_water_sh_e = (mu_waste_water_2_sh_e + mu_waste_water_3_sh_e) / 2

rho_waste_water_2_sh_e= rho_waste_water_2_e
rho_waste_water_3_sh_e=Density(Water;T=T_waste_water[3];P=P_waste_water)
rho_waste_water_sh_e = (rho_waste_water_2_sh_e + rho_waste_water_3_sh_e) / 2

k_waste_water_2_sh_e= k_waste_water_2_e
k_waste_water_3_sh_e=Conductivity(Water;T=T_waste_water[3];P=P_waste_water)
k_waste_water_sh_e = (k_waste_water_2_sh_e + k_waste_water_3_sh_e) / 2

cp_waste_water_2_sh_e= cp_waste_water_2_e
cp_waste_water_3_sh_e=Cp(Water;T=T_waste_water[3];P=P_waste_water)

cp_waste_water_sh_e = (cp_waste_water_2_sh_e + cp_waste_water_3_sh_e) / 2

{Cold fluid}
mu_F_2_sh_e = mu_F_2_e
mu_F_3_sh_e=Viscosity(F$;T=T_F[3];P=P_F[3])
mu_F_sh_e = (mu_F_2_sh_e + mu_F_3_sh_e) / 2

rho_F_2_sh_e = rho_F_2_e
rho_F_3_sh_e=Density(F$;T=T_F[3];P=P_F[3])
rho_F_sh_e = (rho_F_2_sh_e + rho_F_3_sh_e) / 2

k_F_2_sh_e=Conductivity(F$;T=T_F[2];x=x_F[2])
k_F_3_sh_e=Conductivity(F$;T=T_F[3];P=P_F[3])
k_F_sh_e = (k_F_2_sh_e + k_F_3_sh_e) / 2

cp_F_2_sh_e=Cp(F$;T=T_F[2];x=x_F[2])
cp_F_3_sh_e=Cp(F$;T=T_F[3];P=P_F[3])
cp_F_sh_e = (cp_F_2_sh_e + cp_F_3_sh_e) / 2

C_waste_water_sh_e = cp_waste_water_sh_e * m_dot_waste_water
C_F_sh_e = cp_F_sh_e * m_dot_F
C_MIN_sh_e = min(C_waste_water_sh_e; C_F_sh_e)
C_MAX_sh_e = max(C_waste_water_sh_e; C_F_sh_e)

C_R_sh_e = C_MIN_sh_e/C_MAX_sh_e

Q_sh_e = epsilon_sh_e * C_MIN_sh_e * (T_waste_water[3]- T_F[2])

NTU_sh_e = ln((1 - epsilon_sh_e * C_R_sh_e)/(1 -epsilon_sh_e))/(1-C_R_sh_e)

NTU_sh_e = (U_sh_e * A_sh_e) / (C_MIN_sh_e * convert(kJ/K*s;W/K))

A_waste_water_sh_e = A_waste_water_sl_e * N_layer_waste_water_sh_e
A_F_sh_e = A_F_sl_e * N_layer_F_sh_e

A_sh_e = A_F_sh_e*convert(mm^2;m^2) +
A_waste_water_sh_e*convert(mm^2;m^2)

U_sh_e_s&t = 369,2
U_sh_e = U_sh_e_s&t + ((U_sh_e_s&t *30) / 100)

A_ff_waste_water_sh_e = (H_waste_water_e - t_waste_water_e) * (1 -
(n_waste_water_e * t_waste_water_e)) * L_F_e * N_layer_waste_water_sh_e
A_ff_F_sh_e = (H_F_e - t_F_e) * (1 - (n_F_e * t_F_e)) * L_waste_water_e *
N_layer_F_sh_e

N_layer_hot_he_1 = N_layer_waste_water_e +N_layer_waste_water_sh_e
N_layer_cold_he_1 = N_layer_F_e + N_layer_F_sh_e

A_he_1 = A_e + A_sh_e

L_n_e = ceil(N_layer_cold_he_1) * H_F_e + ceil(N_layer_hot_he_1) * H_waste_water_e

A_ff_waste_water_he_1 = (H_waste_water_e - t_waste_water_e) * (1 - (n_waste_water_e * t_waste_water_e)) * L_F_e * ceil(N_layer_hot_he_1)
A_ff_F_he_1 = (H_F_e - t_F_e) * (1 - (n_F_e * t_F_e)) * L_waste_water_e * ceil(N_layer_cold_he_1)

A_he_1_correct = A_waste_water_sl_e * convert(mm^2;m^2) * ceil(N_layer_hot_he_1) + A_F_sl_e * convert(mm^2;m^2) * ceil(N_layer_cold_he_1)

{Heat exchanger 2 }

H_condensate_c = H_F_c
H_condensate_c = 10,3 [mm]

t_condensate_c = t_F_c
t_condensate_c = 0,1 [mm]

L_condensate_c = 200 [mm]
L_F_c = 1100 [mm]

n_condensate_c = n_F_c
n_condensate_c = (1 / 4,9) [mm^(-1)]

N_layer_condensate_c = N_layer_F_c
N_layer_condensate_sh_c = N_layer_F_sh_c
N_layer_condensate_sc_c = N_layer_F_sc_c

l_f_hot_c = l_f_cold_c
l_f_hot_c = 10 [mm]

{Superheater of the condenseer}

Q_sh_c = m_dot_condensate * (h_condensate[4] - h_condensate[5])
Q_sh_c = m_dot_F *(h_F[4] - h_F[5])

h_condensate[4]=Enthalpy(Water;T=T_condensate[4]; P=P_condensate)
T_condensate[5]=Temperature(Water;h= h_condensate[5];P=P_condensate)

{Hot fluid}
mu_F_5_sh_c = mu_F_5_c
mu_F_4_sh_c=Viscosity(F$;T=T_F[4];P=P_F[4])
mu_F_sh_c = (mu_F_5_sh_c + mu_F_4_sh_c)/2

rho_F_5_sh_c = rho_F_5_c
rho_F_4_sh_c=Density(F$;T=T_F[4];P=P_F[4])

rho_F_sh_c = (rho_F_5_sh_c + rho_F_4_sh_c) / 2

k_F_5_sh_c=Conductivity(F$;T=T_F[5];x=x_F[5])
k_F_4_sh_c=Conductivity(F$;T=T_F[4];P=P_F[4])
k_F_sh_c = (k_F_4_sh_c + k_F_5_sh_c) / 2

cp_F_5_sh_c=Cp(F$;T=T_F[5];x=x_F[5])
cp_F_4_sh_c=Cp(F$;T=T_F[4];P=P_F[4])
cp_F_sh_c = (cp_F_4_sh_c + cp_F_5_sh_c) / 2

{Cold fluid}
mu_condensate_5_sh_c = mu_condensate_5_c
mu_condensate_4_sh_c=Viscosity(Water;T=T_condensate[4];P=P_condensate)
mu_condensate_sh_c = (mu_condensate_4_sh_c + mu_condensate_5_sh_c)/2

rho_condensate_5_sh_c= rho_condensate_5_c
rho_condensate_4_sh_c=Density(Water;T=T_condensate[4];P=P_condensate)
rho_condensate_sh_c = (rho_condensate_4_sh_c + rho_condensate_5_sh_c) / 2

k_condensate_5_sh_c= k_condensate_5_c
k_condensate_4_sh_c=Conductivity(Water;T=T_condensate[4];P=P_condensate)
k_condensate_sh_c = (k_condensate_4_sh_c + k_condensate_5_sh_c) / 2

cp_condensate_5_sh_c= cp_condensate_5_c
cp_condensate_4_sh_c=Cp(Water;T=T_condensate[4];P=P_condensate)
cp_condensate_sh_c = (cp_condensate_4_sh_c + cp_condensate_5_sh_c) / 2

C_condensate_sh_c = cp_condensate_sh_c * m_dot_condensate
C_F_sh_c = cp_F_sh_c * m_dot_F
C_MIN_sh_c = min(C_condensate_sh_c; C_F_sh_c)
C_MAX_sh_c = max(C_condensate_sh_c; C_F_sh_c)

C_R_sh_c = C_MIN_sh_c/C_MAX_sh_c

Q_sh_c = epsilon_sh_c * C_MIN_sh_c * (T_F[4]- T_condensate[5])

NTU_sh_c = ln((1 - epsilon_sh_c * C_R_sh_c)/(1 -epsilon_sh_c))/(1-C_R_sh_c)

NTU_sh_c = (U_sh_c * A_sh_c) / (C_MIN_sh_c * convert(kJ/K*s;W/K))

A_condensate_sh_c = A_condensate_sl_c * N_layer_condensate_sh_c
A_F_sh_c = A_F_sl_c * N_layer_F_sh_c

A_sh_c = A_F_sh_c*convert(mm^2;m^2) + A_condensate_sh_c*convert(mm^2;m^2)

U_sh_c_s&t = 477,1
U_sh_c = U_sh_c_s&t + ((U_sh_c_s&t *30) / 100)

A_ff_condensate_sh_c = (H_condensate_c - t_condensate_c) * (1 -
(n_condensate_c * t_condensate_c)) * L_F_c * N_layer_condensate_sh_c

A_ff_F_sh_c = (H_F_c - t_F_c) * (1 - (n_F_c * t_F_c)) * L_condensate_c *
N_layer_F_sh_c

{Condenser}

Q_c = m_dot_condensate * (h_condensate[5] - h_condensate[6])
Q_c = m_dot_F *(h_F[5] - h_F[6])

T_condensate[6]=Temperature(Water;h= h_condensate[6];P=P_condensate)

{Hot fluid}
mu_F_5_c=Viscosity(F$;T=T_F[5];x=x_F[5])
mu_F_6_c=Viscosity(F$;T=T_F[6];x=0)
mu_F_c = (mu_F_5_c + mu_F_6_c) / 2

rho_F_5_c=Density(F$;T=T_F[5];x=x_F[5])
rho_F_6_c=Density(F$;T=T_F[6];x=0)
rho_F_c = (rho_F_5_c + rho_F_6_c) / 2

{Cold fluid}
mu_condensate_5_c=Viscosity(Water;T=T_condensate[5];P=P_condensate)
mu_condensate_6_c=Viscosity(Water;T=T_condensate[6];P=P_condensate)
mu_condensate_c = (mu_condensate_5_c + mu_condensate_6_c)/2

rho_condensate_5_c=Density(Water;T=T_condensate[5];P=P_condensate)
rho_condensate_6_c=Density(Water;T=T_condensate[6];P=P_condensate)
rho_condensate_c = (rho_condensate_5_c + rho_condensate_6_c) / 2

k_condensate_5_c=Conductivity(Water;T=T_condensate[5];P=P_condensate)
k_condensate_6_c=Conductivity(Water;T=T_condensate[6];P=P_condensate)
k_condensate_c= (k_condensate_5_c + k_condensate_6_c) / 2

cp_condensate_5_c=Cp(Water;T=T_condensate[5];P=P_condensate)
cp_condensate_6_c=Cp(Water;T=T_condensate[6];P=P_condensate)
cp_condensate_c= (cp_condensate_6_c + cp_condensate_6_c) / 2

C_condensate_c = cp_condensate_c * m_dot_condensate

Q_c = epsilon_c * C_condensate_c * (T_F[5] - T_condensate[6])

NTU_c = -ln(1 - epsilon_c)

NTU_c = (U_c * A_c) / (C_condensate_c * convert(kJ/K*s;W/K))

A_condensate_sl_c = L_condensate_c * L_F_c * (1 + 2 * n_condensate_c *
(H_condensate_c - t_condensate_c))

A_F_sl_c = L_condensate_c * L_F_c * (1 + 2 * n_F_c * (H_F_c - t_F_c))

A_condensate_c = A_condensate_sl_c * N_layer_condensate_c

A_F_c = A_F_sl_c * N_layer_F_c

A_c = A_F_c*convert(mm^2;m^2) + A_condensate_c*convert(mm^2;m^2)

U_c_s&t = 2036
U_c = U_c_s&t + ((U_e_s&t *30) / 100)

A_ff_condensate_c = (H_condensate_c - t_condensate_c) * (1 - (n_condensate_c * t_condensate_c)) * L_F_c * N_layer_condensate_c
A_ff_F_c = (H_F_c - t_F_c) * (1 - (n_F_c * t_F_c)) * L_condensate_c * N_layer_F_c

{Subcooler of the condenser}

Q_sc_c = m_dot_condensate * (h_condensate[6] - h_condensate[7])
Q_sc_c = m_dot_F *(h_F[6] - h_F[7])

{Hot fluid}
mu_F_6_sc_c = mu_F_6_c
mu_F_7_sc_c=Viscosity(F$;T=T_F[7];P=P_F[7])
mu_F_sc_c = (mu_F_6_sc_c + mu_F_7_sc_c)/2

rho_F_6_sc_c = rho_F_6_c
rho_F_7_sc_c=Density(F$;T=T_F[7];P=P_F[7])
rho_F_sc_c = (rho_F_6_sc_c + rho_F_7_sc_c) / 2

k_F_6_sc_c=Conductivity(F$;T=T_F[6];x=x_F[6])
k_F_7_sc_c=Conductivity(F$;T=T_F[7];P=P_F[7])
k_F_sc_c = (k_F_6_sc_c + k_F_7_sc_c) / 2

cp_F_6_sc_c=Cp(F$;T=T_F[6];x=x_F[6])
cp_F_7_sc_c=Cp(F$;T=T_F[7];P=P_F[7])
cp_F_sc_c = (cp_F_6_sc_c + cp_F_7_sc_c) / 2

{Cold fluid}
mu_condensate_6_sc_c = mu_condensate_6_c
mu_condensate_7_sc_c=Viscosity(Water;T=T_condensate[7];P=P_condensate)
mu_condensate_sc_c = (mu_condensate_6_sc_c + mu_condensate_6_sc_c)/2

rho_condensate_6_sc_c= rho_condensate_6_c
rho_condensate_7_sc_c=Density(Water;T=T_condensate[7];P=P_condensate)
rho_condensate_sc_c = (rho_condensate_6_sc_c + rho_condensate_7_sc_c) / 2

k_condensate_6_sc_c= k_condensate_6_c
k_condensate_7_sc_c=Conductivity(Water;T=T_condensate[7];P=P_condensate)
k_condensate_sc_c = (k_condensate_6_sc_c + k_condensate_7_sc_c) / 2

cp_condensate_6_sc_c= cp_condensate_6_c
cp_condensate_7_sc_c=Cp(Water;T=T_condensate[7];P=P_condensate)
cp_condensate_sc_c = (cp_condensate_6_sc_c + cp_condensate_7_sc_c) / 2
C_condensate_sc_c = cp_condensate_sc_c * m_dot_condensate

C_F_sc_c = cp_F_sc_c * m_dot_F
C_MIN_sc_c = min(C_condensate_sc_c; C_F_sc_c)
C_MAX_sc_c = max(C_condensate_sc_c; C_F_sc_c)

C_R_sc_c = C_MIN_sc_c/C_MAX_sc_c

Q_sc_c = epsilon_sc_c * C_MIN_sc_c * (T_F[6]- T_condensate[7])

NTU_sc_c = ln((1 - epsilon_sc_c * C_R_sc_c)/(1 -epsilon_sc_c))/(1-C_R_sc_c)

NTU_sc_c = (U_sc_c * A_sc_c) / (C_MIN_sc_c * convert(kJ/K*s;W/K))

A_condensate_sc_c = A_condensate_sl_c * N_layer_condensate_sc_c
A_F_sc_c = A_F_sl_c * N_layer_F_sc_c

A_sc_c = A_F_sc_c*convert(mm^2;m^2) + A_condensate_sc_c*convert(mm^2;m^2)

U_sc_c_s&t = 707
U_sc_c = U_sc_c_s&t + ((U_sc_c_s&t *30) / 100)

A_ff_condensate_sc_c = (H_condensate_c - t_condensate_c) * (1 - (n_condensate_c
* t_condensate_c)) * L_F_c * N_layer_condensate_sc_c
A_ff_F_sc_c = (H_F_c - t_F_c) * (1 - (n_F_c * t_F_c)) * L_condensate_c *
N_layer_F_sc_c

N_layer_hot_he_2 = N_layer_F_sh_c + N_layer_F_c + N_layer_F_sc_c
N_layer_cold_he_2 = N_layer_condensate_sh_c + N_layer_condensate_c +
N_layer_condensate_sc_c

A_he_2 = A_sh_c + A_c + A_sc_c

L_n_c = ceil(N_layer_cold_he_2) * H_F_c + ceil(N_layer_hot_he_2) *
H_condensate_c

A_ff_condensate_he_2 = (H_condensate_c - t_condensate_c) * (1 -
(n_condensate_c * t_condensate_c)) * L_F_c * ceil(N_layer_cold_he_2)
A_ff_F_he_2 = (H_F_c - t_F_c) * (1 - (n_F_c * t_F_c)) * L_condensate_c *
ceil(N_layer_hot_he_2)

A_he_2_correct = A_condensate_sl_c * convert(mm^2;m^2) *
ceil(N_layer_cold_he_2) + A_F_sl_c * convert(mm^2;m^2) * ceil(N_layer_hot_he_2)

{Pressure losses}

P_waste_water_real[1] = P_waste_water
P_F_real[1] = P_F[1]
T_F_real[1] = T_F[1]
h_F_real[1] = h_F[1]

P_condensate_real[4]=P_condensate

{Heat exchanger 1}

{Evaporator}

G_hot_e = m_dot_waste_water / (A_ff_waste_water_e*convert(mm^2;m^2))
G_cold_e = m_dot_F / (A_ff_F_e*convert(mm^2;m^2))

f_s_hot_e =((1 / n_waste_water_e) - t_waste_water_e)
f_s_cold_e = ((1 / n_F_e) - t_F_e)

D_h_hot_e = (4 * f_s_hot_e * l_f_hot_e * (H_waste_water_e - t_waste_water_e)) / (2 * (f_s_hot_e * l_f_hot_e + (H_waste_water_e - t_waste_water_e) * l_f_hot_e + (H_waste_water_e - t_waste_water_e) * t_waste_water_e) + t_waste_water_e * f_s_hot_e)
D_h_cold_e = (4 * f_s_cold_e * l_f_cold_e * (H_F_e - t_F_e)) / (2 * (f_s_cold_e * l_f_cold_e + (H_F_e - t_F_e) * l_f_cold_e + (H_F_e - t_F_e) * t_F_e) + t_F_e * f_s_cold_e)

Re_hot_e = (G_hot_e * D_h_hot_e*convert(mm;m)) / mu_waste_water_e
Re_cold_e = (G_cold_e * D_h_cold_e*convert(mm;m)) / mu_F_e

alpha_hot_e = f_s_hot_e / (H_waste_water_e - t_waste_water_e)
alpha_cold_e = f_s_cold_e / (H_F_e - t_F_e)

delta_hot_e = t_waste_water_e / l_f_hot_e
delta_cold_e = t_F_e / l_f_cold_e

gamma_hot_e = t_waste_water_e / f_s_hot_e
gamma_cold_e = t_F_e / f_s_cold_e

ff_hot_e = 9,6243 * Re_hot_e^(-0,7422) * alpha_hot_e^(-0,1856) * delta_hot_e^(0,3053) * gamma_hot_e^(-0,2659) * (1 + (7,669 * 10^(-8) * Re_hot_e^(4,429) * alpha_hot_e^(0,920) * delta_hot_e^(3,767) * gamma_hot_e^(0,236)))^(-0,1)
ff_cold_e = 9,6243 * Re_cold_e^(-0,7422) * alpha_cold_e^(-0,1856) * delta_cold_e^(0,3053) * gamma_cold_e^(-0,2659) * (1 + (7,669 * 10^(-8) * Re_cold_e^(4,429) * alpha_cold_e^(0,920) * delta_cold_e^(3,767) * gamma_cold_e^(0,236)))^(-0,1)

DELTAP_hot_e = (2 * ff_hot_e * L_waste_water_e * convert(mm;m) * G_hot_e^(2)) / (rho_waste_water_e * D_h_hot_e * convert(mm;m))
DELTAP_cold_e = (2 * ff_cold_e * L_F_e * convert(mm;m) * G_cold_e^(2)) / (rho_F_e * D_h_cold_e * convert(mm;m))

P_hot_e_1 = P_waste_water - DELTAP_hot_e * convert(Pa;kPa)
P_cold_e_1 = P_F[2] - DELTAP_cold_e * convert(Pa;kPa)

{First iteration}

11

mu_waste_water_2_e_1 = Viscosity(F$;P = P_hot_e_1;T=T_waste_water[2])
mu_waste_water_e_1 = (mu_waste_water_2_e_1 + mu_waste_water_1_e) / 2

mu_F_2_e_1 = Viscosity(F$;P = P_cold_e_1;x=x_F[2])
mu_F_e_1 = (mu_F_2_e_1 + mu_F_1_e)/2

Re_hot_e_1 = (G_hot_e * D_h_hot_e*convert(mm;m)) / mu_waste_water_e_1
Re_cold_e_1 = (G_cold_e * D_h_cold_e*convert(mm;m)) / mu_F_e_1

ff_hot_e_1 = 9,6243 * Re_hot_e_1^(-0,7422) * alpha_hot_e^(-0,1856) *
delta_hot_e^(0,3053) * gamma_hot_e^(-0,2659) * (1 + (7,669 * 10^(-8) *
Re_hot_e_1^(4,429) * alpha_hot_e^(0,920) * delta_hot_e^(3,767) *
gamma_hot_e^(0,236)))^(-0,1)
ff_cold_e_1 = 9,6243 * Re_cold_e_1^(-0,7422) * alpha_cold_e^(-0,1856) *
delta_cold_e^(0,3053) * gamma_cold_e^(-0,2659) * (1 + (7,669 * 10^(-8) *
Re_cold_e_1^(4,429) * alpha_cold_e^(0,920) * delta_cold_e^(3,767) *
gamma_cold_e^(0,236)))^(-0,1)

rho_waste_water_2_e_1 = Density(F$;P = P_hot_e_1;T=T_waste_water[2])
rho_waste_water_e_1 = (rho_waste_water_2_e_1 + rho_waste_water_1_e) / 2

rho_F_2_e_1 = Density(F$;P = P_cold_e_1;x=x_F[2])
rho_F_e_1 = (rho_F_2_e_1 + rho_F_1_e) / 2

DELTAP_hot_e_1 = (2 * ff_hot_e_1 * L_waste_water_e * convert(mm;m) *
G_hot_e^(2)) / (rho_waste_water_e_1 * D_h_hot_e * convert(mm;m))
DELTAP_cold_e_1 = (2 * ff_cold_e_1 * L_F_e * convert(mm;m) * G_cold_e^(2)) /
(rho_F_e_1 * D_h_cold_e * convert(mm;m))

P_hot_e_2 = P_waste_water - DELTAP_hot_e_1 * convert(Pa;kPa)
P_cold_e_2 = P_F[2] - DELTAP_cold_e_1 * convert(Pa;kPa)

error_hot_e_1 = abs(P_hot_e_1 - P_hot_e_2)
error_cold_e_1 = abs(P_cold_e_1 - P_cold_e_2)

{Second iteration}

mu_waste_water_2_e_2 = Viscosity(F$;P = P_hot_e_2;T=T_waste_water[2])
mu_waste_water_e_2 = (mu_waste_water_2_e_2 + mu_waste_water_1_e) / 2

mu_F_2_e_2 = Viscosity(F$;P = P_cold_e_2;x=x_F[2])
mu_F_e_2 = (mu_F_2_e_2 + mu_F_1_e)/2

Re_hot_e_2 = (G_hot_e * D_h_hot_e*convert(mm;m)) / mu_waste_water_e_2
Re_cold_e_2 = (G_cold_e * D_h_cold_e*convert(mm;m)) / mu_F_e_2

ff_hot_e_2 = 9,6243 * Re_hot_e_2^(-0,7422) * alpha_hot_e^(-0,1856) *
delta_hot_e^(0,3053) * gamma_hot_e^(-0,2659) * (1 + (7,669 * 10^(-8) *

Re_hot_e_2^(4,429) * alpha_hot_e^(0,920) * delta_hot_e^(3,767) *
gamma_hot_e^(0,236)))^(-0,1)
ff_cold_e_2 = 9,6243 * Re_cold_e_2^(-0,7422) * alpha_cold_e^(-0,1856) *
delta_cold_e^(0,3053) * gamma_cold_e^(-0,2659) * (1 + (7,669 * 10^(-8) *
Re_cold_e_2^(4,429) * alpha_cold_e^(0,920) * delta_cold_e^(3,767) *
gamma_cold_e^(0,236)))^(-0,1)

rho_waste_water_2_e_2 = Density(F$;P = P_hot_e_2;T=T_waste_water[2])
rho_waste_water_e_2 = (rho_waste_water_2_e_2 + rho_waste_water_1_e) / 2

rho_F_2_e_2 = Density(F$;P = P_cold_e_2;x=x_F[2])
rho_F_e_2 = (rho_F_2_e_2 + rho_F_1_e) / 2

DELTAP_hot_e_2 = (2 * ff_hot_e_2 * L_waste_water_e * convert(mm;m) *
G_hot_e^(2)) / (rho_waste_water_e_2 * D_h_hot_e * convert(mm;m))
DELTAP_cold_e_2 = (2 * ff_cold_e_2 * L_F_e * convert(mm;m) * G_cold_e^(2)) /
(rho_F_e_2 * D_h_cold_e * convert(mm;m))

P_hot_e_3 =P_waste_water - DELTAP_hot_e_2 * convert(Pa;kPa)
P_cold_e_3 = P_F[2] - DELTAP_cold_e_2 * convert(Pa;kPa)

error_hot_e_2 = abs(P_hot_e_2 - P_hot_e_3)
error_cold_e_2 = abs(P_cold_e_2 - P_cold_e_3)

{Real pressure point 2}

P_waste_water_real[2] = P_hot_e_3
P_F_real[2] = P_cold_e_3

T_F_real[2] = Temperature(F$;P=P_F_real[2];x=x_F[2])
h_F_real[2] = Enthalpy(F$;P=P_F_real[2];x=x_F[2])

{Superheater of the evaporator}

T_F_real[3] = T_F_real[2] + DELTATSUPERHEAT_e

G_hot_sh_e = m_dot_waste_water / (A_ff_waste_water_sh_e*convert(mm^2;m^2))
G_cold_sh_e = m_dot_F / (A_ff_F_sh_e*convert(mm^2;m^2))

Re_hot_sh_e = (G_hot_sh_e * D_h_hot_e*convert(mm;m)) / mu_waste_water_sh_e
Re_cold_sh_e = (G_cold_sh_e * D_h_cold_e*convert(mm;m)) / mu_F_sh_e

ff_hot_sh_e = 9,6243 * Re_hot_sh_e^(-0,7422) * alpha_hot_e^(-0,1856) *
delta_hot_e^(0,3053) * gamma_hot_e^(-0,2659) * (1 + (7,669 * 10^(-8) *
Re_hot_sh_e^(4,429) * alpha_hot_e^(0,920) * delta_hot_e^(3,767) *
gamma_hot_e^(0,236)))^(-0,1)
ff_cold_sh_e = 9,6243 * Re_cold_sh_e^(-0,7422) * alpha_cold_e^(-0,1856) *
delta_cold_e^(0,3053) * gamma_cold_e^(-0,2659) * (1 + (7,669 * 10^(-8) *
Re_cold_sh_e^(4,429) * alpha_cold_e^(0,920) * delta_cold_e^(3,767) *
gamma_cold_e^(0,236)))^(-0,1)

DELTAP_hot_sh_e = (2 * ff_hot_sh_e * L_waste_water_e * convert(mm;m) * G_hot_sh_e^(2)) / (rho_waste_water_e * D_h_hot_e * convert(mm;m))
DELTAP_cold_sh_e = (2 * ff_cold_sh_e * L_F_e * convert(mm;m) * G_cold_sh_e^(2)) / (rho_F_e * D_h_cold_e * convert(mm;m))

P_hot_sh_e_1 = P_waste_water_real[2] - DELTAP_hot_sh_e * convert(Pa;kPa)
P_cold_sh_e_1 = P_F_real[2] - DELTAP_cold_sh_e * convert(Pa;kPa)

{First iteration}

mu_waste_water_3_sh_e_1 = Viscosity(F$;P = P_hot_sh_e_1;T=T_waste_water[3])
mu_waste_water_sh_e_1 = (mu_waste_water_3_sh_e_1 + mu_waste_water_2_sh_e) / 2

mu_F_3_sh_e_1 = Viscosity(F$;P = P_cold_sh_e_1;T=T_F[3])
mu_F_sh_e_1 = (mu_F_3_sh_e_1 + mu_F_2_sh_e)/2

Re_hot_sh_e_1 = (G_hot_e * D_h_hot_e*convert(mm;m)) / mu_waste_water_sh_e_1
Re_cold_sh_e_1 = (G_cold_e * D_h_cold_e*convert(mm;m)) / mu_F_sh_e_1

ff_hot_sh_e_1 = 9,6243 * Re_hot_sh_e_1^(-0,7422) * alpha_hot_e^(-0,1856) * delta_hot_e^(0,3053) * gamma_hot_e^(-0,2659) * (1 + (7,669 * 10^(-8) * Re_hot_sh_e_1^(4,429) * alpha_hot_e^(0,920) * delta_hot_e^(3,767) * gamma_hot_e^(0,236)))^(-0,1)
ff_cold_sh_e_1 = 9,6243 * Re_cold_sh_e_1^(-0,7422) * alpha_cold_e^(-0,1856) * delta_cold_e^(0,3053) * gamma_cold_e^(-0,2659) * (1 + (7,669 * 10^(-8) * Re_cold_sh_e_1^(4,429) * alpha_cold_e^(0,920) * delta_cold_e^(3,767) * gamma_cold_e^(0,236)))^(-0,1)

rho_waste_water_3_sh_e_1 = Density(F$;P = P_hot_sh_e_1;T=T_waste_water[3])
rho_waste_water_sh_e_1 = (rho_waste_water_3_sh_e_1 + rho_waste_water_2_sh_e) / 2

rho_F_3_sh_e_1 = Density(F$;P = P_cold_sh_e_1;T=T_F[3])
rho_F_sh_e_1 = (rho_F_3_sh_e_1 + rho_F_2_sh_e) / 2

DELTAP_hot_sh_e_1 = (2 * ff_hot_sh_e_1 * L_waste_water_e * convert(mm;m) * G_hot_sh_e^(2)) / (rho_waste_water_sh_e_1 * D_h_hot_e * convert(mm;m))
DELTAP_cold_sh_e_1 = (2 * ff_cold_sh_e_1 * L_F_e * convert(mm;m) * G_cold_sh_e^(2)) / (rho_F_sh_e_1 * D_h_cold_e * convert(mm;m))

P_hot_sh_e_2 = P_waste_water_real[2] - DELTAP_hot_sh_e_1 * convert(Pa;kPa)
P_cold_sh_e_2 = P_F_real[2] - DELTAP_cold_sh_e_1 * convert(Pa;kPa)

error_hot_sh_e_1 = abs(P_hot_sh_e_1 - P_hot_sh_e_2)
error_cold_sh_e_1 = abs(P_cold_sh_e_1 - P_cold_sh_e_2)

{Second iteration}

mu_waste_water_3_sh_e_2 = Viscosity(F$;P = P_hot_sh_e_2;T=T_waste_water[3])
mu_waste_water_sh_e_2 = (mu_waste_water_3_sh_e_2 +
mu_waste_water_2_sh_e) / 2

mu_F_3_sh_e_2 = Viscosity(F$;P = P_cold_sh_e_2;T=T_F[3])
mu_F_sh_e_2 = (mu_F_3_sh_e_2 + mu_F_2_sh_e)/2

Re_hot_sh_e_2 = (G_hot_e * D_h_hot_e*convert(mm;m)) /
mu_waste_water_sh_e_2
Re_cold_sh_e_2 = (G_cold_e * D_h_cold_e*convert(mm;m)) / mu_F_sh_e_2

ff_hot_sh_e_2 = 9,6243 * Re_hot_sh_e_2^(-0,7422) * alpha_hot_e^(-0,1856) *
delta_hot_e^(0,3053) * gamma_hot_e^(-0,2659) * (1 + (7,669 * 10^(-8) *
Re_hot_sh_e_2^(4,429) * alpha_hot_e^(0,920) * delta_hot_e^(3,767) *
gamma_hot_e^(0,236)))^(-0,1)
ff_cold_sh_e_2 = 9,6243 * Re_cold_sh_e_2^(-0,7422) * alpha_cold_e^(-0,1856) *
delta_cold_e^(0,3053) * gamma_cold_e^(-0,2659) * (1 + (7,669 * 10^(-8) *
Re_cold_sh_e_2^(4,429) * alpha_cold_e^(0,920) * delta_cold_e^(3,767) *
gamma_cold_e^(0,236)))^(-0,1)

rho_waste_water_3_sh_e_2 = Density(F$;P = P_hot_sh_e_2;T=T_waste_water[3])
rho_waste_water_sh_e_2 = (rho_waste_water_3_sh_e_2 +
rho_waste_water_2_sh_e) / 2

rho_F_3_sh_e_2 = Density(F$;P = P_cold_sh_e_2;T=T_F[3])
rho_F_sh_e_2 = (rho_F_3_sh_e_2 + rho_F_2_sh_e) / 2

DELTAP_hot_sh_e_2 = (2 * ff_hot_sh_e_2 * L_waste_water_e * convert(mm;m) *
G_hot_sh_e^(2)) / (rho_waste_water_sh_e_2 * D_h_hot_e * convert(mm;m))
DELTAP_cold_sh_e_2 = (2 * ff_cold_sh_e_2 * L_F_e * convert(mm;m) *
G_cold_sh_e^(2)) / (rho_F_sh_e_2 * D_h_cold_e * convert(mm;m))

P_hot_sh_e_3 = P_waste_water_real[2] - DELTAP_hot_sh_e_2 * convert(Pa;kPa)
P_cold_sh_e_3 = P_F_real[2] - DELTAP_cold_sh_e_2 * convert(Pa;kPa)

error_hot_sh_e_2 = abs(P_hot_sh_e_2 - P_hot_sh_e_3)
error_cold_sh_e_2 = abs(P_cold_sh_e_2 - P_cold_sh_e_3)

{Third iteration}

mu_waste_water_3_sh_e_3 = Viscosity(F$;P = P_hot_sh_e_3;T=T_waste_water[3])
mu_waste_water_sh_e_3 = (mu_waste_water_3_sh_e_3 +
mu_waste_water_2_sh_e) / 2

mu_F_3_sh_e_3 = Viscosity(F$;P = P_cold_sh_e_3;T=T_F[3])
mu_F_sh_e_3 = (mu_F_3_sh_e_3 + mu_F_2_sh_e)/2

Re_hot_sh_e_3 = (G_hot_e * D_h_hot_e*convert(mm;m)) /
mu_waste_water_sh_e_3

Re_cold_sh_e_3 = (G_cold_e * D_h_cold_e*convert(mm;m)) / mu_F_sh_e_3

ff_hot_sh_e_3 = 9,6243 * Re_hot_sh_e_3^(-0,7422) * alpha_hot_e^(-0,1856) *
delta_hot_e^(0,3053) * gamma_hot_e^(-0,2659) * (1 + (7,669 * 10^(-8) *
Re_hot_sh_e_3^(4,429) * alpha_hot_e^(0,920) * delta_hot_e^(3,767) *
gamma_hot_e^(0,236)))^(-0,1)
ff_cold_sh_e_3 = 9,6243 * Re_cold_sh_e_3^(-0,7422) * alpha_cold_e^(-0,1856) *
delta_cold_e^(0,3053) * gamma_cold_e^(-0,2659) * (1 + (7,669 * 10^(-8) *
Re_cold_sh_e_3^(4,429) * alpha_cold_e^(0,920) * delta_cold_e^(3,767) *
gamma_cold_e^(0,236)))^(-0,1)

rho_waste_water_3_sh_e_3 = Density(F$;P = P_hot_sh_e_3;T=T_waste_water[3])
rho_waste_water_sh_e_3 = (rho_waste_water_3_sh_e_3 +
rho_waste_water_2_sh_e) / 2

rho_F_3_sh_e_3 = Density(F$;P = P_cold_sh_e_3;T=T_F[3])
rho_F_sh_e_3 = (rho_F_3_sh_e_3 + rho_F_2_sh_e) / 2

DELTAP_hot_sh_e_3 = (2 * ff_hot_sh_e_3 * L_waste_water_e * convert(mm;m) *
G_hot_sh_e^(2)) / (rho_waste_water_sh_e_3 * D_h_hot_e * convert(mm;m))
DELTAP_cold_sh_e_3 = (2 * ff_cold_sh_e_3 * L_F_e * convert(mm;m) *
G_cold_sh_e^(2)) / (rho_F_sh_e_3 * D_h_cold_e * convert(mm;m))

P_hot_sh_e_4 = P_waste_water_real[2] - DELTAP_hot_sh_e_3 * convert(Pa;kPa)
P_cold_sh_e_4 = P_F_real[2] - DELTAP_cold_sh_e_3 * convert(Pa;kPa)

error_hot_sh_e_3 = abs(P_hot_sh_e_3 - P_hot_sh_e_4)
error_cold_sh_e_3 = abs(P_cold_sh_e_3 - P_cold_sh_e_4)

{Real pressure point 3}

DELTAP_hot_he_1 = DELTAP_hot_sh_e_3 + DELTAP_hot_e_2
DELTAP_cold_he_1 = DELTAP_cold_sh_e_3 + DELTAP_cold_e_2

P_waste_water_real[3] = P_hot_sh_e_4
P_F_real[3] = P_cold_sh_e_4

h_F_real[3] = Enthalpy(F$;P=P_F_real[3];T=T_F_real[3])

{Compressor}

beta_real = P_F[4] / P_F_real[3]
eta_compressor = 0,88

h_F_real[4] = h_F_real[3] + ((h_F[4] - h_F_real[3]) / eta_compressor)
T_F_real[4] = Temperature(F$;h=h_F_real[4];P=P_F[4])
P_F_real[4] = P_F[4]

G_hot_sh_c = m_dot_F / (A_ff_F_sh_c*convert(mm^2;m^2))
G_cold_sh_c = m_dot_condensate / (A_ff_condensate_sh_c*convert(mm^2;m^2))

f_s_hot_c = ((1 / n_F_c) - t_F_c)
f_s_cold_c = ((1 / n_condensate_c) - t_condensate_c)

D_h_hot_c = (4 * f_s_hot_c * l_f_hot_c * (H_F_c - t_F_c)) / (2 * (f_s_hot_c * l_f_hot_c + (H_F_c - t_F_c) * l_f_hot_c + (H_F_c - t_F_c) * t_F_c) + t_F_c * f_s_hot_c)
D_h_cold_c = (4 * f_s_cold_c * l_f_cold_c * (H_condensate_c - t_condensate_c)) / (2 * (f_s_cold_c * l_f_cold_c + (H_condensate_c - t_condensate_c) * l_f_cold_c + (H_condensate_c - t_condensate_c) * t_condensate_c) + t_condensate_c * f_s_cold_c)

Re_hot_sh_c = (G_hot_sh_c * D_h_hot_c*convert(mm;m)) / mu_F_sh_c
Re_cold_sh_c = (G_cold_sh_c * D_h_cold_c*convert(mm;m)) / mu_condensate_sh_c

alpha_hot_c = f_s_hot_c / (H_F_c - t_F_c)
alpha_cold_c = f_s_cold_c / (H_condensate_c - t_condensate_c)

delta_hot_c = t_F_c / l_f_hot_c
delta_cold_c = t_condensate_c / l_f_cold_c

gamma_hot_c = t_F_c / f_s_hot_c
gamma_cold_c = t_condensate_c / f_s_cold_c

ff_hot_sh_c = 9,6243 * Re_hot_sh_c^(-0,7422) * alpha_hot_c^(-0,1856) * delta_hot_c^(0,3053) * gamma_hot_c^(-0,2659) * (1 + (7,669 * 10^(-8) * Re_hot_sh_c^(4,429) * alpha_hot_c^(0,920) * delta_hot_c^(3,767) * gamma_hot_c^(0,236)))^(-0,1)
ff_cold_sh_c = 9,6243 * Re_cold_sh_c^(-0,7422) * alpha_cold_c^(-0,1856) * delta_cold_c^(0,3053) * gamma_cold_c^(-0,2659) * (1 + (7,669 * 10^(-8) * Re_cold_sh_c^(4,429) * alpha_cold_c^(0,920) * delta_cold_c^(3,767) * gamma_cold_c^(0,236)))^(-0,1)

DELTAP_hot_sh_c = (2 * ff_hot_sh_c * L_F_c * convert(mm;m) * G_hot_sh_c^(2)) / (rho_F_sh_c * D_h_hot_c * convert(mm;m))
DELTAP_cold_sh_c = (2 * ff_cold_sh_c * L_condensate_c * convert(mm;m) * G_cold_sh_c^(2)) / (rho_condensate_sh_c * D_h_cold_c * convert(mm;m))

P_hot_sh_c_1 = P_F_real[4] - DELTAP_hot_sh_c * convert(Pa;kPa)
P_cold_sh_c_1 = P_condensate_real[4] - DELTAP_cold_sh_c * convert(Pa;kPa)

{First iteration}

mu_condensate_5_sh_c_1 = Viscosity(F$;P = P_cold_sh_c_1;T=T_condensate[5])
mu_condensate_sh_c_1 = (mu_condensate_5_sh_c_1 + mu_condensate_4_sh_c) / 2

mu_F_5_sh_c_1 = Viscosity(F$;P = P_hot_sh_c_1;T=T_F[5])
mu_F_sh_c_1 = (mu_F_5_sh_c_1 + mu_F_4_sh_c)/2

Re_hot_sh_c_1 = (G_hot_sh_c * D_h_hot_c*convert(mm;m)) / mu_F_sh_c_1
Re_cold_sh_c_1 = (G_cold_sh_c * D_h_cold_c*convert(mm;m)) / mu_condensate_sh_c_1

ff_hot_sh_c_1 = 9,6243 * Re_hot_sh_c_1^(-0,7422) * alpha_hot_e^(-0,1856) * delta_hot_e^(0,3053) * gamma_hot_e^(-0,2659) * (1 + (7,669 * 10^(-8) * Re_hot_sh_c_1^(4,429) * alpha_hot_e^(0,920) * delta_hot_e^(3,767) * gamma_hot_e^(0,236)))^(-0,1)
ff_cold_sh_c_1 = 9,6243 * Re_cold_sh_c_1^(-0,7422) * alpha_cold_e^(-0,1856) * delta_cold_e^(0,3053) * gamma_cold_e^(-0,2659) * (1 + (7,669 * 10^(-8) * Re_cold_sh_c_1^(4,429) * alpha_cold_e^(0,920) * delta_cold_e^(3,767) * gamma_cold_e^(0,236)))^(-0,1)

rho_condensate_5_sh_c_1 = Density(F$;P = P_cold_sh_c_1;T=T_condensate[5])
rho_condensate_sh_c_1 = (rho_condensate_5_sh_c_1 + rho_condensate_4_sh_c) / 2

rho_F_5_sh_c_1 = Density(F$;P = P_hot_sh_c_1;T=T_F[5])
rho_F_sh_c_1 = (rho_F_5_sh_c_1 + rho_F_4_sh_c) / 2

DELTAP_hot_sh_c_1 = (2 * ff_hot_sh_c_1 * L_F_c * convert(mm;m) * G_hot_sh_c^(2)) / (rho_F_sh_c_1 * D_h_hot_c * convert(mm;m))
DELTAP_cold_sh_c_1 = (2 * ff_cold_sh_c_1 * L_condensate_c * convert(mm;m) * G_cold_sh_c^(2)) / (rho_condensate_sh_c_1 * D_h_cold_c * convert(mm;m))

P_hot_sh_c_2 = P_F_real[4] - DELTAP_hot_sh_c_1 * convert(Pa;kPa)
P_cold_sh_c_2 = P_condensate_real[4] - DELTAP_cold_sh_c_1 * convert(Pa;kPa)

error_hot_sh_c_1 = abs(P_hot_sh_c_1 - P_hot_sh_c_2)
error_cold_sh_c_1 = abs(P_cold_sh_c_1 - P_cold_sh_c_2)

{Second iteration}

mu_condensate_5_sh_c_2 = Viscosity(F$;P = P_cold_sh_c_2;T=T_condensate[5])
mu_condensate_sh_c_2 = (mu_condensate_5_sh_c_2 + mu_condensate_4_sh_c) / 2

mu_F_5_sh_c_2 = Viscosity(F$;P = P_hot_sh_c_2;T=T_F[5])
mu_F_sh_c_2 = (mu_F_5_sh_c_2 + mu_F_4_sh_c)/2

Re_hot_sh_c_2 = (G_hot_sh_c * D_h_hot_c*convert(mm;m)) / mu_F_sh_c_2
Re_cold_sh_c_2 = (G_cold_sh_c * D_h_cold_c*convert(mm;m)) / mu_condensate_sh_c_2

ff_hot_sh_c_2 = 9,6243 * Re_hot_sh_c_2^(-0,7422) * alpha_hot_e^(-0,1856) * delta_hot_e^(0,3053) * gamma_hot_e^(-0,2659) * (1 + (7,669 * 10^(-8) * Re_hot_sh_c_2^(4,429) * alpha_hot_e^(0,920) * delta_hot_e^(3,767) * gamma_hot_e^(0,236)))^(-0,1)
ff_cold_sh_c_2 = 9,6243 * Re_cold_sh_c_2^(-0,7422) * alpha_cold_e^(-0,1856) * delta_cold_e^(0,3053) * gamma_cold_e^(-0,2659) * (1 + (7,669 * 10^(-8) * Re_cold_sh_c_2^(4,429) * alpha_cold_e^(0,920) * delta_cold_e^(3,767) * gamma_cold_e^(0,236)))^(-0,1)

rho_condensate_5_sh_c_2 = Density(F$;P = P_cold_sh_c_2;T=T_condensate[5])
rho_condensate_sh_c_2 = (rho_condensate_5_sh_c_2 + rho_condensate_4_sh_c) / 2

rho_F_5_sh_c_2 = Density(F$;P = P_hot_sh_c_2;T=T_F[5])
rho_F_sh_c_2 = (rho_F_5_sh_c_2 + rho_F_4_sh_c) / 2

DELTAP_hot_sh_c_2 = (2 * ff_hot_sh_c_2 * L_F_c * convert(mm;m) * G_hot_sh_c^(2)) / (rho_F_sh_c_2 * D_h_hot_c * convert(mm;m))
DELTAP_cold_sh_c_2 = (2 * ff_cold_sh_c_2 * L_condensate_c * convert(mm;m) * G_cold_sh_c^(2)) / (rho_condensate_sh_c_2 * D_h_cold_c * convert(mm;m))

P_hot_sh_c_3 = P_F_real[4] - DELTAP_hot_sh_c_2 * convert(Pa;kPa)
P_cold_sh_c_3 = P_condensate_real[4] - DELTAP_cold_sh_c_2 * convert(Pa;kPa)

error_hot_sh_c_2 = abs(P_hot_sh_c_2 - P_hot_sh_c_3)
error_cold_sh_c_2 = abs(P_cold_sh_c_2 - P_cold_sh_c_3)

{Third iteration}

mu_condensate_5_sh_c_3 = Viscosity(F$;P = P_cold_sh_c_3;T=T_condensate[5])
mu_condensate_sh_c_3 = (mu_condensate_5_sh_c_3 + mu_condensate_4_sh_c) / 2

mu_F_5_sh_c_3 = Viscosity(F$;P = P_hot_sh_c_3;T=T_F[5])
mu_F_sh_c_3 = (mu_F_5_sh_c_3 + mu_F_4_sh_c)/2

Re_hot_sh_c_3 = (G_hot_sh_c * D_h_hot_c*convert(mm;m)) / mu_F_sh_c_3
Re_cold_sh_c_3 = (G_cold_sh_c * D_h_cold_c*convert(mm;m)) / mu_condensate_sh_c_3

ff_hot_sh_c_3 = 9,6243 * Re_hot_sh_c_3^(-0,7422) * alpha_hot_e^(-0,1856) * delta_hot_e^(0,3053) * gamma_hot_e^(-0,2659) * (1 + (7,669 * 10^(-8) * Re_hot_sh_c_3^(4,429) * alpha_hot_e^(0,920) * delta_hot_e^(3,767) * gamma_hot_e^(0,236)))^(-0,1)
ff_cold_sh_c_3 = 9,6243 * Re_cold_sh_c_3^(-0,7422) * alpha_cold_e^(-0,1856) * delta_cold_e^(0,3053) * gamma_cold_e^(-0,2659) * (1 + (7,669 * 10^(-8) * Re_cold_sh_c_3^(4,429) * alpha_cold_e^(0,920) * delta_cold_e^(3,767) * gamma_cold_e^(0,236)))^(-0,1)

rho_condensate_5_sh_c_3 = Density(F$;P = P_cold_sh_c_3;T=T_condensate[5])
rho_condensate_sh_c_3 = (rho_condensate_5_sh_c_3 + rho_condensate_4_sh_c) / 2

rho_F_5_sh_c_3 = Density(F$;P = P_hot_sh_c_3;T=T_F[5])
rho_F_sh_c_3 = (rho_F_5_sh_c_3 + rho_F_4_sh_c) / 2

DELTAP_hot_sh_c_3 = (2 * ff_hot_sh_c_3 * L_F_c * convert(mm;m) * G_hot_sh_c^(2)) / (rho_F_sh_c_3 * D_h_hot_c * convert(mm;m))
DELTAP_cold_sh_c_3 = (2 * ff_cold_sh_c_3 * L_condensate_c * convert(mm;m) * G_cold_sh_c^(2)) / (rho_condensate_sh_c_3 * D_h_cold_c * convert(mm;m))

P_hot_sh_c_4 = P_F_real[4] - DELTAP_hot_sh_c_3 * convert(Pa;kPa)
P_cold_sh_c_4 = P_condensate_real[4] - DELTAP_cold_sh_c_3 * convert(Pa;kPa)

error_hot_sh_c_3 = abs(P_hot_sh_c_3 - P_hot_sh_c_4)
error_cold_sh_c_3 = abs(P_cold_sh_c_3 - P_cold_sh_c_4)

{Real pressure point 5}

P_condensate_real[5] = P_cold_sh_c_4
P_F_real[5] = P_hot_sh_c_4

h_F_real[5] = Enthalpy(F$;P=P_F_real[5];x=x_F[5])
T_F_real[5] = Temperature(F$;P=P_F_real[5];x=x_F[5])

{Condenser}

G_hot_c = m_dot_F / (A_ff_F_c*convert(mm^2;m^2))
G_cold_c = m_dot_condensate / (A_ff_condensate_c*convert(mm^2;m^2))

Re_hot_c = (G_hot_c * D_h_hot_c*convert(mm;m)) / mu_F_c
Re_cold_c = (G_cold_c * D_h_cold_c*convert(mm;m)) / mu_condensate_c

ff_hot_c = 9,6243 * Re_hot_c^(-0,7422) * alpha_hot_c^(-0,1856) * delta_hot_c^(0,3053) * gamma_hot_c^(-0,2659) * (1 + (7,669 * 10^(-8) * Re_hot_c^(4,429) * alpha_hot_c^(0,920) * delta_hot_c^(3,767) * gamma_hot_c^(0,236)))^(-0,1)
ff_cold_c = 9,6243 * Re_cold_c^(-0,7422) * alpha_cold_c^(-0,1856) * delta_cold_c^(0,3053) * gamma_cold_c^(-0,2659) * (1 + (7,669 * 10^(-8) * Re_cold_c^(4,429) * alpha_cold_c^(0,920) * delta_cold_c^(3,767) * gamma_cold_c^(0,236)))^(-0,1)

DELTAP_hot_c = (2 * ff_hot_c * L_F_c * convert(mm;m) * G_hot_c^(2)) / (rho_F_c * D_h_hot_c * convert(mm;m))
DELTAP_cold_c = (2 * ff_cold_c * L_condensate_c * convert(mm;m) * G_cold_c^(2)) / (rho_condensate_c * D_h_cold_c * convert(mm;m))

P_hot_c_1 = P_F_real[5] - DELTAP_hot_c * convert(Pa;kPa)
P_cold_c_1 = P_condensate_real[5] - DELTAP_cold_c * convert(Pa;kPa)

mu_condensate_6_c_1 = Viscosity(F$;P = P_cold_c_1;T=T_condensate[6])
mu_condensate_c_1 = (mu_condensate_6_c_1 + mu_condensate_5_c) / 2

mu_F_6_c_1 = Viscosity(F$;P = P_hot_c_1;T=T_F[6])
mu_F_c_1 = (mu_F_6_c_1 + mu_F_5_c)/2

Re_hot_c_1 = (G_hot_c * D_h_hot_c*convert(mm;m)) / mu_F_c_1
Re_cold_c_1 = (G_cold_c * D_h_cold_c*convert(mm;m)) / mu_condensate_c_1

ff_hot_c_1 = 9,6243 * Re_hot_c_1^(-0,7422) * alpha_hot_e^(-0,1856) *
delta_hot_e^(0,3053) * gamma_hot_e^(-0,2659) * (1 + (7,669 * 10^(-8) *
Re_hot_c_1^(4,429) * alpha_hot_e^(0,920) * delta_hot_e^(3,767) *
gamma_hot_e^(0,236)))^(-0,1)
ff_cold_c_1 = 9,6243 * Re_cold_c_1^(-0,7422) * alpha_cold_e^(-0,1856) *
delta_cold_e^(0,3053) * gamma_cold_e^(-0,2659) * (1 + (7,669 * 10^(-8) *
Re_cold_c_1^(4,429) * alpha_cold_e^(0,920) * delta_cold_e^(3,767) *
gamma_cold_e^(0,236)))^(-0,1)

rho_condensate_6_c_1 = Density(F$;P = P_cold_c_1;T=T_condensate[6])
rho_condensate_c_1 = (rho_condensate_6_c_1 + rho_condensate_5_c) / 2

rho_F_6_c_1 = Density(F$;P = P_hot_c_1;T=T_F[6])
rho_F_c_1 = (rho_F_6_c_1 + rho_F_5_c) / 2

DELTAP_hot_c_2 = (2 * ff_hot_c_1 * L_F_c * convert(mm;m) * G_hot_c^(2)) / (
rho_F_c_1 * D_h_hot_c * convert(mm;m))
DELTAP_cold_c_2 = (2 * ff_cold_c_1 * L_condensate_c * convert(mm;m) *
G_cold_c^(2)) / (rho_condensate_c_1 * D_h_cold_c * convert(mm;m))

P_hot_c_2 = P_F_real[5] - DELTAP_hot_c_2 * convert(Pa;kPa)
P_cold_c_2 = P_condensate_real[5] - DELTAP_cold_c_2 * convert(Pa;kPa)

error_hot_c_1 = abs(P_hot_c_1 - P_hot_c_2)
error_cold_c_1 = abs(P_cold_c_1 - P_cold_c_2)

mu_condensate_6_c_2 = Viscosity(F$;P = P_cold_c_2;T=T_condensate[6])
mu_condensate_c_2 = (mu_condensate_6_c_2 + mu_condensate_5_c) / 2

mu_F_6_c_2 = Viscosity(F$;P = P_hot_c_2;T=T_F[6])
mu_F_c_2 = (mu_F_6_c_2 + mu_F_5_c)/2

Re_hot_c_2 = (G_hot_c * D_h_hot_c*convert(mm;m)) / mu_F_c_2
Re_cold_c_2 = (G_cold_c * D_h_cold_c*convert(mm;m)) / mu_condensate_c_2

ff_hot_c_2 = 9,6243 * Re_hot_c_2^(-0,7422) * alpha_hot_e^(-0,1856) *
delta_hot_e^(0,3053) * gamma_hot_e^(-0,2659) * (1 + (7,669 * 10^(-8) *
Re_hot_c_2^(4,429) * alpha_hot_e^(0,920) * delta_hot_e^(3,767) *
gamma_hot_e^(0,236)))^(-0,1)
ff_cold_c_2 = 9,6243 * Re_cold_c_2^(-0,7422) * alpha_cold_e^(-0,1856) *
delta_cold_e^(0,3053) * gamma_cold_e^(-0,2659) * (1 + (7,669 * 10^(-8) *
Re_cold_c_2^(4,429) * alpha_cold_e^(0,920) * delta_cold_e^(3,767) *
gamma_cold_e^(0,236)))^(-0,1)

rho_condensate_6_c_2 = Density(F$;P = P_cold_c_2;T=T_condensate[6])
rho_condensate_c_2 = (rho_condensate_6_c_2 + rho_condensate_5_c) / 2

rho_F_6_c_2 = Density(F$;P = P_hot_c_2;T=T_F[6])
rho_F_c_2 = (rho_F_6_c_2 + rho_F_5_c) / 2

DELTAP_hot_c_3 = (2 * ff_hot_c_2 * L_F_c * convert(mm;m) * G_hot_c^(2)) / (
rho_F_c_2 * D_h_hot_c * convert(mm;m))
DELTAP_cold_c_3 = (2 * ff_cold_c_2 * L_condensate_c * convert(mm;m) *
G_cold_c^(2)) / (rho_condensate_c_2 * D_h_cold_c * convert(mm;m))

P_hot_c_3 = P_F_real[5] - DELTAP_hot_c_3 * convert(Pa;kPa)
P_cold_c_3 = P_condensate_real[5] - DELTAP_cold_c_3 * convert(Pa;kPa)

error_hot_c_2 = abs(P_hot_c_2 - P_hot_c_3)
error_cold_c_2 = abs(P_cold_c_2 - P_cold_c_3)

{Real pressure point 6}

P_condensate_real[6] = P_cold_c_3
P_F_real[6] = P_hot_c_3

h_F_real[6] = Enthalpy(F$;P=P_F_real[6];x=x_F[6])
T_F_real[6] = Temperature(F$;P=P_F_real[6];x=x_F[6])

{Subcooler of the condenser}

G_hot_sc_c = m_dot_F / (A_ff_F_sc_c*convert(mm^2;m^2))
G_cold_sc_c = m_dot_condensate / (A_ff_condensate_sc_c*convert(mm^2;m^2))

Re_hot_sc_c = (G_hot_sc_c * D_h_hot_c*convert(mm;m)) / mu_F_sc_c
Re_cold_sc_c = (G_cold_sc_c * D_h_cold_c*convert(mm;m)) / mu_condensate_sc_c

ff_hot_sc_c = 9,6243 * Re_hot_sc_c^(-0,7422) * alpha_hot_c^(-0,1856) *
delta_hot_c^(0,3053) * gamma_hot_c^(-0,2659) * (1 + (7,669 * 10^(-8) *
Re_hot_sc_c^(4,429) * alpha_hot_c^(0,920) * delta_hot_c^(3,767) *
gamma_hot_c^(0,236)))^(-0,1)
ff_cold_sc_c = 9,6243 * Re_cold_sc_c^(-0,7422) * alpha_cold_c^(-0,1856) *
delta_cold_c^(0,3053) * gamma_cold_c^(-0,2659) * (1 + (7,669 * 10^(-8) *
Re_cold_sc_c^(4,429) * alpha_cold_c^(0,920) * delta_cold_c^(3,767) *
gamma_cold_c^(0,236)))^(-0,1)

DELTAP_hot_sc_c = (2 * ff_hot_sc_c * L_F_c * convert(mm;m) * G_hot_sc_c^(2)) / (rho_F_sc_c * D_h_hot_c * convert(mm;m))
DELTAP_cold_sc_c = (2 * ff_cold_sc_c * L_condensate_c * convert(mm;m) * G_cold_sc_c^(2)) / (rho_condensate_sc_c * D_h_cold_c * convert(mm;m))

P_hot_sc_c_1 = P_F_real[6] - DELTAP_hot_sc_c * convert(Pa;kPa)
P_cold_sc_c_1 = P_condensate_real[6] - DELTAP_cold_sc_c * convert(Pa;kPa)

{First iteration}

mu_condensate_7_sc_c_1 = Viscosity(F$;P = P_cold_sc_c_1;T=T_condensate[7])
mu_condensate_sc_c_1 = (mu_condensate_7_sc_c_1 + mu_condensate_6_sc_c) / 2

mu_F_7_sc_c_1 = Viscosity(F$;P = P_hot_sc_c_1;T=T_F[7])
mu_F_sc_c_1 = (mu_F_7_sc_c_1 + mu_F_6_sc_c)/2

Re_hot_sc_c_1 = (G_hot_sc_c * D_h_hot_c*convert(mm;m)) / mu_F_sc_c_1
Re_cold_sc_c_1 = (G_cold_sc_c * D_h_cold_c*convert(mm;m)) / mu_condensate_sc_c_1

ff_hot_sc_c_1 = 9,6243 * Re_hot_sc_c_1^(-0,7422) * alpha_hot_e^(-0,1856) * delta_hot_e^(0,3053) * gamma_hot_e^(-0,2659) * (1 + (7,669 * 10^(-8) * Re_hot_sc_c_1^(4,429) * alpha_hot_e^(0,920) * delta_hot_e^(3,767) * gamma_hot_e^(0,236)))^(-0,1)
ff_cold_sc_c_1 = 9,6243 * Re_cold_sc_c_1^(-0,7422) * alpha_cold_e^(-0,1856) * delta_cold_e^(0,3053) * gamma_cold_e^(-0,2659) * (1 + (7,669 * 10^(-8) * Re_cold_sc_c_1^(4,429) * alpha_cold_e^(0,920) * delta_cold_e^(3,767) * gamma_cold_e^(0,236)))^(-0,1)

rho_condensate_7_sc_c_1 = Density(F$;P = P_cold_sc_c_1;T=T_condensate[7])
rho_condensate_sc_c_1 = (rho_condensate_7_sc_c_1 + rho_condensate_6_sc_c) / 2

rho_F_7_sc_c_1 = Density(F$;P = P_hot_sc_c_1;T=T_F[7])
rho_F_sc_c_1 = (rho_F_7_sc_c_1 + rho_F_6_sc_c) / 2

DELTAP_hot_sc_c_2 = (2 * ff_hot_sc_c_1 * L_F_c * convert(mm;m) * G_hot_sc_c^(2)) / (rho_F_sc_c_1 * D_h_hot_c * convert(mm;m))
DELTAP_cold_sc_c_2 = (2 * ff_cold_sc_c_1 * L_condensate_c * convert(mm;m) * G_cold_sc_c^(2)) / (rho_condensate_sc_c_1 * D_h_cold_c * convert(mm;m))

P_hot_sc_c_2 = P_F_real[6] - DELTAP_hot_sc_c_2 * convert(Pa;kPa)
P_cold_sc_c_2 = P_condensate_real[6] - DELTAP_cold_sc_c_2 * convert(Pa;kPa)

error_hot_sc_c_1 = abs(P_hot_sc_c_1 - P_hot_sc_c_2)
error_cold_sc_c_1 = abs(P_cold_sc_c_1 - P_cold_sc_c_2)

{Second iteration}

mu_condensate_7_sc_c_2 = Viscosity(F$;P = P_cold_sc_c_2;T=T_condensate[7])
mu_condensate_sc_c_2 = (mu_condensate_7_sc_c_2 + mu_condensate_6_sc_c) / 2

mu_F_7_sc_c_2 = Viscosity(F$;P = P_hot_sc_c_2;T=T_F[7])
mu_F_sc_c_2 = (mu_F_7_sc_c_2 + mu_F_6_sc_c)/2

Re_hot_sc_c_2 = (G_hot_sc_c * D_h_hot_c*convert(mm;m)) / mu_F_sc_c_2
Re_cold_sc_c_2 = (G_cold_sc_c * D_h_cold_c*convert(mm;m)) / mu_condensate_sc_c_2

ff_hot_sc_c_2 = 9,6243 * Re_hot_sc_c_2^(-0,7422) * alpha_hot_e^(-0,1856) * delta_hot_e^(0,3053) * gamma_hot_e^(-0,2659) * (1 + (7,669 * 10^(-8) * Re_hot_sc_c_2^(4,429) * alpha_hot_e^(0,920) * delta_hot_e^(3,767) * gamma_hot_e^(0,236)))^(-0,1)
ff_cold_sc_c_2 = 9,6243 * Re_cold_sc_c_2^(-0,7422) * alpha_cold_e^(-0,1856) * delta_cold_e^(0,3053) * gamma_cold_e^(-0,2659) * (1 + (7,669 * 10^(-8) * Re_cold_sc_c_2^(4,429) * alpha_cold_e^(0,920) * delta_cold_e^(3,767) * gamma_cold_e^(0,236)))^(-0,1)

rho_condensate_7_sc_c_2 = Density(F$;P = P_cold_sc_c_2;T=T_condensate[7])
rho_condensate_sc_c_2 = (rho_condensate_7_sc_c_2 + rho_condensate_6_sc_c) / 2

rho_F_7_sc_c_2 = Density(F$;P = P_hot_sc_c_2;T=T_F[7])
rho_F_sc_c_2 = (rho_F_7_sc_c_2 + rho_F_6_sc_c) / 2

DELTAP_hot_sc_c_3 = (2 * ff_hot_sc_c_2 * L_F_c * convert(mm;m) * G_hot_sc_c^(2)) / (rho_F_sc_c_2 * D_h_hot_c * convert(mm;m))
DELTAP_cold_sc_c_3 = (2 * ff_cold_sc_c_2 * L_condensate_c * convert(mm;m) * G_cold_sc_c^(2)) / (rho_condensate_sc_c_2 * D_h_cold_c * convert(mm;m))

P_hot_sc_c_3 = P_F_real[6] - DELTAP_hot_sc_c_3 * convert(Pa;kPa)
P_cold_sc_c_3 = P_condensate_real[6] - DELTAP_cold_sc_c_3 * convert(Pa;kPa)

error_hot_sc_c_2 = abs(P_hot_sc_c_2 - P_hot_sc_c_3)
error_cold_sc_c_2 = abs(P_cold_sc_c_2 - P_cold_sc_c_3)

{Third iteration}

mu_condensate_7_sc_c_3 = Viscosity(F$;P = P_cold_sc_c_3;T=T_condensate[7])
mu_condensate_sc_c_3 = (mu_condensate_7_sc_c_3 + mu_condensate_6_sc_c) / 2

mu_F_7_sc_c_3 = Viscosity(F$;P = P_hot_sc_c_3;T=T_F[7])
mu_F_sc_c_3 = (mu_F_7_sc_c_3 + mu_F_6_sc_c)/2

Re_hot_sc_c_3 = (G_hot_sc_c * D_h_hot_c*convert(mm;m)) / mu_F_sc_c_3

Re_cold_sc_c_3 = (G_cold_sc_c * D_h_cold_c*convert(mm;m)) / mu_condensate_sc_c_3

ff_hot_sc_c_3 = 9,6243 * Re_hot_sc_c_3^(-0,7422) * alpha_hot_e^(-0,1856) * delta_hot_e^(0,3053) * gamma_hot_e^(-0,2659) * (1 + (7,669 * 10^(-8) * Re_hot_sc_c_3^(4,429) * alpha_hot_e^(0,920) * delta_hot_e^(3,767) * gamma_hot_e^(0,236)))^(-0,1)
ff_cold_sc_c_3 = 9,6243 * Re_cold_sc_c_3^(-0,7422) * alpha_cold_e^(-0,1856) * delta_cold_e^(0,3053) * gamma_cold_e^(-0,2659) * (1 + (7,669 * 10^(-8) * Re_cold_sc_c_3^(4,429) * alpha_cold_e^(0,920) * delta_cold_e^(3,767) * gamma_cold_e^(0,236)))^(-0,1)

rho_condensate_7_sc_c_3 = Density(F$;P = P_cold_sc_c_3;T=T_condensate[7])
rho_condensate_sc_c_3 = (rho_condensate_7_sc_c_3 + rho_condensate_6_sc_c) / 2

rho_F_7_sc_c_3 = Density(F$;P = P_hot_sc_c_3;T=T_F[7])
rho_F_sc_c_3 = (rho_F_7_sc_c_3 + rho_F_6_sc_c) / 2

DELTAP_hot_sc_c_4 = (2 * ff_hot_sc_c_3 * L_F_c * convert(mm;m) * G_hot_sc_c^(2)) / (rho_F_sc_c_3 * D_h_hot_c * convert(mm;m))
DELTAP_cold_sc_c_4 = (2 * ff_cold_sc_c_3 * L_condensate_c * convert(mm;m) * G_cold_sc_c^(2)) / (rho_condensate_sc_c_3 * D_h_cold_c * convert(mm;m))

P_hot_sc_c_4 = P_F_real[6] - DELTAP_hot_sc_c_4 * convert(Pa;kPa)
P_cold_sc_c_4 = P_condensate_real[6] - DELTAP_cold_sc_c_4 * convert(Pa;kPa)

error_hot_sc_c_3 = abs(P_hot_sc_c_3 - P_hot_sc_c_4)
error_cold_sc_c_3 = abs(P_cold_sc_c_3 - P_cold_sc_c_4)

{Real pressure point 7}

P_condensate_real[7] = P_cold_sc_c_4
P_F_real[7] = P_hot_sc_c_4

h_F_real[7] = Enthalpy(F$;P=P_F_real[7];T=T_F_real[7])
T_F_real[7] = T_F_real[6] - DELTAT_sc

DELTAP_hot_he_2 = DELTAP_hot_sc_c_4 + DELTAP_hot_c_3 + DELTAP_hot_sh_c_3
DELTAP_cold_he_2 = DELTAP_cold_sc_c_4 + DELTAP_cold_c_3 + DELTAP_cold_sh_c_3

COP_real_cycle = (h_F_real[3] - h_F_real[1]) / (h_F_real[4] - h_F_real[3])

{Economic analysis}

N_work_hours_year = 8000 [h/year]
N_year = 20 [year]

Cost_he_1=635,14*A_he_1^0,778*0,81553
Cost_he_2=635,14*A_he_2^0,778*0,81553

W_dot_compressor = ((h_F[4] - h_F_real[3]) / eta_compressor) * m_dot_F
C_operating_compressor = ((h_F[4] - h_F_real[3]) / eta_compressor) *
convert(kJ/s;kW) * m_dot_F * N_work_hours_year * 0,065
C_operating_compressor_act =
sum(((C_operating_compressor*0,81553)/(1+0,1)^l);l=1;N_year)

C_investment_compressor=3,11 * 2517 * W_dot_compressor^0,7849

C_mantenience_compressor = C_investment_compressor * 0,1
{10% of the compressor cost}
C_mantenience_c_actualyzed =
sum((C_mantenience_compressor/(1+0,1)^l);l=1;N_year)

C_total = Cost_he_1 + Cost_he_2 + C_investment_compressor +
C_operating_compressor_act + C_mantenience_c_actualyzed

saving = Q_he_2 * convert(kJ/s;kW) * N_work_hours_year * 0,0834
saving_actualyzed=sum((saving/(1+0,1)^l);l=1;N_year)

net_saving = saving_actualyzed - C_total
{Enviromental analysis}

SEF_Europe = 0,460 [tonCO_2/MWh]
SEF_Scandinavian_countries = 0,222 [tonCO_2/MWh]

SEF_gas_oil = 0,267 [tonCO_2/MWh]
SEF_residual_oil = 0,279 [tonCO_2/MWh]

CO2_e_HP_year_europe = (((h_F[4] - h_F_real[3]) / eta_compressor) *
convert(kJ/s;kW) * m_dot_F * N_work_hours_year) * (SEF_europe * 10^(-3))
CO2_e_HP_life_europe = CO2_e_HP_year_europe * N_year

CO2_e_HP_year_Scandinavia = (((h_F[4] - h_F_real[3]) / eta_compressor) *
convert(kJ/s;kW) * m_dot_F * N_work_hours_year) * (SEF_Scandinavian_countries *
10^(-3))
CO2_e_HP_life_Scandinavia = CO2_e_HP_year_Scandinavia * N_year

CO2_emission_boiler_go_year = Q_he_2 * convert(kJ/s;kW) * N_work_hours_year *
SEF_gas_oil * 10^(-3)
CO2_emission_boiler_go_life = CO2_emission_boiler_go_year * N_year
CO2_emission_boiler_ro_year = Q_he_2 * convert(kJ/s;kW) * N_work_hours_year *
SEF_residual_oil * 10^(-3)
CO2_emission_boiler_ro_life = CO2_emission_boiler_ro_year * N_year

Efficient heat recovery from industrial processes using heat pump: A review

Pierfrancesco Fava

Department of Energy and Process Engineering
Norwegian University of Science and Technology
27.01.2016

Abstract

The main aim of this thesis is to show the possibilities that heat pumps hold within the industrial sectors in high-temperature applications, easing their inclusion within this field.The developed case of study is a highly efficient heat recovery system for industrial applications using HP technology. This system is to be inserted into the Kyknos transformation implant, located in Savalia, Greece, a factory that uses fresh vegetables to produce all kinds of canned tomato products. It will estimate its performances, especially the reduction of primary energy consumption, within a broader analysis of the pollutants released and of its economic efficiency, by drawing a comparison with the same situation if the recovery system had not been used.

Introduction

According to the International Energy Agency, the industrial sector absorbs 31% of the primary energy generated globally, only a little less than the transportation sector. It is clear that these systems need improvement, if we wish to strongly reduce polluting emissions.

In order to do so, there is a tendency to reduce the consumption of primary energy by recovering heat and materials that would otherwise become waste.

Heat pumps technology is making its way in this trend: it has already been used for some time in space heating and, more recently, in the industrial sector.

This system allows heat recovery from a low temperature source to a source with a higher energetic level by introducing work in the system. The result of this technology, therefore, is the reduction of primary energy within a process, but not its complete substitution. This technology is mainly applied to low temperatures, with a few cases of temperature raising above 80 °C, even though it is already well-established for a number of industrial processes, such as wood drying, and in the food and chemical industry.

For this reason, studies on pilot plants are carried out in order to establish this technology fit also for these uses, which will surely give high benefits as a result.

I gave a great deal of importance to the choice of the refrigerant fluid, which has been chosen among a range of natural fluids. To make this choice, simulations for each refrigerant fluid selected for the study have been carried out using the Engineering Equation Solver software, which helped in determining the most performant fluid for the specific given case.

Case of Study

The developed case of study is a highly efficient heat recovery system for industrial applications using HP technology. This system is to be inserted into the Kyknos transformation implant, located in Savalia,

1

Greece, a factory that uses fresh vegetables to produce all kinds of canned tomato products. This project is part of a broader European project to reduce emissions.

The main energy consuming process of the implant is the generation of steam at 180° C of temperature and 10 bar of pressure, which is used for treating vegetables, peeling and cooking tomatoes, thermic treatments on vegetables, cooking and sterilization of the cookers. Four oil powered boilers currently produce the steam flow.

Another important stream within the implant is the waste water flow, containing tomato particles that shall later be filtrated.

Finally there is the high temperature condense and pressure which are sent to the boilers, which will then produce the steam used by the implant internally. The table below shows the characteristics of the stream analyzed above.

Stream	Temperature [°C]	Pressure [bar]
Steam	180	10
Waste water	50	1
Condensate	95	10

Table1: Stream Summary

The purpose of this heat recovery system is to absorb heat from the waste water flow, downstream of the filtering, raise its temperature level and release it to the stream of condense going towards the boilers in order to pre-heat it and thus reduce the fuel consumption of the boilers.

To obtain this result, a Mechanical Vapour Compression heat pump (MVC) is used: it will work between the temperatures supplied by the manager of the factory, as shown below.

Stream	Mass flow [ton/h]	Inflow Temp. [°C]	Outflow Temp. [°C]
Waste water	20	50	47
Condensate	16	95	100

Table 2: HP stream characteristic

The study has been conducted taking into account the limits of the temperatures of the thermic sources mentioned above.

The following figure shows the layout of the implant, with all the equipment necessary for its working.
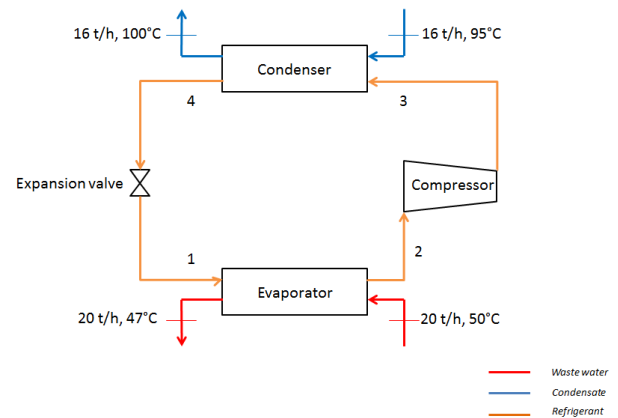
Figure 1: HP layout

As the diagram above shows, there are an evaporator, a compressor, a condenser and an expansion valve. Considering the refrigerant's cycle within the implant, the following conditions will take place in quick succession:

1. low-temperature heat, necessary for the refrigerant evaporation, is exchanged within the evaporator;
2. the steam is sent to the compressor where its energetic level is increased;
3. the steam is sent to the condenser, where it will release heat at high temperature;
4. the condense is dispatched to the expansion valve that brings the fluid back to its initial conditions.

Further considerations can be made about the refrigerant. Because of the nature of this project, only natural fluids were used, since they present a limited danger for the environment. A list of refrigerants particularly appropriate for this process was drawn up from academic literature, with special regards to the constraints on the maximum

2

permissible operating temperatures and their critical pressure.

Below is the list of the refrigerants which will be used in the study reported here:

Ammonia (R-717)

Butane (R-600)

Isobutane (R-600a)

R-245fa

Even though the latter is not a natural refrigerant, it was used in the study to make a comparison with the traditional refrigerants (HFC).

Hypothesis and boundary conditions

For the definition of the system and the evaluation of its performances, a simulation model was created with the aid of the Engineering Equation Solver (EES) software.

It is to be noted that the almost static case will be considered, thus without analyzing how the system works during its startup and switch off, and generally during transients.

When considering the heat exchange, the supposition was that no heat losses towards the exterior would occur, considering the heat exchangers as adiabatic. The heat exchange along the longitudinal wall was neglected and the phase changings were considered happening at stable pressure and temperature. [1]

First of all, the ideal study of the system was considered, adding further hypothesis later on, which would then be removed during the analysis of the real case.

The losses within the heat exchangers were ignored, the compression is considered isentropic and the expansion inside the valve isenthalpic.

Ideal Model

In order to determine the cycle of the heat pump, the starting point was the evaporator outlet section. Considering the superheating temperature difference in this point, the minimum temperature at which two fluids inside the first exchanger can be close is recorded. The temperature of the fluid entering the compressor was thus determined.

Since the inlet temperature is known, by removing the difference of superheating temperature the result will be the temperature of the working fluid at the end of the evaporation stage. This point can be determined since the temperature of the fluid and its strength are both known. Using specific functions implemented in the software, it was possible to determine all of the thermo-dynamical properties of the fluid in this state.

Using these functions, if two thermo-dynamical properties of a fluid in the same state are known, it is possible to determine any other of its proprieties, given that the fluid is listed in the database. The following function was used in this particular case. Similar functions were used in other sections of the heat exchanger.

$$P_i = pressure(T = T_i; x = x_i)$$

The pressure when exiting the evaporator is then determined; the pressure drops within the heat exchangers will be ignored, since we are analyzing the ideal case. It is clear that the pressure and temperature when entering the exchanger are known. This is a bivariate area, so the enthalpy of the entering section of the evaporator is not known, but it will be determined later with the analysis of the condenser.

The following chart shows the typical trend of a heat exchange inside the evaporator.

Figure 2: Heat transfer of the evaporator R-717

The following step is the analysis of the second heat exchanger. There is an area where the vapour exiting from the compressor is de-superheated, and another where the condensation of the refrigerant occurs, followed by a sub-cooling process until the desired temperature is reached. Therefore, it is more complicated to identify the section where the minimal temperature approach occurs. To do so, another temperature difference - called approach temperature difference ($\Delta T_{approch}$) – is defined: it represents the difference between the considerable temperature of the inlet fluid and that of the fluid flowing out of one of the ends of the exchangers. In this case, the ingoing fluid will be the condense that will be heated, and the outflowing fluid will be the refrigerant. This means that, if we change this parameter, we can change the extent of the minimum temperature approach between the fluids.

This parameter is set to 10°C.

By doing so, the thermodynamic characteristics of the end of the condensation are defined univocally. The temperature of the fluid to which heat is going to be released is added to the sub-cooling temperature difference and the approach temperature difference. The function is as follows:

$$T_{F_6} = T_{condensate_6} + \Delta T_{sc} + \Delta T_{approch}$$

After determining this temperature value, since it has to be on the lower limiting curve,

we can find pressure, enthalpy and entropy using the aforementioned functions.

Consequently, the characteristic of the beginning of condensation can be determined, since temperature and strength are known and that section needs to be on the upper limiting curve.

The point of compression end can be determined, ignoring also the pressure drops this time, for the same reasons explained before. Knowing the pressure inside the condenser, and since the compression is isentropic, the characteristics of the end of the compression are determined univocally.

In the same way, the characteristics of the refrigerant coming out of the heat exchanger are determined.

Once the enthalpy of the refrigerant fluid coming out of the condenser is determined, it is possible to define the starting point of the vaporization inside the first heat exchanger thanks to an isenthalpic expansion inside a valve.

The following is the typical trend of the process inside a condenser.

Figure 3: Heat transfer of the condenser R-717

In order to determine ΔT_{pp} inside the condenser and identify the section in which it will be positioned, it is necessary to apply the energy conservation equation to the different sections of the second exchanger, and to verify where the minimum temperature difference between the two fluids occurs.

4

By fixing the temperatures of the sources, it is possible to determine the ideal cycle of the heat pump.

The following image is the ideal cycle of an HP which uses R – 717 as a refrigerant in the p – h planes. When the same considerations are applied to the other refrigerant fluids, the results are similar graphics that can be found in the appendixes of this writing.

Figure 4: Ideal Cycle for R-717

Preliminary dimensioning of the machines

Once the cycle of the HP is determined, it is necessary to dimension the other machines. The process focused more on the heat exchangers, while the compressor was chosen from a catalogue.

The information needed for choosing the compressor is: the volumetric flow rate of the fluid transitioning, the maximum exhaust temperature, the pressure reached by the system, and the pressure ratio that the compressor needs.

In order to determine this information, the following equation of energy conservation needs to be applied. The function is applied to the first heat exchanger in the case of the stream from which heat needs to be recovered – which is the stream of waste water.

$$Q_{he_1} = \dot{m}_{waste\ water}(h_{waste\ water_3} - h_{waste\ water_1})$$

Through this process, we could determine the heat exchanged by the first heat exchanger. Applying the same equation to the refrigerant fluid, while knowing the enthalpies when entering and exiting the machine, the refrigerant mass flow can be determined.

To choose the compressor from a catalogue, we will need to determine the volumetric flow rate.

The last value necessary is the compression pressure ratio, that is defined as the ratio between the maximum and minimum pressure of the cycle.

$$\beta = \frac{P_{max}}{P_{min}}$$

First of all, in order to design the heat exchanger, it is necessary to choose the refrigerant fluid that will be used, and the operating pressures and temperature.

Later, we will need to choose the kind of heat exchanger to be used. In this case study, there are two possible scenarios: the first one employs a shell and tube heat exchanger, while the second one uses compact plate-fin exchangers.

The first step is the thermic sizing of the heat exchanger using the $\varepsilon - NTU$ method, that I will briefly describe.

This method expresses the exchanged heat using the following equation:

$$Q = \varepsilon C_{min}(T_{hi} - T_{Ci})$$

ε is the efficiency of the heat exchanger, which is defined as the ration between the thermic power exchanged in the analyzed conditions, and the maximum thermic power that could be exchanged – such as in the case of infinite exchange surfaces.

$$\varepsilon = \frac{Q}{Q_\infty}$$

5

Within the ratio, the minimum per hour thermic capacity of the fluids employed in the thermic exchange C_{min} is taken into consideration; it is the result of the mass flow for the specific heat at constant pressure.

For this method to be applicable, the value needs to be constant. For this exact reason, we will perform a separate analysis for each portion of the exchanger where a significant change of the per hour thermic capacity occurs, as in the case of the phase change of the refrigerant. Each portion of the exchanger thus identified will be consequently considered as a separate machine.

Because of this, the analysis of the exchangers inside the model has been split in different parts. For the first exchanger, two areas were identified: the evaporator and the superheater. The second exchanger, on the other hand, has an area where the vapour is de-superheated, an area where the condensation occurs, and another area where the steam is subcooled.

The number of transfert unit NTU is defined as:

$$NTU = \frac{uA}{C_{min}}$$

Where A is the surface through which the heat exchange happens, and u is the global heat exchange coefficient.

Using the considerations drawn from the energy conservation equation, the exchanged thermic power was determined; moreover, since the cycle was defined, the temperatures are known. Therefore, it is possible to calculate the heat exchanger efficiency. [2]

After calculating its efficiency, the following ratio can be used to determine the value of NTU:

$$NTU = \frac{\ln(\frac{1 - \varepsilon C_R}{1 - \varepsilon})}{(1 - C_R)}$$

This equation can be applied only to counterflow shell and tube exchangers with only one tubepass -side, with no phase change occurring. The term C_R represents the ratio between the maximum and minimum thermic capacity of the fluids involved in the heat exchange.

$$C_R = \frac{C_{max}}{C_{min}}$$

The equation is not valid, however, when a phase change occurs, since the fluid affected by this phenomenon will have a per hour thermic capacity that will tend towards infinity, therefore the parameter will have that same value.

In this case, the equation that needs to be used is the following:

$$NTU = -\ln(1 - \varepsilon)$$

The next value to be determined is the exchange surface of the evaporator. To do so, we first need to find the global heat exchange coefficient of this scenario, which is not known to us beforehand.

The following equation designs a method used to determine the global heat exchange coefficient:

$$U = \left(\left(\frac{1}{\alpha_{shell}}\right) + R_{shell} + \left(\frac{d_{internal}}{d_{external}}\right)(R_{tube} + \left(\frac{1}{\alpha_{tube}}\right))\right)^{-1}$$

The values R_{tube} and R_{shell} respectively represent the coefficients of tube side and shell side fouling. These status parameters can reduce the global heat exchange coefficient, so as to oversize the exchange surfaces to take into account the fouling of the surfaces, a consequence of the regular use of the machine.

The latter coefficient has been determined for both the exchangers using appropriate values drawn from the literature. [3] In order to determine the tube side coefficient, the

following formulation by Dittus-Boelter [4] was employed:

$$\alpha_{tube} = 0{,}023 \left(\frac{\lambda_{tube}}{d_{internal}}\right) Re_{tube}^{0,8} Pr_{tube}^{(1/3)}$$

The formulation can only be applied to the liquid phase; determining the coefficient during the phase change appears to be more complex.

Nevertheless, a specific database inside the software can be used to calculate the average exchange coefficient inside the tubes if phase change should occur.

This function takes into account convective and nucleation-evaporation, according to Saha's reports (1982) [5]

$$\alpha_{tube} = Flow_{Boiling,\text{avg}}(\text{Fluid}; \text{T}_{\text{sat}}; \text{G}_{tube}; \text{d}_{internal}; \text{x}_{in}; \text{x}_{out}; q''; Horizontal)$$

Where *G* is the mass velocity, which represents the mass flow for surface unit represented by the passage surface and q" is the thermic power for surface unit.

A similar function was used when considering condensation. The only further parameter needed was the wall temperature of the tubes during condensation. The following formulation is how the function was reported inside the code.

$$\alpha_{tube} = Cond_{horizontube,\text{avg}}(\text{Fluid}; \text{T}_{\text{sat}}; \text{T}_{\text{wall}}; \dot{m}; \text{d}_{internal}; \text{x}_{in}; \text{x}_{out})$$

It is now possible to calculate the global heat exchange coefficient for the exchanger or a section of it.

Plate and fin heat exchangers has similar relations with regards to its thermal dimensioning.

On the other hand, the process to calculate the heat exchange coefficient is different. In this case, given how difficult it is to determine the exchange coefficient if a phase change is occurring, the choice has been to increase by

30% the exchange coefficient identified for the shell and tube exchanger. The experience has later validated this choice.
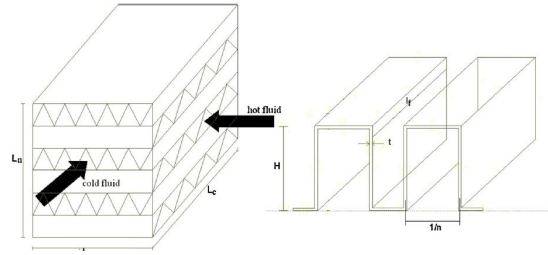
Figure 5: Plate & Fin heat exchanger layout (V. Patel 2014)

At this point, it is necessary to define two surfaces, one touched by the hot fluid and the other one touched by the cold fluid; their sum will determine the total heat exchange surface, on which the cost of the machine will depend, among other factors.

Following are the relations used to determine such surfaces. [6]

$$A_h = L_h L_c N_h [1 + 2n_h(H_h - t_h)]$$

$$A_c = L_c L_h N_c [1 + 2n_c(H_c - t_c)]$$

$$A = A_h + A_c$$

For this type of machinery, it is also necessary to determine the passage surface, which does not appear to be immediate, due to the particular arrangement of the corrugated sheets. The following formulations relate to this issue.

$$A_{ff_h} = (H_h - t_h)(1 - n_h t_h)L_c N_h$$

$$A_{ff_c} = (H_c - t_c)(1 - n_c t_c)L_h N_c$$

Real model

In order to determine the characteristics of the equipment, the ideal cycle needed to be defined; the definition of the real cycle, on the other hand, needed the determination of the actual characteristics of the implant components.
Once the temperature of the refrigerant entering the compressor is known, it is necessary to determine the temperature at

the end of the compression. Knowing the compression end pressure, a result drawn from the analysis of the ideal cycle, will allow to univocally define such point on the plane *p-h*. This is because, despite the ideal case conditions, the compression is not isentropic anymore, consequently pressure drops will occur, which will generate entropy and thus result in a further increase of the temperature of the cooling fluid after going through the compression.

The pressure at the beginning of the compression is already known in the light of the considerations that will be made further on in the study; thus, the next step is to calculate the actual pressure ratio of compression, using the same formulation shown in the previous chapters.

Once this is done and the compressor is chosen from catalog as shown above, the determination of the isentropic efficiency of the compressor is carried out: this can be easily achieved from the nameplate information of the component.

We then proceed to calculate the enthalpy of the end compression using the following formulation.

$$h_{F\,real4} = h_{F\,real3} + \frac{(h_{F4} - h_{F\,real3})}{\eta_{compressor}}$$

After calculating this value and knowing the pressure of the compression end, the point is determined univocally; the appropriate functions within the software mentioned previously can now determine the remaining thermodynamic properties of the refrigerant.

For the calculation of the real cycle, the starting point was the input section of the first heat exchanger.

Firstly, the pressure and temperature of the entering point to the evaporator were fixed. The methodology here described determined the conditions occurring when leaving the exchanger.

The correlations reported in the following paragraphs were used to calculate the pressure drops within the tubes, with the average thermodynamic properties of the fluid in the evaporator inlet sections and in the section at the end of the evaporation process referring to the ideal case. After determining the pressure drops of the given section, the new pressure at the end of the evaporation process in the heat exchanger was determined; knowing its title allows to determine, using the functions implemented within the software, the new outlet temperature of that section of the tube bundle.

At this point, pressure drops were calculated again using the average properties and updating them with the new pressures and temperatures found. A new value for the pressure drops is thus determined; lastly, the new pressure and temperature of the end of evaporation section are calculated.

This process is iterative; it repeats itself until the conditions previously chosen occur.

An error δ is defined: it identifies the difference between the pressure found in the previous case, and the pressure found in the following case. If the value is less than $10^{-3}\,Pa$, the process stops, because the real pressure at the end of the analyzed portion of the exchanger has been found.

A clearer definition of the error is shown below.

$$\delta_i = P_{i-1} - P_i$$

The procedure must be repeated for each portion taken into consideration during the dimensioning of the heat exchanger.

The process for the second heat exchanger is similar; the only difference is that the thermodynamic characteristics at the end of the compression are known.

8

The same procedure was used to determine the real cycle with the aid of the compact plate-fin heat exchangers.

The formulas below were used for the calculation of the pressure drops inside the exchangers; the analysis of shell and tube exchangers will come first, followed by that of plate-fin exchangers.

When talking about shell and tube exchangers, it is important to separate what happens on the tube side and what happens on the shell side. [18]

The formulation used in this case is the following:

$$\Delta P_{shell} = \frac{\rho_{shell} v_{shell}^2}{2} f_{shell} n_{pass_{shell}} \left(\frac{L}{b}\right) \left(\frac{D_{internal_{shell}}}{D_{eq}}\right)$$

This equation appears to be valid if the Reynolds number values on the shell side are less than 40000.

There are various geometric factors inside the formulation: the diameter of the shell enclosing the equipment, the equivalent diameter - defined as the ratio between the pass surface of the tube and the perimeter of the same -, the distance between the baffles, the number of shell side passes, the friction factor - representative coefficient of the frictional losses caused by the passage of the fluid inside the shell - which depends on the conditions of the flow.

The friction factor is defined as follows.

$$f_{shell} = 2 \times 0{,}72 Re_{shell}^{-0,15}$$

The formulation above is to be considered valid in the case of a fully developed turbulent flow; in case of laminar flow, the coefficient would depend linearly on the Reynolds number.

The flow inside the tubes will now be defined using relations similar to the previous case.

The formulation below determines the pressure drops.

$$\Delta P_{tube} = \frac{\rho_{tube} v_{tube}^2}{2} (f_{tube} + 4) n_{pass_{tube}} \left(\frac{L}{d_{internal}}\right)$$

$$f_{tube} = \sqrt{(1{,}82 \times \log_{10} Re_{tube}) - 1{,}64}$$

The following relation is used to calculate the pressure drops of plate and fin heat exchangers. [6]

$$\Delta P = \frac{2fLG^2}{\rho D_h}$$

The friction factor is the last parameter to be evaluated. For this type of heat exchangers a correlation, validated by experimental data, was discovered: it allows to evaluate f regardless of the flow regime; this is extremely important in case of off-design, although this specific treatment was not analyzed in this study. [7]

$$f = 9{,}6243 Re^{-0,7422} \alpha^{-0,1856} \delta^{0,3053} \gamma^{-0,2659} (1 + 7{,}669 \times 10^{-8} Re^{4,429} \alpha^{0,920} \delta^{3,767} \gamma^{0,236})^{0,1}$$

This parameter need the introduction of other geometric coefficients.

$$\alpha = \frac{f_s}{H - t}; \quad \delta = \frac{t}{l_f}; \quad \gamma = \frac{t}{f_s}; \quad f_s = \left(\frac{1}{n} - t\right)$$

Results

Before the results an analysis of the relevant parameters and performances of HPs follows.

The heat transfer at high temperature Q_d, is equal to the heat transfer from the source at low temperature Q_s plus the amount of high energy input W.

$$Q_d = Q_s + W$$

Therefore, it is possible to define the coefficient of performance for heat pumps COP, which is represented by the ratio

between the purposed effect and the energy required to obtain it. [8]

$$COP = Q_d/W$$

Presented below are the results from the simulations using the refrigerants mentioned above.

It should be reminded that these results were achieved with the same pinch point temperature difference (10 ° C) inside the evaporator and the condenser, in order to make this comparison.

Refrigerant	ΔT_{ppe}	ΔT_{she}	ΔT_{ppc}	ΔT_{scc}	ṁ [kg/s]	p_4 [kPa]	β	T_4 [K]	COP
R717	10	5			0,084	7302	5,405	459	2,807
R600a	10	15	10	3	0,4835	2381	5,415	383,4	1,998
R600	10	15			0,387	1845	7,571	383,3	1,941
R245fa	10	15			0,734	1574	10,65	384	1,967

Table 3: Ideal Cycle Simulation Result

As the chart shows, the highest coefficient of performance appears when the refrigerant *R-717* is used. The cause is the superheating value of the steam before entering the compressor, which turns out to be considerably greater for the other refrigerants because of the peculiar shape of the state diagram.

As a matter of fact, if such value were not imposed, the last stage of the compression would have happened inside the upper limiting curve.

Despite this necessity, a simulation was carried out imposing the same ΔT_sh found in the literature like in the case of R-717. Despite the whole coefficient of performance arose up to the value of 2.2, it appears to be rather lower than the value obtained in the case of ammonia nevertheless.

A decisive factor on which the value of the coefficient of performance depends, is the minimum temperature value at which the two flows in the evaporator can be combined. This value establishes the temperature of the refrigerant fluid downstream of the heat resulting from the recovery of heat, which would have otherwise been thrown outside. Since the temperature that needs to be reached inside the condenser is already

fixed, the higher is the temperature reached by the coolant by refrigerant during the heat recovery, the less work will need to be supplied by the compressor in order to achieve the desired characteristics in the condenser.

Figure 6: COP Ideal Cycle vs ΔT_{pp_e} for R-717

Nevertheless a variation of the coefficient of performance will occur in the real case, caused by a combination of effects.

The first one is related to difference between the outlet pressure from the heat exchanger and its input pressure; the latter will be lower, thus varying the enthalpy exiting from the machine. This means that the value of the numerator in the formula of the COP will change; the modification is not very relevant if the standard rules on pressure drops are applied.

The second effect is caused by the pressure drops within the compressor, which will further rise its outlet temperature. This means that the enthalpy of the fluid entering the capacitor will be greater than the one calculated in the ideal case. This will determine the increase of the denominator in the formulation of the COP.

The coefficient of performance in the real case will therefore be smaller, with respect to the one of the ideal case.

The following summary tables include the geometric quantities of the two different types of heat exchangers, and the cycle performances with these configurations

Refrigerant	ΔT_{ppe}	ΔT_{she}	ΔT_{ppc}	ΔT_{scc}	$\dot{m}$ [kg/s]	β	p_4 [kPa]	T_4 [K]	T4 real [K]	COP ideal	COP real
R717	10	5	10	3	0,084	5,405	7302	459	470	2,807	2,469

Table 4: Real Cycle Simulation Result

	R717	n_{tube}	d_e [mm]	d_i [mm]	pass [mm]	$n_{pass\,tube}$	$n_{pass\,shell}$	$D_{i\,shell}$ [mm]	Pitch	CPT	Total lenght [m]	Tot. surface [m²]
S&T	Heat exchanger 1	10	19,05	14,83	23,8	1	1	91,57	square	0,85	4,515	2,67
	Heat exchanger 2	10	19,05	14,83	23,8	1	1	92,85	square	0,85	4,968	3,02

Table 5: Real Cycle S&T heat exchangers characteristics $\Delta T_{pp_e} = 10° C$

	5,69

		H [mm]	t [mm]	L_{hot} [mm]	L_{cold} [mm]	l_f [mm]	n [mm⁻¹]	S_{layer} surface [m²]	Total surface [m²]
PFHE	Heat exchanger 1	10,3	0,1	200	1000	10	0,2041	1,033	2,065
	Heat exchanger 2			1100	200			1,136	2,272

Table 6: Real Cycle Plate&Fin heat exchangers characteristics $\Delta T_{pp_e} = 10° C$

	4,337

Economic analysis

The entire modeling was carried out with a well determined value of the ΔT_{pp} of the evaporator which was assumed as given. It is now necessary to determine the structural setting of the system with the best performance. For this purpose the following economic analysis was conducted; its function is the minimization of the costs that need to be met to change as suggested the existing plant.

In order to do so, the parameter ΔT_{pp_e} was changed; the exchange surface of the evaporator, and the amount of heat

recovered on which the coefficient of performance depends, are governed by this parameter. This will also determine a variation of the operating costs of the compressor: as the COP increases, the purchase cost of the electrical work required to drive the compressor is reduced.

The estimate cost of the plant has an error margin of ± 25%.

Assuming that the system would work 8,000 hours a year for 20 years, the cost of the electrical work supplied by the network was considered to be 0.12 € / kWh.[9]

The manufacturing firm of the compressor, Mykom, provided the purchase price for its alternative volumetric compress HS series

The determination of the cost of the heat exchangers in the case of shell and tube exchangers exploited a series of cost correlations whose validity scope was extended in order to determine the cost of these machines also in the case of limited exchange surfaces.

The correlation used is the Hall correlation; nevertheless, this formulation has a validity range function of the diameter of the shell which cannot be smaller than 60 $inch^2$. [10]

The correlation is the following:
$$C_{heat\ exchanger\$} = 8500 + 409A^{0,85}$$

This value represents the cost of the machine installed during the year referenced in the correlation whose result was the cost of the equipment, 2003.

To determine the current cost of the equipment, it will be necessary to multiply this cost for the ratio between the cost indexes of the reference year and the indexes of the current one, as shown in the following formulation. [11]

$$C_{real,heat\ exchanger\$} = C_{heat\ exchanger\$}\left(\frac{I_{equipment\ cost\ index\ 2003}}{I_{equipment\ cost\ index\ 2015}}\right)$$

The cost is expressed in dollars: it will have to be converted in euros. To change the currency, the amount has to be multiplied by the following factor $0,81553\frac{€}{USD}$. [9]

The relation used to calculate the cost of the compact heat exchangers is the following.[12]

$$C_{heat\ exchanger\$} = 231A^{0,639}$$

The following formula too has its separate range of validity; as a matter of fact, the exchange surface must be between the following values: $4,65\ m^2 < A < 836\ m^2$.

Now, the calculation of the operating costs is analyzed. The costs for the handling of the compressor are defined by the following relation.

$$C_{operating\ compressor\$} = \left(\frac{h_{F\ 4real} - h_{F\ 3real}}{\eta_{compressor}}\right)\dot{m}_F N_{working\ hours}C_{electricity}$$

This relation represents the yearly cost of the purchase of electric work expressed in dollars; to have the price in euros, it is necessary to multiply the entire factor above by the conversion factor mentioned above.

What must be determined is the discounted cost of the total expenditure due to the purchase of electrical work to power the compressor during the entire lifetime of the system. This was the formula used to determine the compound actualized rate, with an interest rate of $i = 0.1$.

$$C_{operating\ compressor,ctualyzed} = \sum_{k}^{N_{year}} \frac{C_{operating\ compressor€}}{(1 + i)^k}$$

Other operating costs are represented by the maintenance costs of the compressor.

They were calculated as a percentage of the purchase cost of the component, ranging from 2 to 10%. [13] In the specific case, given the size of the component, the maintenance cost was set to 10% of the basic cost of the compressor.

Once the overall costs are determined, the next stage is the minimization of these costs using the ΔT_{pp_e}. This factor is changed from the value taken as a reference when choosing the refrigerant, until it reaches values lower than the Celsius degree. As a result, since the exchange surfaces are not extremely sizeable, the heat exchanger will also turn out to be not very expensive; it will thus affect less the total cost, compared to the benefits obtained from the reduction of the operating costs of the heat exchanger.

Naturally, if the cancellation of the ΔT_{pp_e} is imminent, the cost of the exchange surfaces will diverge.

For this reason, the ΔT_{pp_e} value was set at 3 °C for technological reasons.

The last calculation is to determine the cost that should have been borne in order to buy fuel oil, had this recovery system had not been introduced.

This cost equals the thermal power that is exchanged, multiplied by the number of operating hours per year and the cost per heating kWh produced by the fuel oil. This value comes to € 0.0834 / kWh.

$$C_{oil} = Q_{he_2}N_{working\ hours}C_{kWh\ from\ oil}$$

It will then have to be actualized, like in the previous cases.

Environmental analysis

Naturally, the economic aspect is not the only parameter to analyze when verifying if a technological solution is appropriate. The environmental impact is as much important, especially during these hard times in which all countries are facing the needs of planet Earth: reducing emissions is necessary to stop global warming.

The solution analyzed, by employing heat recovery, can reduce carbon dioxide atmospheric emissions.

Using the standards SEF emission factor and knowing the combustible used, it will be possible to determine the quantity of carbon dioxide that would have been introduced into the atmosphere due to the combustion of fuel oil, had the heat recovery system designed not been used. [14]

The formulation used is the same for both the emissions caused by oil combustion, and those deriving from the purchase of electrical work from the network.

$$CO_{2\,emission} = \left(\frac{h_{F4real} - h_{F3real}}{\eta_{compressor}}\right)\dot{m}_F N_{working\ hours}SEF$$

Conclusion

The present experiment shows the potentiality of heat pumps, a technology that has widespread application in the space conditioning field.

They are already used in the industrial sector too, for instance within a number of drying systems in the food, wood and paper industry and in the chemical industry; nevertheless, their use was limited to temperatures lower than 90 °C, with very few exceptions. Therefore, this technology has not yet fully expressed its potentialities in the production industry at higher temperatures.

Therefore, this project is an example of innovative experimentation aimed at proving the aptitude of this technology to possible applications in contexts of production characterized by higher temperatures. As a matter of fact, in the case studied, the condense, whose energetic level is increased, reaches a temperature of 100 ° C.

This temperature is reached by raising the refrigerant temperature up to 185° C, providing heat with a temperature of about 110° C through the condenser.

The refrigerant fluids used for these high-temperature applications were also analyzed, and the refrigerant fluid *R-717* turned out to be the most performing.

This result has even greater relevance when considering the environmental impact: natural refrigerants are proven to be superior to synthetic ones (an example is the *R-245fa* fluid, analyzed during the study).

This solution has a double advantage. Firstly, it is economically convenient, since the introduction of the heat recovery system produces savings. However, the most

important effect is the reduction of carbon dioxide emissions; as a matter of fact, in the best case, the emission reduction amounts to almost 80%, compared to a case where fuel oil exclusively provides the thermal power needed by the fluid to raise its temperature.

In the current socio-economic context, great importance is given to environmental issues and to the impact that emissions can have on the planet; these results can represent the essential success factor that would help to spread the use of heat pumps in high-temperature applications, with a consequent decrease of industrial emissions.

Another important result is the mathematical model that was developed to guide the designing process and maximizing the results. The model can be applied to any industrial context, with only some simple modifications that need to be carried out based on the constraints of the heat recovery and on the dimensions of the equipment; it will thus allow to easily determine the ideal cycle, the preliminary sizing of the machines and finally the real cycle.

This model, which was designed in specialized development environments, can be largely adjusted to specific parameters; it takes into account the constraints of each solution, and it adapts its development to such constraints, highlighting the most interesting results.

Further projects

This work is only an example, though significant, of the potential that heat pumps have in the industrial sector: they would improve the primary energy consumption, and reduce atmospheric carbon dioxide emissions.

In the future, other studies that could be carried out, could include heat recoveries of larger entity: they would probably give even greater results in terms of cost and emission reduction.

The present case used a mechanical vapour-compression closed-cycle heat pump (CCC); a valid alternative is represented by absorption heat pumps, which have already been used in high-temperature applications.

These heat pumps can reach even higher temperatures, but they tend to have a superior complexity level.

The aim of this study is to further develop similar projects that can stimulate the spreading of this heat recovery system in high-temperature industrial fields; as a result, the sector technological level would increase, leading to better performances of the implants and, in conclusion, more economical and environmental-conscious productions.

References

[1] Warren M. Rohsenow and James P. Hartnett, Young I. Cho, 1998. Handbook of heat transfer. 3rd ed. New York: McGrow-Hill;

[2] Gregory Nellis, Sanford Klein, 2012. Heat transfer. Cambridge University Press

[3] http://www.hcheattransfer.com;

[4] Marwan Chamoun, Romual Rulliere, Philippe Haberschill, Jean Francois Berail, 2012. Dynamic model of an industrial heat pump using water as refrigerant. *International Journal of Refrigeration,* [online] Available at: http://www.sciencedirect.com/science/article/pii/S0140700711003082 [Accessed November 2015];

[5] S. A. Klein, 2013. Engineering Eqation Solver. Available at: http://www.fchart.com;

[6] Vivek Patel, Vimal Savsani, 2014. Optimization of a plate-fin heat exchanger design through an improved multi-objective teaching-learning based optimization (MO-ITLBO) algorithm. *Chemical Engineering Research and Design,* [online] Available at: http://www.sciencedirect.com/science/article/pii/S0263876214000732 [Accessed November 2015];

[7] Raj M. Manglik, Arthur E. Bergles 1994. Heat transfer and pressure drop correlations for the rectangular offset strip and fin compact heat exchanger. *Experimental thermal and fluid science* [online] Available at: http://www.sciencedirect.com/science/article/pii/089417779400096Q [Accessed November 2015];

[8] Bohdan Soroka, 2015. *Application Note - Industrial Heat Pumps.* [pdf] European Copper Institute.

Available at: http://www.leonardo-energy.org/sites/leonardo-energy/files/Cu0118%20-%20Industrial%20Heat%20Pumps%20-%20v2.pdf [Accessed August 2015];

[9] Antonio C. Caputo, Pacifico M. Pelagagge, Paolo Salini 2008. Heat exchanger design based on economica optimization. *Applied Thermal Engineering* [online] Available at: http://www.sciencedirect.com/science/article/pii/S1359431107002839 [Accessed December 2015];

[10] Marcel Taal, Igor Bulatov, Jiri Klemeš, Petr Stehlìk 2003. Cost estimation and energy price forecast for economic evaluation of retrofit project. *Applied Thermal Engineering* [online] Available at: http://www.sciencedirect.com/science/article/pii/S1359431103001364 [Accessed December 2015];

[11] M&S equipment economical index;

[12] Marcel Taal, Igor Bulatov, Jiri Klemeš, Petr Stehlìk 2003. Cost estimation and energy price forecast for economic evaluation of retrofit project. *Applied Thermal Engineering* [online] Available at: http://www.sciencedirect.com/science/article/pii/S1359431103001364 [Accessed December 2015];

[13] Turton, Bailie, Whiting,Shaeiwitz, Bhattacharyya, 2012. Analysis, Synthesis and Design of Chemical Processes, 4rd ed. Prentice Hall;

[14] Convenant of Mayors, 2006. Technical annex to the SEAP template instructions document: the emission factors. [pdf] Convenant of Mayors.